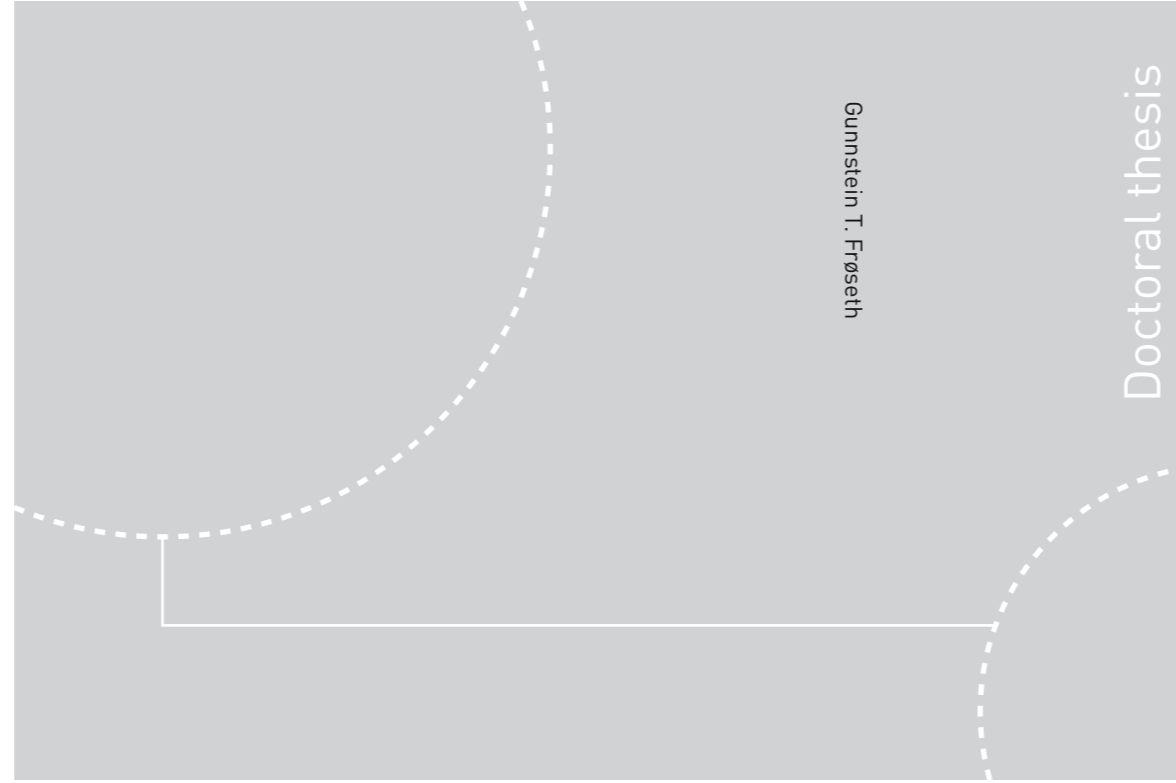


ISBN 978-82-326-3748-5 (printed ver.)  
ISBN 978-82-326-3749-2 (electronic ver.)  
ISSN 1503-8181



Doctoral theses at NTNU, 2019:73

Gunnstein T. Frøseth

# Load model of historic traffic for fatigue life estimation of Norwegian railway bridges

Doctoral theses at NTNU, 2019:73

**NTNU**  
Norwegian University of Science and Technology  
Thesis for the Degree of  
Philosophiae Doctor  
Faculty of Engineering  
Department of Structural Engineering

 **NTNU**  
Norwegian University of  
Science and Technology

 **NTNU**

 **NTNU**  
Norwegian University of  
Science and Technology

Gunnstein T. Frøseth

# Load model of historic traffic for fatigue life estimation of Norwegian railway bridges

Thesis for the Degree of Philosophiae Doctor

Trondheim, May 2019

Norwegian University of Science and Technology  
Faculty of Engineering  
Department of Structural Engineering



Norwegian University of  
Science and Technology

**NTNU**  
Norwegian University of Science and Technology

Thesis for the Degree of Philosophiae Doctor

Faculty of Engineering  
Department of Structural Engineering

© Gunnstein T. Frøseth

ISBN 978-82-326-3748-5 (printed ver.)  
ISBN 978-82-326-3749-2 (electronic ver.)  
ISSN 1503-8181

Doctoral theses at NTNU, 2019:73

Printed by NTNU Grafisk senter

# Preface

This thesis is submitted in partial fulfillment of the requirements for the degree *Philosophiae Doctor* at the Norwegian University of Science and Technology (NTNU). The work has been carried out at the Department of Structural Engineering, Faculty of Engineering. Professor Anders Rönquist and Professor Ole Øiseth have supervised the work. This thesis consists of a collection of three papers, one that is published in an international peer reviewed journal and two that are submitted for publication.

Gunnstein Thomas Frøseth,

Trondheim, Norway  
February 24, 2019



# Publications

## Included publications

The following papers are included in this thesis:

- I: G. T. Frøseth and A. Rönnquist. Evolution of load conditions in the Norwegian railway network and imprecision of historic railway load data. *Structure and Infrastructure Engineering*, 15(2):152–169, 2019. doi: 10.1080/15732479.2018.1504087
- II: G. T. Frøseth and A. Rönnquist. Finding the train composition causing greatest fatigue damage in railway bridges by Late Acceptance Hill Climbing. 2018. Submitted for journal publication
- III: G. T. Frøseth and A. Rönnquist. Load model of historic traffic for fatigue life estimation of Norwegian railway bridges. 2019. Submitted for journal publication

## Declaration of authorship

Gunnstein T. Frøseth is the first author and Anders Rönnquist is the second author of all papers (I–III) included in this thesis. Gunnstein T. Frøseth came up with the ideas, gathered the data, implemented the theory, obtained numerical results, performed analysis and wrote the manuscripts in all three papers. Anders Rönnquist discussed the work and provided constructive criticism which increased the scientific quality of the papers.

### Other scientific contributions

The following papers are related to the topic of this thesis and are published in journals and conference proceedings during the PhD study:

- 1) G. T. Frøseth, P. Nåvik, and A. Rönnquist. Operational displacement estimations of railway catenary systems by photogrammetry and the integration of acceleration time series. 2016. Accepted for publication in *International Journal of Railway Technology*
- 2) G. T. Frøseth, A. Rönnquist, D. Cantero, and O. Øiseth. Influence line extraction by deconvolution in the frequency domain. *Computers & Structures*, 189: 21–30, Sept. 2017. doi: 10.1016/j.compstruc.2017.04.014
- 3) G. T. Frøseth and A. Rönnquist. System Reliability Analysis of Steel Railway Bridge Based on Historic Rolling Stock Records. In *13th Nordic Steel Construction Conference*, Tampere, Finland, 2015. Tampere University of Technology. ISBN 978-952-15-3579-6
- 4) G. T. Frøseth, P. Nåvik, and A. Rönnquist. Close range photogrammetry for measuring the response of a railway catenary system. In *Proceedings of the Third International Conference on Railway Technology: Research, Development and Maintenance*, Stirlingshire, UK, 2016. Civil-Comp Press. doi: 10.4203/ccp.110.102
- 5) G. T. Frøseth, A. Rönnquist, and O. Øiseth. Operational Modal Analysis and Model Updating of Riveted Steel Bridge. In *Proceedings of the 34th IMAC, A Conference and Exposition on Structural Dynamics*, volume 2 of *Dynamics of Civil Structures*. Springer International Publishing, 2016. doi: 10.1007/978-3-319-29751-4\_23
- 6) G. T. Frøseth, A. Rönnquist, and O. Øiseth. Prediction Error in Strain Response in Finite Element Simulations with Moving Load Formulation of Train Passages of Open Deck Steel Bridges. In *First International Conference on Rail Transportation: Railway Development, Operations, and Maintenance*, Chengdu, China, 2017. ASCE. doi: 10.1061/9780784481257.077

# Abstract

Material fatigue is the primary damage mechanism in steel railway bridges and ultimately causes material fracture and eventually component and system failure. It is essential that the infrastructure owner can predict and monitor the state of material fatigue in the bridge stock to avoid bridge collapse due to the catastrophic consequences to human life and environment as well as economic cost. Fatigue life assessment of railway bridges is also necessary to ensure that limited funds for maintenance and renewal of the infrastructure is managed in the most efficient manner. Given the vital role of a well managed, reliable and safe railway infrastructure to a functioning modern society and the large number of steel railway bridges in the railway infrastructure, fatigue life assessment of steel railway bridges is of key importance to industrialized countries all around the world.

The state of the fatigue damage mechanism depends strongly on the loading history of the material. The loading history of the material is determined by the historic traffic on the railway infrastructure, and the remaining fatigue life of a railway bridge therefore depends on the historical traffic conditions at the bridge site. Historical traffic conditions in the railway infrastructure has long been a neglected field of research on fatigue life assessment of railway bridges. Furthermore, the traffic conditions in a railway network is strongly heterogeneous, data on traffic conditions at one site in a railway network is therefore generally not applicable to the traffic conditions at another location in the railway network.

This thesis considers historical loads on the Norwegian railway network and establishes a conservative load model of the historical loads for fatigue life estimation of steel railway bridges. The available data on historical loads on the Norwegian railway network between 1854 and the present is compiled. The load conditions in the railway network is established through documentation of the geometry and loads on the rolling stock, permissible loads and speed on the lines in the network and rules for train operation. It is concluded that the precise load conditions at a particular bridge generally cannot be determined due to lack of relevant data. A novel methodology to find the most damaging train, given all possible locomotives and wagons for a particular period and traffic type is developed. The methodology determines the conservative load case and allows prediction of the remaining fa-



tigue life of railway bridges with the available data. The significance of historical traffic on fatigue life of railway bridges is considered and it is concluded that traffic prior to 1900 can be neglected in fatigue life estimation of Norwegian bridges. Passenger and freight traffic after 1900 has a significant contribution to fatigue damage due to moderate fatigue damage potential for some structural components and relatively high number of train passages on certain lines in the railway network.

A general framework for establishing and calibrating a load model to the conservative load case is presented. The framework is used to develop a conservative load model of historic freight and passenger traffic for efficient assessment of bridges in the Norwegian railway network.

# Acknowledgments

A thesis should include acknowledgment of those who have directly or indirectly made a contribution to the work presented therein. This is my attempt at acknowledging those who contributed to this thesis.

I am grateful to Bane Nor and Jernbanedirektoratet (formerly Jernbaneverket) for funding and supporting this thesis, for showing great interest in the work that has been performed and adopting any result and conclusion from this work. Special acknowledgments are made to Arne Vik, John Magne Hembre and Åsmund Tøsse. The contribution from others are certainly not forgotten, particularly those in the bridge engineering group or those working on the Hell bridge project.

I am also grateful to the scientific, administrative and technical staff at the Department of Structural Engineering. Most of you have helped me with something in relation to this thesis at some point. Terje Petersen deserves a special mention for our trips to various bridges and the fun I had on those.

To my current and former colleagues at the Structural Dynamics group; Thank you for all the coffee breaks, I have enjoyed myself in your company and learned something from most of you. I acknowledge Øyvind Wiig Petersen for his patience, you have endured these years in room 3-104 without a single complaint<sup>1</sup>. The members of Last Day are acknowledged for every last day. I hereby unacknowledge Knut Andreas Kirkestuen Kvåle, stealer of fonts and proponent of long floppy bridges.

My main supervisor, and good friend, Anders Rönnquist has my sincerest and deepest gratitude. You have provided guidance in both scientific and non-scientific aspects of life in the past few years and have been instrumental in making this thesis and who I am today.

I also acknowledge Ole Øiseth, Daniel Cantero, Oddvin Ørjasæther and Petter Nåvik for the discussion and collaboration on other scientific projects. I have learned a lot from each of you.

My mother and father should be acknowledged, not only for gifting the world with at least one healthy and highly capable boy, but also to instill in me that I must either get a job or continue my studies. Luckily, I am either lazy and/or bad

---

<sup>1</sup>Even more impressive if you know that I periodically used a buckling spring keyboard

at finding jobs which meant that I continued to the pinnacle of our education system and produced the thesis you are now reading. Thank you mom. Thank you dad.

Then, finally, I must acknowledge the greatest contributor beside myself to this thesis. Simone, not only have you made life a pleasure for more than a decade, you have also helped me with reading, discussions and even preparing scientific measurement equipment. Thank you for everything.

# Contents

<b>Preface</b>	<b>i</b>
<b>Publications</b>	<b>iii</b>
<b>Abstract</b>	<b>v</b>
<b>Acknowledgments</b>	<b>vii</b>
<b>1 Introduction</b>	<b>1</b>
1.1 Background and motivation . . . . .	1
1.1.1 Current research needs . . . . .	3
1.2 Fatigue life analysis . . . . .	4
1.2.1 Remaining fatigue life by fracture mechanics . . . . .	4
1.2.2 Remaining fatigue life by damage accumulation . . . . .	5
1.3 Stress cycles in railway bridges . . . . .	6
1.3.1 Stress cycles in railway bridges due to traffic loads . . . . .	7
1.4 Fatigue load models . . . . .	9
1.4.1 What is “relevant traffic data”? . . . . .	10
1.4.2 Lack of relevant traffic data . . . . .	11
1.4.3 Requirements of a fatigue load model . . . . .	13
1.5 Objectives and scope . . . . .	15
1.5.1 Objectives . . . . .	15
1.5.2 Scope . . . . .	16
1.6 Outline of thesis . . . . .	16
<b>2 Evolution of load conditions in the Norwegian railway network and im- precision of historic railway load data</b>	<b>19</b>
2.1 Introduction . . . . .	20
2.2 Historic axle loads . . . . .	22
2.2.1 Locomotives . . . . .	22
2.2.2 Freight wagons . . . . .	23

2.2.3	Passenger wagons and multiple units . . . . .	25
2.2.4	Permissible loads on a track . . . . .	27
2.2.5	Train speed . . . . .	27
2.3	Rolling stock geometry and design . . . . .	29
2.3.1	Geometry and design of locomotives . . . . .	29
2.3.2	Geometry and design of wagons . . . . .	32
2.4	Train geometry and composition . . . . .	36
2.4.1	Mixed train traffic . . . . .	36
2.4.2	Train traction type . . . . .	37
2.4.3	Number of wagons in trains . . . . .	37
2.5	Discussion . . . . .	40
2.5.1	Relevance of presented data to actual loads in the railway network . . . . .	40
2.5.2	Evolution of load conditions in the Norwegian railway network . . . . .	40
2.5.3	Nature of the presented data . . . . .	47
2.5.4	Use of imprecise data in service life estimation . . . . .	48
2.5.5	Relevance of findings and discussion to foreign railways . . . . .	49
2.6	Conclusions . . . . .	50
<b>3</b>	<b>Finding the train composition causing greatest fatigue damage in railway bridges</b>	<b>53</b>
3.1	Introduction . . . . .	53
3.2	Theory . . . . .	56
3.2.1	Fatigue damage . . . . .	56
3.2.2	Response generation by influence lines . . . . .	57
3.3	Formulation, notation and problem statement . . . . .	58
3.3.1	Trains, locomotives and wagons instead of axle position and load magnitudes . . . . .	58
3.3.2	Notation, solution space and problem statement . . . . .	59
3.4	Solving the problem – Finding the most damaging train . . . . .	60
3.4.1	Exact solution . . . . .	60
3.4.2	Approximate solution . . . . .	60
3.5	Examples . . . . .	63
3.5.1	Train sets and influence lines to evaluate heuristics . . . . .	63
3.5.2	Performance of random sampling and Hill Climbing . . . . .	66
3.5.3	Influence of the history length on the performance of the LAHC heuristic . . . . .	68
3.5.4	Behavior and performance of LAHC with larger train sets . . . . .	69
3.6	Discussion . . . . .	74
3.6.1	Selecting the history length and number of trials . . . . .	74
3.6.2	Defining the train set . . . . .	76

3.7	Conclusions . . . . .	80
<b>4</b>	<b>Load model of historic traffic for fatigue life estimation of Norwegian railway bridges</b>	<b>83</b>
4.1	Introduction . . . . .	84
4.2	Properties of the proposed fatigue load model . . . . .	86
4.2.1	The load model should be conservative . . . . .	86
4.2.2	The load model should be consistent . . . . .	87
4.3	Methodology . . . . .	89
4.3.1	Formulation of the optimization problem . . . . .	90
4.3.2	Fatigue damage calculation . . . . .	92
4.3.3	Representing structural components in the infrastructure . . .	92
4.3.4	Historic traffic conditions in the Norwegian railway network .	94
4.4	Results and discussion . . . . .	95
4.4.1	Fatigue damage potential and significance of historical loads .	95
4.4.2	Load model based on existing reference trains . . . . .	98
4.4.3	Which and how many new reference trains? . . . . .	100
4.4.4	Proposed load model . . . . .	103
4.4.5	Can a load model be used on structural components that it was not calibrated for? . . . . .	105
4.5	Conclusion . . . . .	108
	Appendices . . . . .	110
4.A	Definition of train sets . . . . .	110
4.B	Definition of fatigue load model of historic traffic . . . . .	113
<b>5</b>	<b>Conclusion</b>	<b>117</b>
5.1	Concluding remarks . . . . .	117
5.2	Suggestions for further work . . . . .	119
	<b>References</b>	<b>121</b>



# Chapter 1

## Introduction

### 1.1 Background and motivation

Construction of the Norwegian railway infrastructure started in 1851 with the 68 km long line, *Hovedbanen*, between Oslo and Eidsvold. The Norwegian railways continued its expansion the next century, reaching a peak length of around 4500 km and was largely completed in 1962 with *Nordlandsbanen* between Trondheim and Bodø [17]. Today's railway network consists of 3857 km of railway lines available for commercial traffic [69], and is primarily the same as it was in 1962, with the exception of discontinued lines and the new 64 km long Gardermobanen which finished in 1999. Table 1.1 shows a summary of the main lines in regular traffic and gives an overview of the Norwegian railway network.

The majority of the railway infrastructure in Norway was therefore completed more than 50 years ago. Most of the original components of the infrastructure has been renewed several times over the history of the railways, but bridges are a notable exception due to the considerable investment cost and interruption to the railway operation associated with the replacement of them. Figure 1.1 shows the construction year of bridges with different building materials in the current Norwegian railway network.

During the initial expansion of the railway network, timber bridges were almost exclusively being constructed due to the high availability and low cost of timber in Norway. This changed at the end of the 19th century when steel became much cheaper and widely available [97]. From the beginning of the 20th century, a number of stone arch bridges were constructed, but steel was the primary material used in both the construction of new bridges and also in the replacement of existing timber bridges. Reinforced concrete was not commonly used until the 1930s, but has been the dominating construction material used in new bridges from the middle of the 20th century [55]. The current distribution of construction material in railway bridges is about 50% concrete, 40% steel and the rest are stone or steel-concrete



Table 1.1: Active railway lines in the Norwegian railway infrastructure. The table represents all lines longer than 30 km and more than 97 % of the railway infrastructure measured in route length and number of bridges.

Line	Termini		Construction	Length [km]	Bridges
Nordlandsbanen	Trondheim	Bodø	1873 – 1962	729	300
Sørlandsbanen	Drammen	Stavanger	1869 – 1944	546	498
Dovrebanen	Eidsvoll	Trondheim	1857 – 1921	475	327
Rørosbanen	Hamar	Støren	1869 – 1877	384	227
Bergensbanen	Hønefoss	Bergen	1875 – 1913	371	204
Østfoldbanen-west	Oslo	Kornsjø	1873 – 1879	169	131
Vestfoldbanen	Drammen	Eidanger	1875 – 1882	140	98
Gjøvikbanen	Oslo	Gjøvik	1894 – 1902	124	73
Kongsvingerbanen	Lillestrøm	Charlottenberg	1857 – 1862	115	62
Raumabanen	Dombås	Åndalsnes	1908 – 1924	114	106
Solørbanen	Kongsvinger	Elverum	1890 – 1910	94	31
Meråkerbanen	Hell	Storlien	1873 – 1882	70	47
Hovedbanen	Oslo	Eidsvoll	1851 – 1854	68	66
Gardermobanen	Etterstad	Eidsvoll	1992 – 1999	64	24
Østfoldbanen-east	Ski	Rakkestad	1873 – 1882	55	31
Randsfjordbanen	Hokksund	Hønefoss	1863 – 1868	54	22
Bratsbergbanen	Eidanger	Nordagutu	1875 – 1917	47	45
Drammenbanen	Oslo	Drammen	1869 – 1872	41	27
Ofofbanen	Narvik	Vassijaure	1898 – 1902	39	7
Arendalsbanen	Nelaug	Arendal	1894 – 1910	36	17
Roa–Hønefoss	Roa	Hønefoss	1898 – 1909	32	27
			1851 – 1999	3767	2370

composite bridges.

Considering the age distribution of the bridges in the current railway network, fig. 1.1 shows that the majority of the oldest bridges in the railway network are steel bridges, e.g. there are more steel bridges constructed before 1970 ( $\approx$  50 yrs. ago) than the combined number of concrete and stone bridges constructed before 1970. The figure also shows that the majority of steel railway bridges in the Norwegian railway network was designed and constructed before 1960, which means that about a third of all bridges in the current railway network are steel railway bridges, designed and constructed before 1960.

Two major aspects of steel bridge engineering design has changed from 1960 and until today. Firstly, the design loads have changed significantly both in terms of load magnitude, spatial distribution and frequency. Also, the actual traffic loads have significantly changed character, e.g. from steam locomotives to diesel and electric locomotives, higher operational speeds and wagon design. This means that steel bridges in the Norwegian railway network were designed and constructed for different traffic conditions than what is present in the railway infrastructure today and what is predicted for the future. Secondly, the fatigue damage mechanism was not properly understood until the second half of the 20th century [109]. Further-

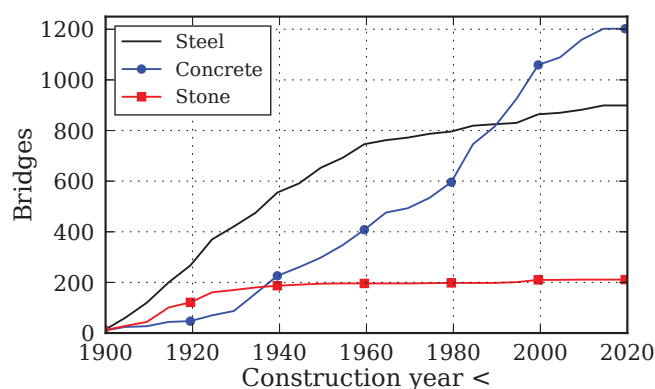


Figure 1.1: Cumulative distribution of construction year of bridges in the Norwegian railway network.

more, the appropriate fatigue endurance data was not available before the 1970s and 1980s [39, 57]. The ability of engineers to perform a thorough fatigue design analysis was therefore limited due to lack of knowledge and necessary data.

The fatigue damage mechanism is a cumulative damage mechanism which evolves by repeated loading and unloading of the material. The number of loading and unloading cycles induced by traffic in railway bridges, and also therefore the fatigue damage, increases for each train that passes the bridge. Eventually, the fatigue life of steel bridges runs out and components and even the entire bridge structure must be repaired or replaced. The changes to historic traffic conditions in the railway infrastructure and lack of consideration and understanding for the fatigue damage mechanism in bridge design raise further concerns about the safety and continued use of the old steel railway bridges. Furthermore, the large number of these bridges in the railway network and the cost associated with replacing them makes it infeasible to swap them out in the foreseeable future. It is also undesirable from an economic and environmental perspective to replace bridges that have sufficient capacity and safety levels.

For the infrastructure owner, it is therefore essential to estimate the remaining fatigue life of these steel railway bridges such that the most critical bridges to fatigue failure can be identified and the limited resources for maintenance and renewal can be applied in the most efficient way.

### 1.1.1 Current research needs

Fatigue life analysis involves a model for the fatigue resistance of the component and a model for the fatigue loads applied to the component. The fatigue resistance

of typical railway bridge components is now well established after extensive research in the second half of the 20th century. Unfortunately, there are no fatigue load models in the literature that are directly applicable for fatigue life analysis of bridges in the Norwegian railway network.

Lack of a representative load model for the Norwegian railway network prevents assessment of remaining fatigue life of old steel bridges and thereby severely limits the ability to efficiently maintain and renew the railway network.

There is an immediate need for a fatigue load model that represent historic loads in the Norwegian railway network.

## 1.2 Fatigue life analysis of steel railway bridges

Fatigue is a mechanism where cracks initiate and grow in a material due to repeated loading and unloading of the material. Fatigue failure occurs when the fatigue cracks have grown to a critical length and the remaining cross section cannot resist the applied load. The fatigue life of a material can be divided into two periods *crack initiation* and *crack growth*. In the crack initiation period, cracks develop in the material due to cyclic slip and crack nucleation, and are generally limited to a single or a few grains. The crack growth rate in the crack initiation period is dependent on the conditions at the material surface and more specifically on the geometric stress concentrations due to surface roughness, material faults and component design. In the crack growth period, a crack grows into the material and the crack front is exposed to a larger number of grains. Hence it depends on the average bulk properties of the material rather than the stress concentrations at the surface [110].

The distinction between crack initiation and crack growth phase is significant from a fatigue life analysis point of view because the fatigue phenomenon depends on different specimen properties for the two periods, i.e. micro structure and surface conditions in the crack initiation phase and the bulk material properties in the crack growth phase.

### 1.2.1 Remaining fatigue life by fracture mechanics

Fracture mechanics is applicable if the fatigue mechanism is in the crack growth phase and an initial crack size is available for the analysis. For steel railway bridges the fracture mechanical approach is relevant for estimating the remaining fatigue life if a crack can be identified in the bridge, e.g. an actual crack is found during inspection, or if it is reasonable to assume an initial crack length, e.g. if the intervals of an inspection scheme is to be determined [80] or a damage tolerant approach is

acceptable [76]. These are, however, special cases. Typically when estimating the remaining fatigue life of a railway bridge, there is no initial crack size available. Both the crack initiation period as well as the crack growth period must be included to get reasonable estimate of the remaining fatigue life. Without going into more detail on fatigue life estimation by fracture mechanics, it is relevant to note that a description of the magnitude and number of loading cycles is also necessary with the fracture mechanical approach [4, 18, 110].

### 1.2.2 Remaining fatigue life by damage accumulation

In the typical case of estimating the remaining fatigue life of a railway bridge, where there is no initial crack size available, the current state of the fatigue mechanism is unknown. The crack initiation period as well as the crack growth period must then be included in the analysis of remaining fatigue life. The fatigue life of a structural component is in this case determined by a combination of a fatigue endurance model and a damage accumulation model. The fatigue endurance model defines the number of cycles  $N$  from a uncracked and perfect material to fatigue failure for a component subjected to repeated application of stress range  $S$ . A fatigue endurance model therefore defines the entire fatigue life of the component subjected to constant amplitude loading. A simple and commonly used fatigue endurance model is a power law known as Basquin's relation,

$$N(S) = CS^{-b} \quad (1.1)$$

where  $C$  and  $b$  are the fatigue endurance parameters established by experimental tests for different structural details. As mentioned in section 1.1, the fatigue endurance of typical railway bridge components was not established prior to designing these structures, much of the research has therefore focused on determining the fatigue endurance of railway bridge components [1, 2, 11, 21, 34, 38, 96, 102, 103, 108]. A review of previous fatigue tests of steel bridge components and composition into a fatigue endurance catalog can be found in Taras and Greiner [119]. Typical variants of Basquin's relation used in fatigue life estimation of steel railway bridges are piece wise functions consisting of two or more power laws specified for different domains of  $S$ , see e.g. [23, 28].

The fatigue endurance model defines the fatigue life when the component is subjected to repeated application of a single and constant stress range magnitude  $S$ . The response in a railway bridge generally consists of a combination of different stress ranges  $[S_1, S_2, \dots, S_k]$ , and a damage accumulation model must be introduced to find the combined total damage from these cycles. A number of different damage accumulation models have been proposed in the literature [37]. The most commonly used accumulation model is Miner summation,

$$D = \sum_{i=1}^k \frac{1}{N(S_i)} \quad (1.2)$$

where the total fatigue damage  $D$  is the sum of damage contributions  $\frac{1}{N(S)}$  from each stress cycle  $S$ . The component fails when the fatigue damage reaches some critical level  $D_c$ .

The remaining fatigue life of a component at a particular point in time depends on the fatigue damage introduced by past stress cycles applied to the component and the fatigue damage induced by future stress cycles. If  $D_0$  is the fatigue damage introduced by past stress cycles, and  $D_1$  is the yearly fatigue damage introduced by the future stress cycles, the remaining fatigue life of the structural component is given in years  $t$  as

$$t = \frac{D_c - D_0}{D_1} \quad (1.3)$$

### 1.3 Determining stress cycles in railway bridges

The previous section described two approaches to obtain an estimate of the remaining fatigue life of a component. In either approach it is necessary to estimate the future stress cycles induced in the material, and in the damage accumulation approach it is also necessary to describe the past stress cycles applied to the material such that the current state of the fatigue mechanism can be established.

Stress cycles can be determined by either measuring them directly on the bridge in service or by estimating them by numerical models of traffic and bridge. Measuring stress cycles directly is generally the most accurate approach because it avoids the uncertainty associated with numerical models and the necessary input data [50, 76, 77]. Measurements can also be used to update the bridge model and reduce the uncertainty in obtaining stress cycles in a modeling approach [26, 98]. Obtaining the stress cycles by measuring them directly is expensive compared to estimating them from numerical models due to high installation and maintenance cost, and are therefore limited to a few critical components [72, 115]. Furthermore, measured stress cycles are only representative of the bridge behavior and traffic conditions at a particular point in time, since the structural behavior and traffic conditions change over time due to deterioration and structural modification of bridges [12] and technological advances and demands for trains [52].

Numerical models are therefore in general necessary to obtain a complete stress cycle history and the remaining fatigue life of old steel railway bridges. In the numerical modeling approach, the stress response is obtained by modeling the bridge and the external loads that induce stress cycles in railway bridges. The typical ap-

proach to modeling of railway bridges for fatigue assessment involve a multi-level finite element model with truss and beam elements to capture stresses in plain structural members and global bridge behavior, and sub-models of shell and solid elements to obtain stresses in plates and structural details such as fillets, rivets and rivet holes [3, 60–62, 64, 71].

Stress response in railway bridges are induced by external loads applied to the structure, and any variable external loading applied to a railway bridge will induce stress cycles in the bridge material. The sources of variable loading on railway bridges are traffic loads and environmental loads. Traffic loads will generally have higher load intensity and application frequency. For instance, hundreds of trains may pass a bridge in a day and a train may have more than one hundred axles, each weighing over 20 tn. Heavy snow, on the other hand, only occurs a few times each year and snow is seldom allowed to accumulate on railway bridges such that the load intensity is negligible compared to those from traffic loading. Strong winds are also limited to a few times each year and due to the relatively modest dimensions of old steel railway bridges, the wind loads are small compared to those from traffic. Due to their high load intensity and application frequency compared to environmental loads, one may conclude that:

Traffic loads are the only loads that need to be considered when estimating the remaining fatigue life of old steel railway bridges.

### 1.3.1 Stress cycles in railway bridges due to traffic loads

Consider fig. 1.2 which shows a train with eight axles and the corresponding static load function  $f(x)$  of that train along a spatial coordinate  $x$ .

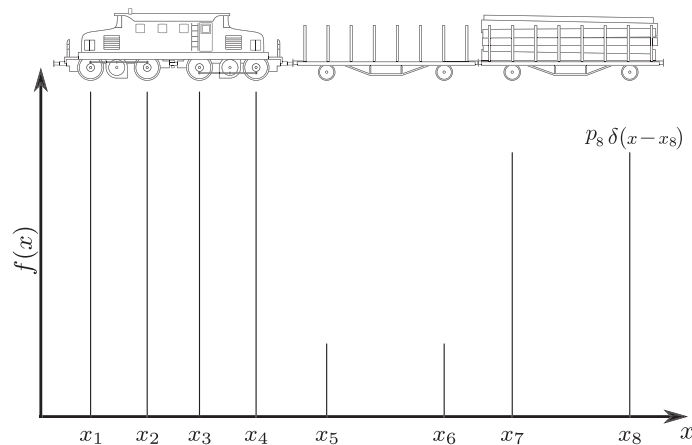


Figure 1.2: Load function for a train with eight axles.

The figure shows that each axle  $i$  has a position  $x_i$  and a load magnitude  $p_i$ . The static loading  $f(x)$  of a train on the substructure is then more formally defined by

$$f(x) = \sum_{i=1}^{n_p} p_i \delta(x - x_i) \quad (1.4)$$

where  $n_p$  denotes the number of axles in the train and  $\delta(x)$  is the Dirac delta function.

The influence line  $l(x)$  is the response<sup>1</sup> of a structure subjected to a unit load moving along a predefined load path with spatial coordinate  $x$ . The influence line can either be estimated by a numerical model [15, 30, 68] or from measurements on the structure [47, 94]. If the influence line belongs to a structure that can be considered linear, i.e. the principle of super position holds, then the static response  $z_0(s)$  in a structural detail can be determined by taking the convolution of the influence line and the load function,

$$z_0(s) = (l * f)(s) \quad (1.5)$$

where  $(*)$  denotes the convolution operator and  $s$  is the shift variable which can be interpreted as the distance that the train has moved along the load path of the influence line.

The complete response in a structure generally consists of both a static and a dynamic part. The common approach to estimate the response in old steel railway bridges for the purpose of fatigue analysis is to estimate the static response with influence lines and the dynamic response by applying a dynamic amplification factor, see e.g. [6, 60, 104]. The dynamic amplification in a bridge depends on several properties of train, track and bridge, examples include the speed of the train, the condition at the wheel-rail interface and the dynamic properties of both the train and the bridge. These effects are typically included as a dynamic amplification factor  $\Phi$  which is the ratio between the total response over the static response. Several dynamic amplification factors for fatigue life assessment of bridges have been proposed in the literature [60], and they typically depend on the speed of the train  $v$  and the characteristic length  $L$  of the influence line under investigation, i.e. the dynamic amplification factor is a function of train speed and characteristic length  $\Phi(v, L)$ . Using this definition, and introducing eq. (1.4) into eq. (1.5), the total response  $z(s)$  in a structural detail is defined by

$$z(s) = \Phi(v, L) \cdot \sum_{i=1}^{n_p} p_i l(s - x_i) \quad (1.6)$$

---

<sup>1</sup>Response is any measurable quantity, e.g. moment, shear, stress, deflection...

If  $l(x)$  is the influence line of stress in a structural detail, then  $z(s)$  is the stress response induced in that structural detail by a passing train. The stress cycles  $[S_1, S_2, \dots, S_k]$  can then be extracted from the stress response by a cycle counting algorithm, e.g. the rainflow cycle counting algorithm [5, 35].

In summary to this section on stress cycles in railway bridges, traffic loads are generally the only loads that need to be considered in fatigue life estimation of bridges. The number and magnitude of stress cycles induced in a structural component by a train depends on the speed of the train, the number of axles in the train, the axle positions and axle load magnitudes. A description of these parameters as well as the number of trains that pass a bridge are therefore necessary to determine the stress cycles that are applied to railway bridges by traffic, i.e. a load model is necessary to estimate the remaining fatigue life of railway bridges.

## 1.4 Load models for fatigue life estimation of railway bridges

The load model is a key component of fatigue life estimation of railway bridges because it determines the stress cycles that the material is subjected to. A load model that is an accurate representation of actual traffic is therefore essential to obtain accurate estimates of remaining fatigue life of railway bridges [61, 72, 74, 99].

In general, a fatigue load model consists of a reference load and a corresponding set of calibration factors. The load models available in the literature can be classified into two different types:

- The reference load is a collection of standard trains that are modeled on real trains. The calibration factors are then typically the composition of these trains into a traffic mix, see e.g. [59, 60, 123] or the fatigue trains in annex D of the Eurocode [27].
- The reference load is a single artificial load case, see e.g. LM71 of the Eurocode [27], with a set of calibration factors that take into account the traffic type, traffic intensity and structural parameters, e.g. the lambda factors for LM71 in the Eurocode [27].

Regardless of the type of fatigue load model which is used, the fundamental idea is that the load model introduces the same fatigue damage as the actual traffic when applied to a bridge, i.e. the fatigue load model and the actual traffic introduce equivalent fatigue damage in bridges in the infrastructure [57]. This is achieved by adjusting (calibrating) the calibration factors of the load model with relevant data on traffic in the infrastructure.

Calibrating a fatigue load model for fatigue life estimation of all bridges in a railway network is not a trivial task. A major problem is that traffic in a railway



network is heterogeneous, i.e. the traffic that pass one bridge may have completely different characteristics from the traffic at another bridge [118]. This is also the case for bridges located on the same line and only a short distance from each other, e.g. if a factory is located between two bridges, all traffic from that factory typically only pass one of them. The past traffic conditions of one particular bridge is therefore in general different from the traffic conditions at another bridge. This means that a load model of past traffic loading which is calibrated for, e.g. British railways [59, 60], Swedish and Danish railways [117] or European railways [123] is not directly applicable to Norwegian railways, and perhaps only to the few locations they were calibrated for. In general, a load model must be calibrated to the particular bridge under investigation to obtain realistic estimates of the remaining fatigue life due to the heterogeneous traffic conditions in a railway network.

Load models must be calibrated with relevant traffic data for the particular bridge under investigation.

#### 1.4.1 What is “relevant traffic data”?

Equation (1.6) shows that basic variables of trains that influence the stress response in a bridge are the train speed, axle loads and axle spacing. Relevant traffic data is then any data that can be used to determine these basic variables.

The sources of relevant traffic data for calibration of load models for railway bridges can be categorized either as primary or secondary data sources. The primary sources of data are direct measurements of train speed, axle loads and axle spacings. Ideally, all these variables should be recorded for each train passage of a bridge such that the exact realization of the traffic at a bridge is known. Alternatively, these variables are recorded in the form of histograms and correlation maps such that the traffic is known in a statistical sense. Several authors have reported direct measurements of the basic variables in the literature [67, 81, 111, 121], but these efforts are generally of short duration and limited to a few locations in the railway network.

Primary sources of data are therefore in general limited to a few bridges in the infrastructure, and are only covering a small fraction of all traffic of the entire history of the bridge. This claim is evidenced by the large body of case studies on remaining fatigue life of railway bridges, which generally either *assume* historic traffic conditions or estimate them from secondary sources, see e.g. [1, 6, 13, 19, 20, 33, 60, 73, 100, 104–106, 120].

Secondary sources of data on traffic in a railway network are all other data that can be used to estimate the basic variables of trains, i.e. the train speed, axle loads and axle spacing. Among the examples of secondary sources of data are:

- Primary sources of data for other location and time periods [6, 120].
- Rolling stock data, e.g. axle load limits and geometry of locomotives, passenger and freight wagons [19, 33, 60].
- Operation statistics, e.g. locomotive, wagon, train distance traveled, transported goods, average axle loads and number of passengers [1, 6, 20].
- Infrastructure data, e.g. regulation of train length, train speed, axle loads and documented changes to infrastructure [1, 33, 117].

A major problem associated with estimating basic variables from secondary data sources is that the data which is available is not the “correct” or “sufficient” data for the estimation problem. Is it possible to estimate the speed of a train at a bridge without actually measuring the speed?

The issue of insufficient data is perhaps best explained from a mathematical perspective; recall that an equal number of equations and unknown variables are necessary to find a unique solution to a system of equations. Equation (1.6) shows that there are two unknowns for each axle (magnitude and spacing) and one for the train speed, i.e. there are  $(2 \cdot n_p + 1)$  unknown variables to define a train. One equation is obtained for every *distinct* and *relevant* piece of information that is gathered from secondary sources, e.g. one equation is obtained if the mean axle loads of the wagons of a train are established from operational statistics. Reasonable assumptions may also provide a large number of equations, e.g. one equation per two-axle wagon can be obtained if it is assumed that both axles of a wagon are equally loaded.

A typical freight train has roughly fifty axles, if the mean axle load of these wagons can be determined and one can safely assume that the axles on each wagon is equally loaded, one would still need another fifty unique and relevant pieces of information to define the load of that train. There might be cases where it is possible to establish the loads by secondary sources, but in general it is simply infeasible to locate this much information/data on each train in traffic from secondary sources. Since primary data sources generally does not exist and secondary sources of data does not provide sufficient amounts of data, one may conclude that:

There is generally a lack of relevant traffic data for load model calibration.

#### 1.4.2 Lack of relevant traffic data

The issue with lack of data in estimation problems is that the estimation problem becomes under-constrained or under-specified. In the context of estimating a train on a railway bridge, this means that the data is not able to uniquely identify one

train that the data must correspond to, but rather a number of different trains that are all possible given the data.

To illustrate this point and problems associated with lack of data, consider a case where we are tasked with determining the fatigue life of a simply supported bridge due to bending stresses at mid-span. Through the primary and secondary data sources we are able to establish that one particular train is the only traffic that has passed the bridge. The number of passages and the speed of each passage is known by direct measurements. The train consist of a locomotive, with known axle loads and geometry, followed by twenty wagons with known and identical geometry. The data sources show that eighteen of the twenty wagons are fully loaded and two of them are empty. The only piece of information that is lacking is therefore the ordering of the full and empty wagons, i.e. are the empty wagons placed together or separated by fully loaded wagons and are the empty wagons at the front, back or mixed in with the fully loaded wagons?

Figure 1.3 shows the ratio between the minimum and maximum fatigue damage induced in the simply supported beam bridge with different lengths  $L$ , when considering all possible permutations of the order of the twenty wagons in the train. Fatigue damage is calculated with Basquins relation eq. (1.1) for different  $b$ 's and Miner's damage accumulation rule eq. (1.2). Stress cycles extracted by rainflow cycle counting.

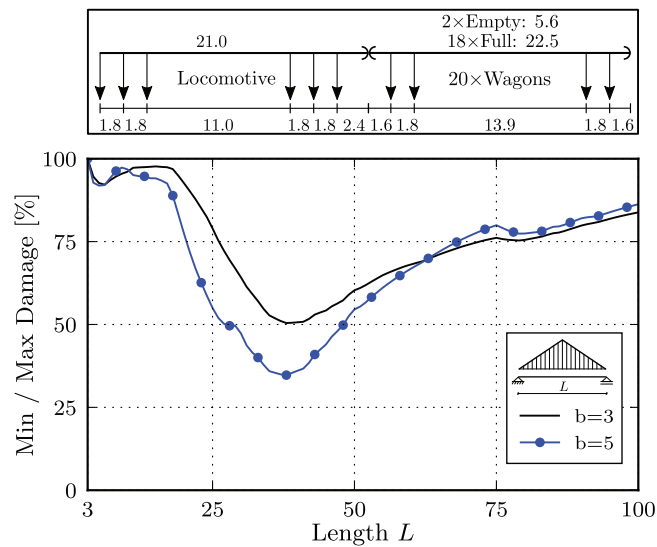


Figure 1.3: Ratio between minimum and maximum damage at mid-span due to bending moment from ordering of full and empty wagons.  $b$  refers to the exponent in Basquins equation.

The figure shows that the ordering of full and empty wagons in the train is not insignificant to the estimated fatigue damage in these type of bridges, e.g. for bridge lengths  $L \approx 40$  the fatigue damage of the least damaging ordering is roughly 50% of most damaging ordering of wagons. The data in this case cannot help us decide which train is more probable or likely, the data can only tell us that it is one of the trains between and including the least damaging train and the most damaging train.

Lack of relevant data means that a set of possible loads corresponds to the available data, rather than a single unique load case.

### 1.4.3 Requirements of a load model for assessment of steel railway bridges

A fatigue life analysis considers the available data on resistance of the components in the infrastructure and the available data on fatigue loading applied to the component to establish the time to failure. In section 1.4.2 it was argued that, due to the lack of relevant traffic data, there are a set of possible fatigue loadings that could have applied to the component. Which of these loadings should be used when considering the remaining fatigue life of the bridge components and the objectives of the fatigue life assessment of steel railway bridges?

The primary objective of a fatigue life assessment of steel railway bridges is to *ensure that the bridge is safe to operate*. Fulfilling this objective is generally necessary from a legal standpoint, but it is also ethically and economically motivated. If a railway bridge collapses during train operation, the direct and indirect monetary cost, loss of lives and loss of reputation are catastrophic to both the train operator and the infrastructure owner. The infrastructure owner must therefore ensure and document that the bridge is safe to operate.

The only way to meet the primary objective of fatigue life assessment, given that there is a set of possible load cases that cannot be given any preference over one another, is to select the load case that introduces the maximum fatigue damage in the material, i.e. a conservative assumption is made about the data. Making a conservative assumption when faced with lack of data is well established in good engineering practice and ensures that the estimated fatigue life is at least as long as predicted by the analysis, i.e. a safe prediction of the remaining fatigue life is obtained. This approach to lack of data is also advocated in the literature on fatigue life estimation of railway bridges, see e.g. assumptions made on load models in [1, 33]. A load model for assessment of steel railway bridges should therefore be conservative to fulfill the primary objective of fatigue life assessment of steel railway bridges.

Another objective of fatigue life assessment is to rank the structural components

and bridges in the infrastructure from critical to safe to allow efficient management of the infrastructure. It has already been established that the fatigue load model should be conservative, but what if the load model is more conservative<sup>2</sup> for one structural component than it is for another structural component? The issue then is that the component which the load model is less conservative for will be ranked less critical than the other component, solely because the load model induces inconsistent levels of fatigue damage in the two components. This means that if a load model does not induce consistent levels of fatigue damage, the load model introduces a bias in the ranking of structural components and the second objective of the fatigue life assessment is possibly violated. A load model for fatigue life assessment of steel railway bridges should therefore introduce consistent levels of fatigue damage in different structural components to allow efficient management of the railway infrastructure.

Given a set of possible load cases, the conservative load case should be assumed in fatigue life estimation of railway bridges.

---

<sup>2</sup>A load model may be more conservative for one structural component than another because the stress response induced in a structural component depends on both the characteristics of the load and the characteristics of the structural component, see  $l(x)$  in eq. (1.6)

## 1.5 Objectives and scope

### 1.5.1 Objectives

The primary objective of this thesis is to develop a conservative load model of historic traffic loads for fatigue life estimation of bridges in the Norwegian railway network. To accomplish this goal the following research objectives must be realized.

**Describe available historic load data for estimation of remaining fatigue life of steel railway bridges** Section 1.4 discussed the importance of calibrating fatigue load models with relevant traffic data for fatigue life estimation of a bridge. Currently, there is no concise compilation available of past traffic data for the Norwegian railway network that is suitable for fatigue load model calibration. This also means that there is no clear overview of what data is in fact available or how it can be used in fatigue load model calibration. One objective of this thesis is therefore to gather and describe relevant historic load data for use in fatigue life estimation of bridges in Norway and discuss how this data can be used in such a task.

**Develop a methodology to determine the conservative load case given the available load data for the Norwegian railways** Section 1.4.1 established that there is generally a lack of relevant traffic data for fatigue load calibration and section 1.4.2 showed that lack of data means that a set of possible loads which corresponds to the data are found rather than one unique load case. Furthermore, section 1.4.3 established that a fatigue load model should be conservative to fulfill the objectives of a fatigue life analysis. This means that one must identify which of the possible load cases induces the most fatigue damage in an arbitrary structural component to fulfill the objectives of a fatigue life analysis. One of the objectives of this thesis is therefore to develop a methodology that can identify the most severe fatigue load case, given by the available traffic data for the Norwegian railways.

**Determine the significance of historic loads in fatigue life estimation** Section 1.3 identified any past and future train as the fatigue loads that must be considered in analysis of the remaining fatigue life of railway bridges. This does not however mean that all trains will have a significant influence on the fatigue damage analysis, e.g. one might expect that trains from one period generally induces fatigue damage that are orders of magnitude lower than trains from another period. This ultimately means that the traffic from certain periods may be neglected from the analysis without any significance to the estimated remaining fatigue life. One of the objectives of this thesis is therefore to determine the significance of historical loads on fatigue life estimation of railway bridges such that fatigue analysis

can be simplified and made as efficient as possible by omitting traffic loads that are insignificant to fatigue life.

**Establish a conservative fatigue load model based of the available Norwegian traffic data** The second research objective of this thesis establishes a methodology that finds a load case for each structural component that is conservative. A conservative estimate of the fatigue life of a structural component can be obtained by determining the conservative load case with the methodology presented in the second research objective above and combining this with the number of train passages for the particular bridge in the infrastructure. It is, however, impractical and inefficient to apply the methodology of finding the most severe load case every time a structural component is to be assessed. A more efficient approach is to establish a load model which induces the same fatigue damage as the conservative load case in a wide range of different structural components. One objective of this thesis is therefore to establish and calibrate a conservative fatigue load model for use in the fatigue life estimation of Norwegian railway bridges.

### 1.5.2 Scope

The focus of this thesis is on developing a load model from available data on past traffic loads in the regular Norwegian railway network. The load conditions at the iron ore lines *Ofofbanen* and *Dunderlandsbanen* are not emphasized in the investigation and are considered outside the scope of this thesis. This thesis only considers data that are available in the literature or from established measurement programs, i.e. measurements on the current traffic conditions will not be performed as part of this thesis.

## 1.6 Outline of thesis

Chapter 2 describes the historical load conditions in the Norwegian railway network. The available data on rolling stock, traffic and infrastructure for the entire history of the railways are presented. The nature of the available data and how the data can be used in fatigue life assessment of steel railway bridges is also discussed.

Chapter 3 develops a novel methodology to utilize all data presented in chapter 2 and find the train composition that causes greatest fatigue damage induced in an arbitrary structural component by traffic from a specific period. The methodology therefore identifies the conservative load case for a specific train type and period in the railway network.

Chapter 4 presents the fatigue load model of historic traffic for Norwegian railways. The desired properties of a fatigue load model for steel railway bridges are

established. A general framework for load model calibration that satisfies the desired properties of a fatigue load model is developed. Fatigue damage potential and significance of historical loads to fatigue life of steel railway bridges in the Norwegian railway network is considered. The impatient reader finds the proposed load model in section 4.B.

Chapter 5 concludes this thesis with the main findings and suggestions for future work.





## Chapter 2

# Evolution of load conditions in the Norwegian railway network and imprecision of historic railway load data

Gunnstein T. Frøseth and Anders Rönnquist,  
*Structure and Infrastructure Engineering*, vol. 15(2):152-169, 2019.

### Abstract

This paper describes historic load conditions in the Norwegian railway network to improve estimates of the remaining service life of bridges. Data on rolling stock, traffic and infrastructure throughout the history of the railway are presented. Axle loads, geometry, design, composition and operation of both passenger and freight trains have changed several times since the initial construction. The capacities of both rolling stock and infrastructure influence the load conditions in a railway network. Historic loads may have been more severe than modern loads for certain structural details. A probability distribution of load variables for a specific bridge cannot be obtained in the general case. Future research directions and suggestions for the use of non-probabilistic data in estimating the service life of bridges are discussed.

## 2.1 Introduction

Technological advances and population and trade growth have led to increasing axle loads and train speeds, placing higher demands on the ageing railway infrastructure. The existing infrastructure must be assessed under conditions of increased operational demands to ensure safe operation of the transportation system. Numerical models are essential in this regard due to the vast number of components requiring assessment. Numerical models are used to determine the appropriate actions and predict the condition of many parts of the infrastructure, e.g., bridges [61, 62, 65]. The importance of load conditions at the site is common to all such assessment tasks.

Bridges are structures with very long service lives and represent essential infrastructure components. A large portion of Europe's oldest bridges are made of steel [116]. Fatigue is one of the primary damage mechanisms in steel bridges, and crack initiation, as well as crack growth, is governed by the load history at the site. In the absence of data on historic loading conditions at a bridge site, the current train loadings and traffic intensity are commonly applied to the entire history of the structure in service life estimation. Hayward [52, 53] presents train loads on bridges in the British rail network throughout its history and shows that both axle weights and train speeds evolved tremendously from the first railways to today's modern railways. As the fatigue damage mechanism is highly sensitive to the magnitude of the stress range, assuming today's traffic over the history of the structure will yield grossly conservative results [63]. Ignoring historic loads can, on the other hand, overestimate the remaining service life, as such loads may have contributed significantly to the fatigue damage of certain details, as shown by Pipinato et al. [105] and more recently by Imam and Salter [59].

A better understanding of the historic loading conditions of the railway infrastructure will improve an evaluation of the existing infrastructure and facilitate a better allocation of limited resources to maintenance and renewal, therefore being essential to achieving both economic management of the infrastructure and an environmentally sustainable society. Several authors have previously proposed load models for service life estimation of railway bridges due to fatigue damage.

Åkesson [1] suggests a simple load model, considering an *equivalent freight train*. It is assumed to have axle loads equivalent to the current maximum axle load during the entire history of the bridge. The use of an equivalent freight train is also suggested in Sustainable Bridges [116], in which the concept is extended to include the evolution of axle loads and allow for variations in train composition and wagon geometry. Details of past changes of axle loads and geometry are lacking; additionally, no recommendations regarding the selection of locomotive and wagon geometry, train type, train composition or traffic intensity are provided. Pipinato and Modena [101] adapt the model but, similarly, do not present any further details

of the historic fatigue load model.

Imam et al. [60] present a model of historic load conditions of British railways. The model divides the railway history into two periods, 1900-1970 and 1970-present. For the period from 1970 to the present, the fatigue for trains of medium traffic type defined in BS5400-10 [23] is used. The load model prior to 1970 is divided further into three sub-periods, each defined by three different trains, i.e., freight, passenger and local suburban trains. Each train has a particular locomotive with various geometries and axle loads; the passenger and freight wagons vary in axle loads, while the wagon geometry is unchanged throughout the entire period 1900–1970. The load model is extended in [59] to lines with only passenger trains or only freight trains, with the study also including a description of geometry ranges of locomotives, freight wagons and passenger wagons of the rolling stock prior to 1970.

Although Imam and Salter [59] present certain data on the ranges of values of the rolling stock geometry, the current literature lacks a concise overview of the variations and ranges of variables defining the train loads. Specifically, data are needed on the ranges of possible axle load magnitudes and geometry of locomotives, freight wagons and passenger wagons, as well as on the composition and operation of trains, e.g., the number and type of wagons and locomotive speeds applicable to a train. Without such data, it is not possible to assess the uncertainty associated with service life estimates or identify parameters that the service life estimate is most sensitive to.

Two major contributions to the theory of service life estimation of railway bridges are made in this paper. First, it presents data for the loads, design and geometry of rolling stock, as well as available data relevant to the composition of trains throughout the railway's history to further assess the uncertainty associated with service life estimates. A foreign reader can adapt and extend the presented data to other countries' railways. Second, this paper provides a general discussion of the nature of available load data for specific bridges in the network. In general, the probability distribution of all load variables cannot be determined. The implications of this insight for the current practice are discussed, and future research directions are provided.

This paper is organised as follows. Section 2.2 and section 2.3 present data on the evolution of the axle loads, geometry and design of rolling stock available to the railway network throughout the railways' history. Section 2.4 considers the composition and operation of trains. Section 2.5 summarises the data presented in this paper, discusses the nature and characteristics of data on historic railway loads, and suggests further data uses and directions of research in estimating the service life of bridges.

## 2.2 Historic axle loads

### 2.2.1 Locomotives

The data on locomotive axle loads have been primarily gathered from Aspenberg [9], Bjerke et al. [16] and Norges Statsbaner [85]. Figure 2.1 shows the evolution of the maximum axle load and the relationship with the maximum secondary axle loads of locomotives used in the Norwegian railway network.

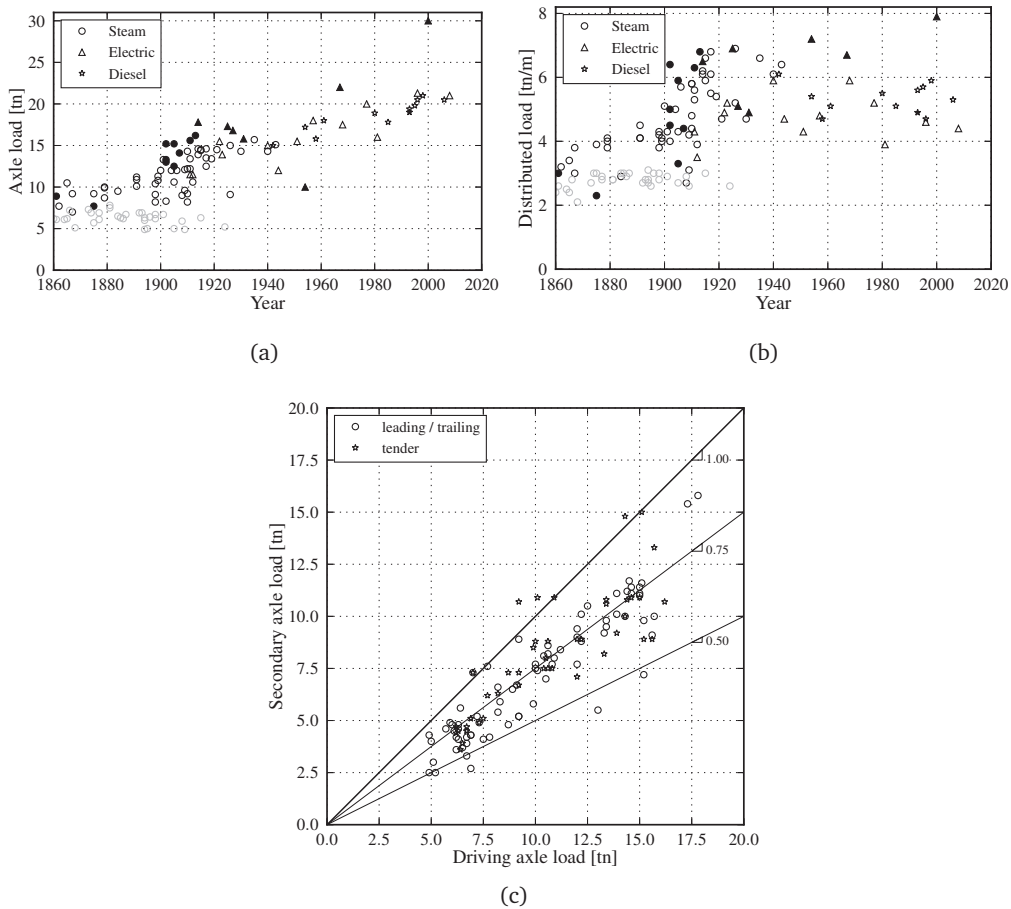


Figure 2.1: (a) Evolution of the maximum axle load of locomotives, (b) distributed load across buffers and (c) relationship between axle loads on the driving and secondary axles of the locomotive, i.e., leading, trailing and tender axles. Filled markers indicate locomotives used on the iron ore lines. Grey markers indicate narrow gauge locomotives.

The maximum axle load of locomotives has increased, going through roughly four different levels during the railway's history. Prior to 1900, the maximum axle load of locomotives was 11 tn. The maximum axle load increased rapidly to 15 tn after 1900. In the fifties, the axle loads of trains increased again to 18 tn, with the maximum axle loads continuing to rise, reaching 21 tn for today's locomotives. Note that locomotives used for the iron ore lines at Ofot- and Dunderlandsbanen generally have the highest loadings; however, the movements of such locomotives are restricted to the mentioned lines. Such locomotives are therefore not considered further in the presented description. The delivery year does not necessarily indicate that the locomotive was in widespread use throughout the railway network, as the first delivery was often used to test the design before making further acquisitions.

An interesting pattern of the distributed loading of locomotives is shown in fig. 2.1b. The distributed load increased significantly around 1900 and approached 7 tn/m around 1920 for several steam locomotives. The distributed loading of subsequent electric and diesel locomotives used in regular traffic has not surpassed 6 tn/m, i.e., the distributed loading over the buffer length was the highest for steam locomotives built after 1900.

Figure 2.1c shows that the driving axles are generally the most heavily loaded axles of locomotives. This is explained by the tractive effort of a locomotive being limited by the friction between the driving axles and the rails. The loads of leading and trailing axles on locomotives are generally in the range of 50 % to 100 % of the driving axle load, with a modulus of 75 % between leading/trailing and driving axle loads being a reasonable assumption based on a visual inspection of the figure. The tender axle load can be higher than that of the driving axle for certain locomotives, however, the tender axle load changes as stores of water and coal are depleted; hence, the tender axle loads presented in the figure represent the upper bounds.

The narrow-gauge locomotives (grey markers) have a significantly lower maximum axle load than their standard-gauge counterparts. Data on the evolution of the axle loads of narrow-gauge freight and passenger wagons have not been found; however, as narrow-gauge locomotives have significantly lower axle loads than standard-gauge locomotives, it can also be argued that the wagons used on narrow-gauge lines similarly had lower axle loads than standard-gauge wagons.

### 2.2.2 Freight wagons

Historic data have been compiled from [86], including amendments that were published periodically during the railways' history. The newest data have been obtained from the national vehicle register of rolling stock. Figure 2.2 depicts the axle loads of freight wagons.

The maximum load imposed by Norwegian freight wagons changed in stages.

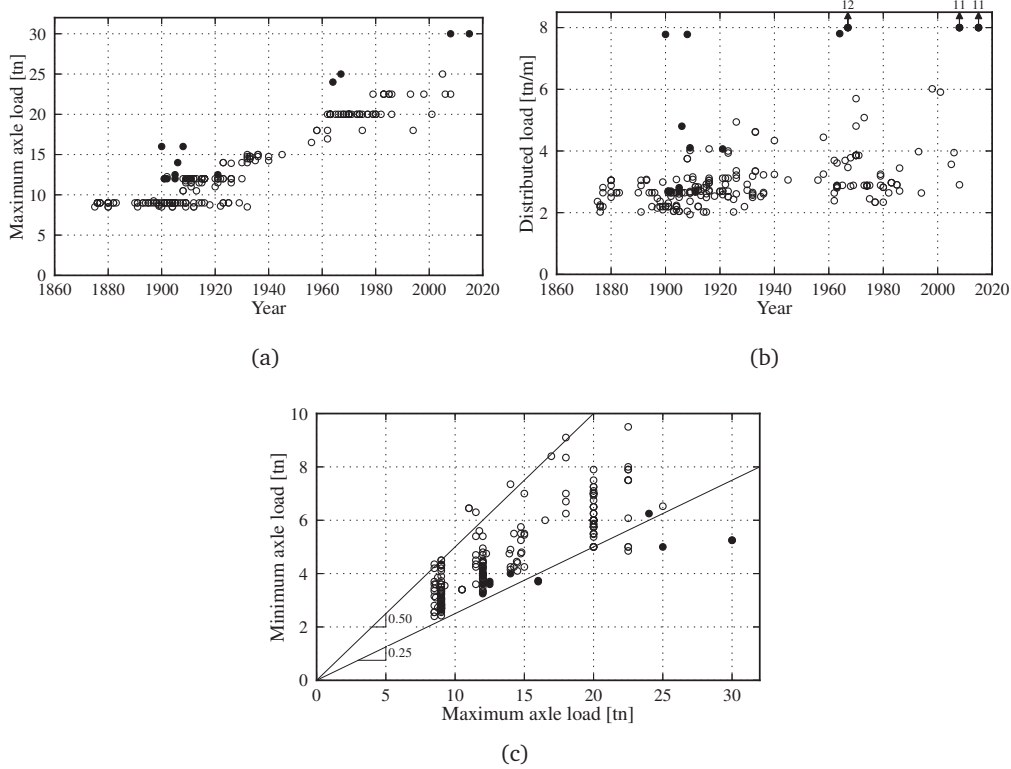


Figure 2.2: (a) Evolution of maximum axle load, (b) evolution of distributed load, and (c) relationship between axle loads of full and empty freight wagons. Filled markers indicate freight wagons that were used on iron ore lines.

Prior to 1900, the maximum axle loads of freight wagons in the general railway network was 9 tn, increasing to 12 tn at the turn of the century. In 1932, the first wagons with 15 tn axle loads were delivered and put into service. From 1956, a new class of freight wagons was introduced with 18 tn axle loads.

After the Second World War, UIC introduced a series of standard two-axle freight wagons together with the standard running gear. The standardised single-axle and bogie suspension had an axle load capability of 20 tn [70]. The Norwegian rail administration adopted standardised freight wagons and running gear in 1966, while the previously classified 18 tn wagons were modified to comply with the UIC standard. The standardised UIC running gear of freight wagons was upgraded during the 1980s to 22.5 tn after extensive experimental measurements had been performed in the European railway network [66]. Since the introduction of standardised freight wagons and running gear, the variation in the maximum axle loads

of freight wagons has declined, as shown by fig. 2.2a. The highest permissible axle loads of wagons registered to date are those of special flat wagons built and registered in 2003. Such wagons have the maximum axle load of 25 tn and are used for timber transport on certain lines in the southeastern parts of the railway network under a dispensation from the general permissible loads.

Figure 2.2b shows that the maximum distributed loading of freight wagons was below 3 tn/m until 1910, 5 tn/m until 1970 and below 6 tn/m until 1998, i.e., the maximum distributed loading of freight wagons increased over time. Figure 2.2c depicts the relationship of the axle loads between full and empty wagons. The axle load of an empty wagon can be assumed to be 25 % to 50 % of the maximum axle load. Certain wagons have a higher than 25 % maximum axle load, as certain types of goods require special heavier wagons, e.g., an empty insulated thermal wagon weighs more than a flatbed wagon for intermodal transport.

### 2.2.3 Passenger wagons and multiple units

The historic data on passenger wagons and multiple units have been compiled from [87, 90]. The axle load of a passenger wagon is determined by the number of passengers present in the wagon. The maximum number of passengers is determined by the number of seats  $n_{\text{seats}}$  and the available area for standing passengers. The available area of a wagon comprises the aisle and the areas near the wagon entrances. Herein, two passengers per metre are assumed to be standing over the wagon buffer length  $L_{\text{buffer}}$  to account for non-seated passengers. Hence, the total number of passengers  $n_{\text{passengers}}$  of a fully loaded passenger wagon is given by:

$$n_{\text{passengers}} = n_{\text{seats}} + 2 \cdot L_{\text{buffer}} \quad (2.1)$$

Figure 2.3 shows the evolution of axle loads and the relationship between the axle loads of full and empty passenger wagons and motorised units, assuming that each passenger weighs 75 kg.

The maximum axle weight of passenger wagons was approximately 9 tn until 1910, subsequently increasing to approximately 11 tn by the 1950s, when a series of wagons with steel bodies was introduced with 12 tn axle load. The maximum axle load of passenger wagons has generally remained around 12 tn until the present, with the exceptions to this general description being a series of two-axle steel wagons in 1928 that were not used extensively for transportation, a restaurant wagon in 1953 and a sleeper wagon in 1986. The sleeper wagon of NSB type 7 is still commonly used in long-distance overnight trains.

The first multiple unit was introduced in 1931; fig. 2.3a shows that motorised units have the highest axle loads among wagons used for passenger transport. The non-motorised multiple units have historically had the same axle loads as regular passenger wagons; however, starting from 1990, the non-motorised multiple unit



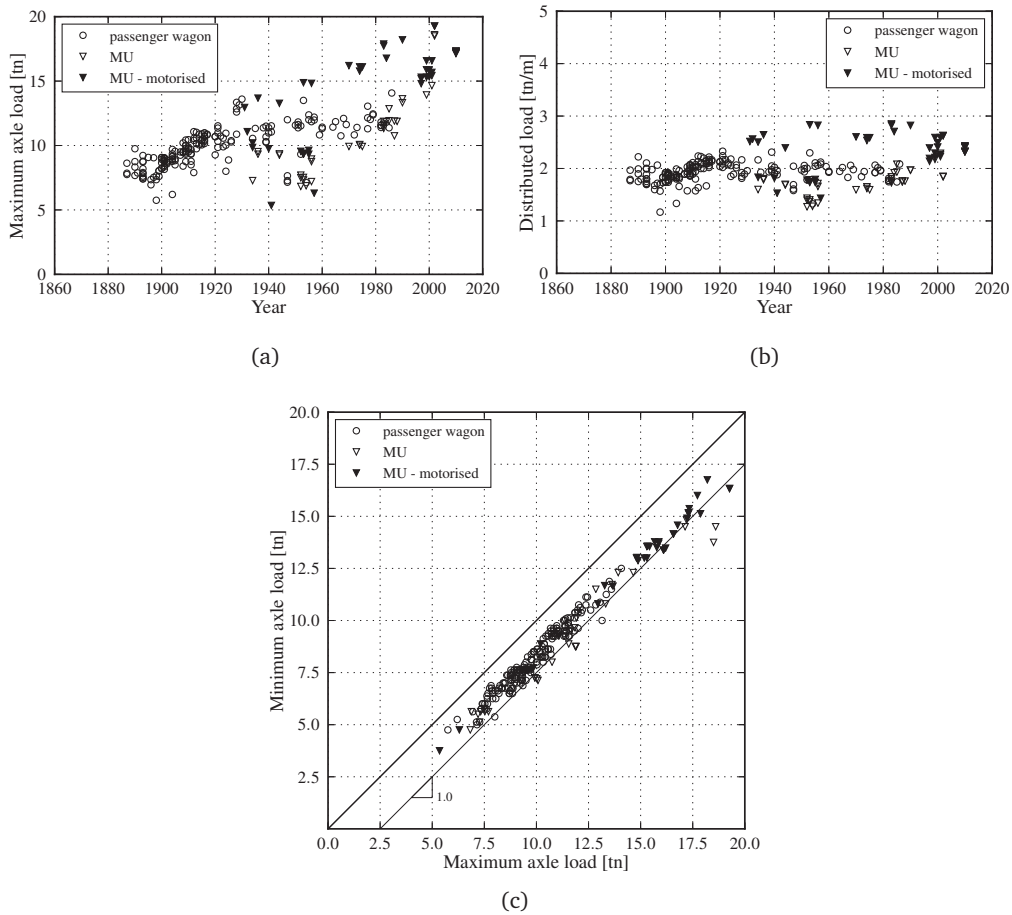


Figure 2.3: (a) Evolution of axle loads of passenger wagons and multiple units, (b) evolution of distributed load, and (c) relationship between axle loads of empty and full units.

wagons have had higher axle loads. The axle loads of motorised multiple units are roughly comparable to those of locomotives of the time.

The distributed loading of passenger wagons depicted in fig. 2.3b has remained relatively unchanged throughout the entire railways' history at around 2 tn/m. The distributed load of a motorised multiple unit followed the same trend, i.e., the distributed loading has remained unchanged slightly below 3 tn/m.

Figure 2.3c shows that subtracting 2.5 tn per axle from the maximum axle load of a wagon yields a good approximation of an empty wagon weight for regular passenger wagons and motorised wagons. The weight of 2.5 tn per axle corresponds to approximately 130 passengers of average weight of 75 kg. The number of pas-

senger seats in passenger wagons has varied between 20 and 80 throughout the entire history, while certain newer multiple units accommodate up to 120 seated passengers.

#### 2.2.4 Permissible loads on a track

The permissible load on a particular line during a period provides an upper bound on the load experienced by bridges along the line. The data are gathered from network statements issued by the infrastructure owner, i.e., historically Norges Statsbaner [88], and, since 2003, from the *network statement* available under EU Directive 2012/34/EU. Figure 2.4 shows the permissible axle loads in the railway network in various years.

Permissible axle loads ranged from 7 tn to 17 tn in the first half of the previous century. The pattern became more uniform around 1950, with the permissible axle load being 15 tn as a general rule. It remained so until around 1960, when the *Modernisation and rationalisation-plan* [58] (MR-plan) was ordered and put into effect by the Norwegian parliament. Higher axle loads and speeds were two of the explicit goals of the MR-plan to improve the railways' competitiveness relative to other modes of transportation. According to the MR-plan, the axle loads were increased to 18 tn, remaining at that level until 1984, as shown in fig. 2.4c. Another change in permissible axle load was made in 1985 to 20.5 tn, with a further increase to 22.5 tn in 1989. By 1996, most of the Norwegian railway network had reached the current standard with the permissible axle load of 22.5 tn.

#### 2.2.5 Train speed

The train speed affects both the quasi-static and dynamic components of the load exerted by the train on the infrastructure.

##### Locomotive speed

Figure 2.5 shows the maximum speed of locomotives and motorised units throughout the railways' history. Prior to 1900, the maximum speed of locomotives was 70 km/h. The fastest steam locomotive was NSB Type 30 with the nominal top speed of 90 km/h, introduced to the network in 1913. Diesel- and electric-powered locomotives reached speeds of 100 km/h around 1940. After 1950, the maximum speed increased until reaching the maximum speed of 200 km/h of modern electric locomotives and multiple units. Historically, there has not been a clear difference in speed between locomotives and motorised units, with the fastest locomotives having approximately the same top speed as motorised units.



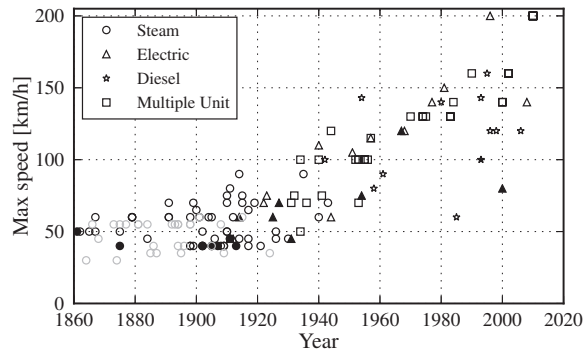


Figure 2.5: Maximum speed of locomotives and multiple units. Filled markers indicate locomotives used on the iron ore lines. Grey markers indicate narrow gauge locomotives.

Table 2.1: Maximum speeds of passenger and freight trains according to the infrastructure owner's regulations, speeds are given in km/h.

Train\Year	1950	1970	1990	2000	2016
Passenger	90	120	130	160	210
Freight	65	80	80	80	100

No representative data on infrastructure-imposed speed limits prior to 1950 have been found.

## 2.3 Rolling stock geometry and design

### 2.3.1 Geometry and design of locomotives

**Design** The classification system presented in UIC [122] is adopted in the following discussion on locomotive design and geometry. Figure 2.6 shows the number of driving axles and the locomotive class as a percentage of the total number of locomotives used in regular traffic by year. The figure includes all steam locomotives with tenders and electric/diesel locomotives with more than three driving axles. Motorised units are not represented in the figure.

Prior to 1900, locomotives had at most three driving axles, increasing to four at the turn of the century, five around 1930 and eventually six around the start of the second half of the previous century. The reason for increases in the number of driving axles during the railways' history relates to the demand for higher axle loads and train speeds. The maximum tractive effort a locomotive can generate to pull a set of wagons is limited by the friction force between the driving wheels and

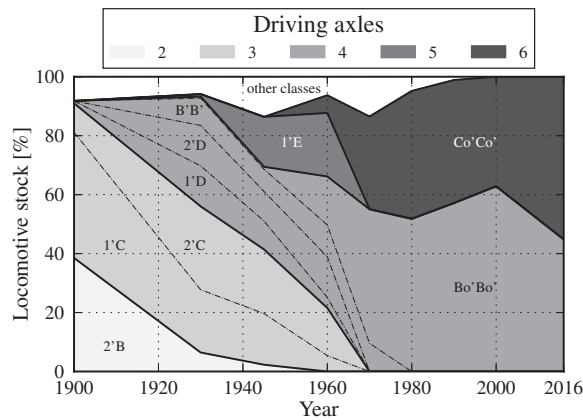


Figure 2.6: Axle arrangement and number of driving axles of locomotives used in regular traffic.


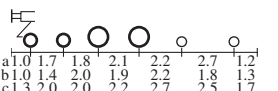
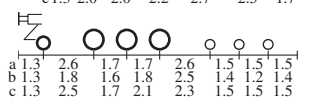
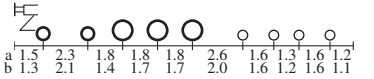
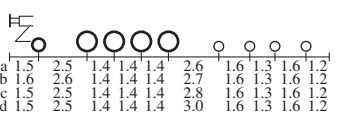
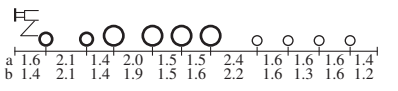
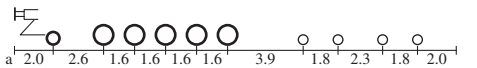
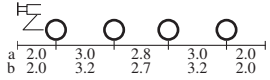
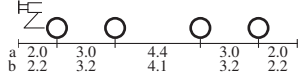

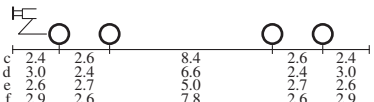
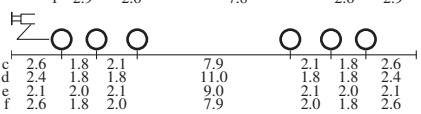
the rails. To increase the tractive effort of a locomotive, given the restriction on the permissible axle load on the track, it is necessary to increase the number of driving axles.

Figure 2.6 includes only steam locomotives with tenders, i.e., a locomotive connected to a wagon with a supply of fuel and water. Tender locomotives had a larger range and were the primary steam locomotive type used in regular traffic. Tank steam locomotives, on the other hand, were primarily used in shunting service, although some tank locomotives were also used in regular service trains, either as assistance locomotives on steep ascents or in local passenger traffic around major cities, with additional details on such uses provided in the following subsection on locomotive geometry. The majority of steam locomotives had one or two lead axles in addition to the driving axles. Electric and diesel power locomotives used in regular traffic featured four and six driving axles. The earliest electric locomotives had both leading and trailing axles; however, the modern electric and diesel locomotives are all without leading or trailing axles. In steam locomotives, the driving axles are in one group, while in electric and diesel locomotives, they are generally grouped into two bogies.

**Geometry** The geometry of Norwegian locomotives varies according to the locomotive's design. Table 2.2 shows the dimensions of locomotive classes identified in the previous section. Note that the steam tank locomotive, class 1'C1't, is also included, as it was used in local passenger trains around the larger cities [16] before multiple units took over the task as suburban trains.

Perhaps the overall greatest deviation in the dimensions of steam locomotives is

Table 2.2: Geometry of the most numerous locomotives of each class. Coverage indicates the percentage represented by the respective locomotives in the total number of locomotives of the class. The axle load column refers to the axle loads on the driving axles for each geometry (a-f). Figure 2.6 and table 2.3 provide information on time periods that the locomotives were operating within.

Class	Geometry	Coverage	Axle load (a/b/...)
Steam locomotives –1970			
1'C1't		43%	15
2'B-2		88%	10 / 7 / 11
1'C-3		90%	11 / 7 / 10
2'C-2'2'		83%	15 / 12
1'D-2'2'		87%	12 / 14 / 15 / 15
2'D-2'2'		100 %	15 / 12
1'E-2'2'		92%	15
Diesel/electric locomotives –1980			
B'B'		100 %	15 / 12
Bo'Bo'		94 %	16 / 18
Co'Co'		100 %	17 / 18
Diesel/electric locomotives 1980–			
Bo'Bo'		81 %	21 / 21 / 20 / 21
Co'Co'		92 %	20 / 21 / 21 / 19

○ lead/trail    ○ drive    ○ tender

observed in the smallest locomotives, i.e., class 2'B-2 and 1'C-3 locomotives. Such locomotives are the oldest representatives of a period when the standardisation across different lines was not yet implemented. The most significant deviations among the other steam locomotives are observed in the distances between different axle types, i.e., the distances between the leading wheel(s) and the driving wheels, and between the driving wheels and the tender wheels. The deviations in the distances between driving wheels is generally small.

Table 2.2 also shows that the driving axles on steam locomotives are in general more closely spaced than those on electric/diesel locomotives. Driving axles on steam engines are all coupled together, while those on electric and diesel locomotives are powered by at least two separate engines. A comparison of the 1'D-2'2' steam locomotive with the B'B' diesel/electric locomotive illustrates this point clearly, as the maximum distance between driving axles on the steam engine is 1.4 m, compared to the minimum distance of 3.0 m for the B'B electric and diesel/locomotives. The distributed load intensity for the steam locomotive may therefore be higher than that for the diesel/electric counterpart, even if the axle loads are lower.

The axle loads of the driving axles are also included in table 2.2. The axle loads of the lead/trail and tender axles of steam locomotives can generally be obtained from fig. 2.1c, i.e., the lead/trail and tender axle loads can be assumed to be 75 % of the driving axle load.

### 2.3.2 Geometry and design of wagons

The geometry of wagons is described by the distance from the buffer to wheelset centre  $a$ , the centre-centre distance between wheelsets  $b$ , and the distance between wheels in a bogie wheelset  $c$ , as shown in fig. 2.7. Figure 2.7 also shows the most common examples of wagon designs: two-axle wagons, (four-axle) bogie wagons and (six-axle) Jacobs bogie wagons.

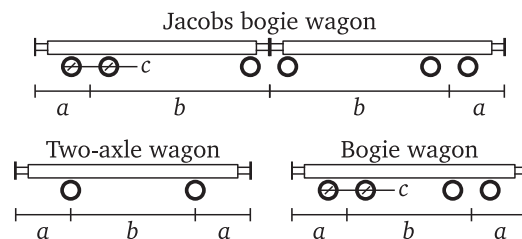


Figure 2.7: Geometry of two-axle wagons, bogie wagons and Jacobs bogie wagons.

### Freight wagons

**Design** Two-axle and bogie freight wagons have been in service throughout the history of the Norwegian railway network. The Jacobs bogie wagons did not join the rolling stock until the very end of the 20th century. Figure 2.8 shows the relative number of wagons of each design among freight wagons since 1900.

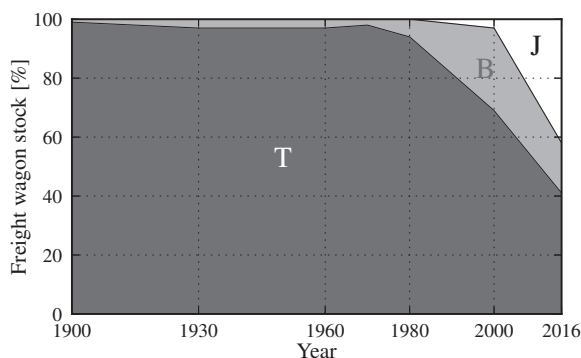


Figure 2.8: Shares of two-axle (T), bogie (B) and Jacobs bogie (J) freight wagons available in the rolling stock.

Between 1900 and 1970, the two-axle freight wagons dominated the rolling stock. Around 1970, flat bogie wagons were introduced for intermodal transport, i.e., semi-trailer and container transport. During the 80s, bogie wagons were also introduced for other types of freight transport, with approximately 30% of the rolling stock in 2000 being bogie wagons. In 1993, the Jacobs bogie wagon was introduced into the freight rolling stock, becoming popular quickly due to the possibility of carrying full length semi-trailers, as well as combinations of conventional-length containers. The current national vehicle register shows that approximately 40% of wagons are two-axle wagons, 20% are bogie wagons and 40% are Jacobs bogie wagons.

**Geometry** The right side of fig. 2.9 shows the geometry data for freight wagons. The total length  $L$  of wagons is across the buffers for two-axle and bogie wagons, in contrast to the end- to mid-buffer measurement for Jacobs wagons. In general, the maximum length of freight wagons increases over time. Comparison of the changes in the dimensions of two-axle wagons in fig. 2.9 to the evolution of axle loads in fig. 2.2a makes it possible to identify the introduction of new ‘generations’ of wagons around 1930, 1960 and 1980.

The changes in the dimensions of bogie and Jacobs bogie wagons are not as clear as those of two-axle wagons. This is likely explained by the primary freight



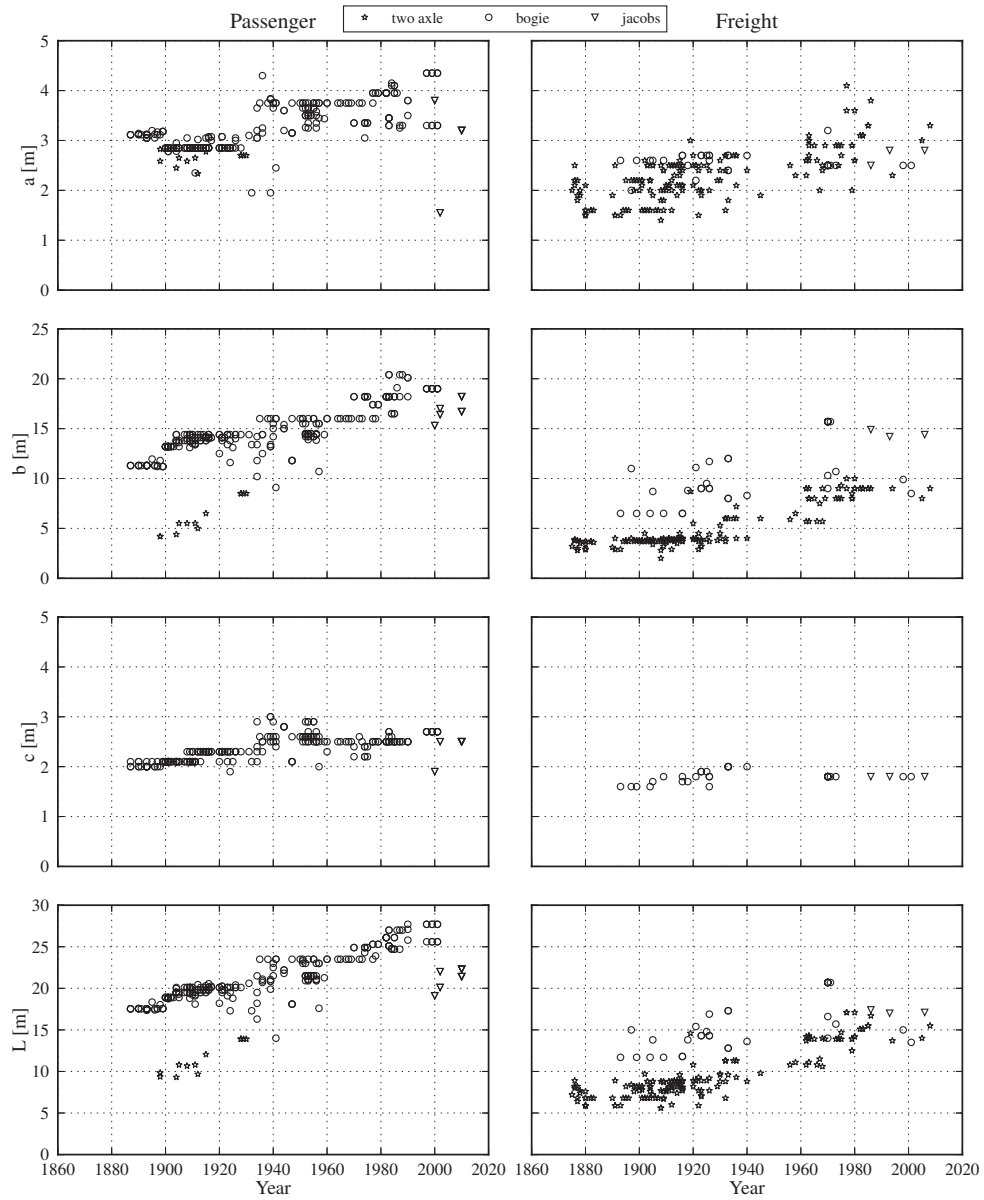


Figure 2.9: Geometry of passenger wagons and multiple units (left) and freight wagons (right).

type design being two-axle wagons prior to the introduction of standardised wagons by UIC in the 1960s. The bogie wagons were not developed and used in regular traffic and therefore were not as diversified as two-axle wagons.

Note that the buffer-wheelset distance  $a$  and the wheel distance  $c$  in a bogie for bogie and Jacobs bogie freight wagons remained unchanged for the last part of the previous century at  $a \approx 2.5$  m and  $c \approx 1.8$  m. As bogie and Jacobs wagons were not used extensively until the last part of the previous century, the geometry of such wagons can be considered to only vary with  $b$ .

Figure 2.10 shows the variables  $a$  and  $b$  for freight wagons. For two-axle wagons, there is a positive correlation between the two variables, i.e., an increasing  $b$  implies an accompanying increase of  $a$ . For bogie and Jacobs bogie wagons, there is no apparent correlation between these variables. Although not presented in any figure, the data show no clear correlation between  $a$  and  $c$  or between  $b$  and  $c$  for freight wagons.

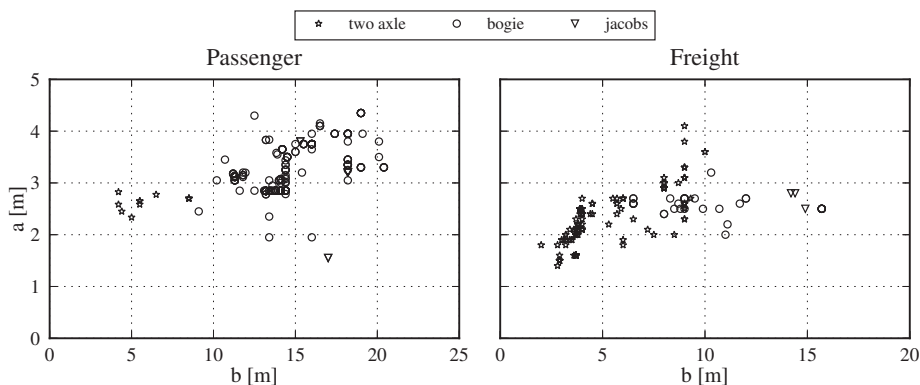


Figure 2.10: Geometric variables  $a$  and  $b$  for passenger wagons and multiple units (left) and freight wagons (right).

### Passenger wagons and multiple units

**Design** The designs of passenger wagons and multiple units have largely remained the same. Note that the motorised wagons of multiple units do not generally differ from non-motorised wagons. In 1903, two-axle and bogie wagons each constituted approximately one half of the available passenger rolling stock. This changed rapidly, with passenger wagons and multiple units in use after 1900 being almost exclusively four-axle bogie wagons. Compared to two-axle wagons, bogie wagons provide the passengers a smoother and more comfortable ride. Jacobs bogie wagons are found on the newest multiple units, i.e., multiple units introduced after

2003. The following discussion focuses on the bogie and Jacobs bogie wagons, as these are the wagons used for regular traffic. Data for two-axle wagons are, however, included in fig. 2.9 for completeness.

**Geometry** Figure 2.9 shows that the overall dimensions of passenger wagons and multiple units increased over time. There are several distinct steps in the evolution of the dimensions. The change around 1900 should be considered together with the increased axle loads of passenger wagons, as displayed by fig. 2.3a, and is likely to be due to an increase in permissible axle loads around 1900. A significant increase in dimensions can also be observed around 1930 due to a change from wood to steel for the material used to construct passenger wagons. Similar increases in  $a$ ,  $b$  and  $L$  can be observed around the mid-70s and 80s with the introduction of two entirely new classes of passenger wagons, NSB type 5 and 7. A part of the modernisation plan during the 60s, 70s and 80s involved increasing the overall speeds on train lines, again requiring the removal of small-radii curves and track profile that previously limited the wagon dimensions. Figure 2.10 shows no strong correlation between the geometric variables  $a$  and  $b$  for passenger wagons. Similar plots have been constructed for  $a - c$  plotted against  $b - c$ ; however, no correlation structure was observed.

## 2.4 Train geometry and composition

The particular composition of a train, i.e., the locomotive and the wagons, defines the distribution and magnitude of the load and has a large influence on the response history the train produces when it passes a bridge. This section presents the relevant data on the composition of trains.

### 2.4.1 Mixed train traffic

Trains can be categorised as passenger, freight or mixed trains. The latter consist of both passenger and freight wagons and have been used on lines with traffic volume too low to support passenger-only or freight-only trains. The use of mixed trains during the initial years after a line opened is a common feature of all lines.

The use of mixed trains was already limited in 1935, with only 6 % of the total train running distance performed by mixed trains [29]. The last mixed trains were in service until 1968 [91]. Mixed trains are unfit for both freight and passenger traffic, as their use places restrictions on the stopping frequency and loading time of freight and extends passengers' transit time. On any line with *significant* passenger or freight traffic, the mixed train type was abandoned in favour of freight-only and passenger-only trains. It is therefore reasonable to assume that a significant

portion of passenger and freight transport has been performed by passenger-only or freight-only trains throughout most of the railway history.

### 2.4.2 Train traction type

Figure 2.11 depicts the use of various types of tractive vehicles as a share of the total running distance of such vehicles. Data for the period after 1998 have not been obtained.

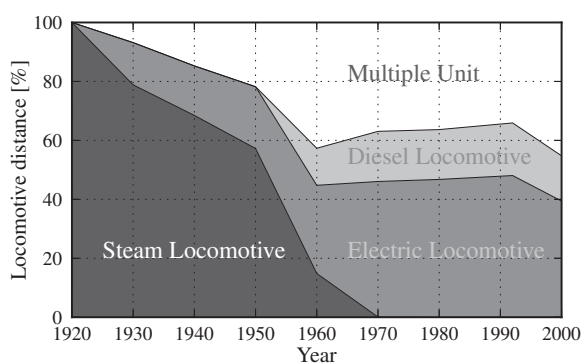


Figure 2.11: Various tractive types' shares of the total running distance.

The steam locomotive was the only type of tractive vehicle used in the Norwegian railway network until 1923 when electric locomotives were introduced. Electrification continued over the following decades until 1970, when Dovrebanen was fully electrified [9]. In 1954, diesel locomotives were put into regular service, while, at the same time, the rail administration officially abandoned the steam engine technology, with the last steam engine being decommissioned in 1971.

Multiple units were introduced around 1930 and quickly became an important part of the tractive vehicle stock, especially for local and shorter-distance passenger traffic. From 1960, multiple units were also used in regional trains and are currently important to both local and regional passenger traffic, with approximately 40 % of all tractive distance since 1960 being provided by multiple units.

### 2.4.3 Number of wagons in trains

The number of wagons in a train is governed by economic, practical and technical factors. Historic data on train (locomotive) running distance and axle running distance for passenger and freight wagons are available in Central Bureau of Statistics of Norway [29] and Norges Statsbaner [91, 92] for the period 1935–1998. An

estimate of the average number of axles in trains can therefore be obtained by dividing the axle running distance by the train running distance. Figure 2.12 shows the average number of axles estimated using the data obtained from the above source.

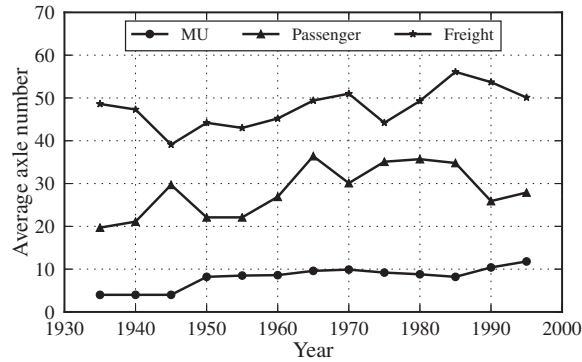


Figure 2.12: Average axle number in different train types.

The lengths of all train types tend to increase, with the freight trains having the most axles. The average number of axles of freight trains varied between 40 and 50 prior to 1980 and from 50-55 after 1980. As the majority of freight wagons prior to 1980 were two-axle freight wagons, as shown by fig. 2.8, the average number of wagons of freight trains has ranged between 20 and 25 two-axle wagons. The increase in the use of bogie wagons from around 1980 might also explain the increase in the number of axles after 1980. For the period 1980–2000, an estimate of the number of wagons can be obtained by assuming 80% two-axle wagons, 20% bogie wagons and 55 axles, resulting in an average of 21 wagons in freight trains. No data for the average number of axles are available for the period after 2000, while the composition of the available rolling stock changed significantly when Jacobs bogie wagons were introduced; however, as the average number of wagons during most of the railways' history has been in the range of 20–25, it is reasonable to assume that the average number of wagons in freight trains is presently similar. The average number of wagons in freight trains for the period after 1985 is therefore also in the range of 20 to 25.

Passenger trains and multiple units has generally been four-axle bogie wagons throughout the entire railways' history. Figure 2.12 indicates that passenger trains had close to 20 axles, or 5 wagons, prior to 1960. In the period between 1960 and 1985, the average number of axles on passenger trains was between 30 and 35, or approximately 8 wagons. After 1985, the average number of wagons decreased to approximately 7 wagons.

The average number of axles on multiple units has increased steadily from 4 in

the 1930s to 8 in 1950 and 12 in the 1990s, corresponding to one wagon prior to 1950, two wagons after 1950, and three wagons after 1990.

#### **Limits on the number of wagons in trains**

The lower limit on the number of wagons in a train is determined by the transport value of the goods being transported. The first multiple units consisted of a single wagon, while the current shortest multiple unit consists of only two wagons. Prior to multiple units, i.e., before 1930, locomotive-hauled passenger trains were used in suburban service; it is reasonable to assume that such suburban trains consisted of one or two passenger wagons when multiple unit length after 1930 is considered. Most multiple units could be joined together and driven in tandem, with the maximum length of multiple units therefore being twice the length of a multiple unit of the time. Furthermore, assuming that multiple units were used on lines with the lowest traffic intensity, the minimum number of wagons in locomotive-hauled passenger trains can be estimated by the maximum multiple unit length, i.e., 2 wagons during 1900–1960, 3 wagons during 1960–1985 and 5 wagons after 1985. The lower limit on freight wagons is more challenging to estimate due to a lack of relevant data; however, considering that the average number of freight wagons is three to four times the average number of passenger wagons, a minimum of 10 freight wagons can be assumed for freight trains throughout the railways' history.

The brake system, the capacity of coupling between wagons, the platform length at stations and the passing loop length of single-track lines all influence the maximum length of trains [54, 88], with all such factors considered in the following discussion of freight and passenger train length.

For passenger trains, the maximum number of axles has primarily been restricted by the braking capacity of the train. The maximum length due to brake conditions depends on the maximum allowable speed, with higher speeds demanding a stronger brake capacity. Passenger trains have during the history of railways been limited to approximately 80 axles, i.e., 20 four-axle bogie wagons, at a speed of 50 km/h.

For freight trains, the maximum train length has been approximately 50 wagons, as determined by the passing loop length of the track and the coupling capacity between the wagons in the train. Technically, neither factor can be considered to impose a strict or hard limit on the train length. For instance, the issue of coupling capacity between wagons can be mitigated by introducing an assistance locomotive at the middle or end of the train at the steepest ascents [88]. Similarly, the passing loop length only restricts the shorter passing train, i.e., the shorter train is diverted to the passing loop and waits until the longer train passes [54]. Practically, however, it is preferable to avoid the use of assistance locomotives due to the added cost of an extra locomotive and driver; additionally, factors other than

train length have to be considered when scheduling the use of passing loops, e.g., express passenger trains having a higher priority than freight trains such that the freight train must be diverted to the passing loop.

## 2.5 Discussion

### 2.5.1 Relevance of presented data to actual loads in the railway network

The data presented in this paper is largely based on the permissible loads on infrastructure and rolling stock. In theory, the permissible loads establish the bounds for the loads on the infrastructure. It is, however, important to acknowledge that the actual loads on the infrastructure may exceed these bounds.

The discrepancy between the actual loads and the permissible loads can only be determined by performing measurements on actual traffic. Unfortunately, such measurements are not available for the Norwegian railway network and they are also scarce in the international literature. One exception are axle load measurements reported by [67], which indicate that approximately 2.5% of all axles exceed the permissible axle load on a line with mixed passenger and freight traffic in the Swedish railway network. Obviously, these results are valid only to the traffic at the specific line and period of acquisition. On lines with system traffic, such as iron ore lines, one might also expect systematic overloading of wagons such that a much larger proportion of the axles exceed the permissible loads. Regardless of the proportion of axles that exceed the permissible loads, it is clear that permissible loads are exceeded by actual loads.

On the other hand, the consequences of significantly exceeding permissible loads on railways are severe. Failure of a bridge due to overloading of wagons or derailment of a train due to high speed are generally catastrophic in terms of human life and economic cost. It is therefore reasonable to assume that the maximum loads of actual traffic will be related to the permissible loads on rolling stock and infrastructure.

In any case, without actual load measurements or other available data, permissible loads are the best available estimators for the bounds on actual load conditions in the railway network.

### 2.5.2 Evolution of load conditions in the Norwegian railway network

Table 2.3 shows an overview of the data presented for the general railway network.

Table 2.3: Summary of data for the rolling stock and train composition during the history of the Norwegian railways.

Train composition					
Period	Train type	Locomotive / Motorised unit	Max speed	Wagon type	Number of wagons, $N$
-1900	LS	1'C1't	70 km/h	T+B	$\hat{N} = 1, N \in [1, 2]$
	P	2'B-2	70 km/h	T+B	$\hat{N} = 5, N \in [1, 20]$
	F	1'C-3	50 km/h	T	$\hat{N} = 20, N \in [10, 50]$
1900-30	LS	1'C1't	75 km/h	B	$\hat{N} = 1, N \in [1, 2]$
	P	2'B-2   2'C-2'2'   2'D-2'2'	90 km/h	B	$\hat{N} = 5, N \in [1, 20]$
	F	1'C-3   1'D-2'2'	65 km/h	T	$\hat{N} = 23, N \in [10, 50]$
1930-60	LS	B(13, 3.6, 15.0, 2.5)	90 km/h	B	$\hat{N} = 2, N \in [1, 4]$
	P	2'C-2'2'   2'D-2'2'   B'B'	90 km/h	B	$\hat{N} = 5, N \in [2, 20]$
	F	1'D-2'2'   1'E-2'2'   B'B'	65 km/h	T	$\hat{N} = 23, N \in [10, 50]$
1960-85	LS	B(16, 3.8, 16.0, 2.5)	120 km/h	B	$\hat{N} = 2, N \in [1, 4]$
	P	B'B'   Bo'Bo'[a-b]   Co'Co'[a-b]	120 km/h	B	$\hat{N} = 8, N \in [3, 20]$
	F	B'B'   Bo'Bo'[a-b]   Co'Co'[a-b]	80 km/h	T + B	$\hat{N} = 25, N \in [10, 50]$
1985-2000	LS	B(18, 3.8, 18.0, 2.6)	160 km/h	B	$\hat{N} = 3, N \in [2, 6]$
	P	Bo'Bo'[a-f]   Co'Co'[a-f]	160 km/h	B	$\hat{N} = 7, N \in [5, 20]$
	F	Bo'Bo'[a-f]   Co'Co'[a-f]	80 km/h	T + B	$\hat{N} = 25, N \in [10, 50]$
2000-	LS	B(18, 3.8, 18.0, 2.6)	160 km/h	B + J	$\hat{N} = 3, N \in [2, 6]$
	P	Bo'Bo'[c-f]   Co'Co'[c-f]	160 km/h	B + J	$\hat{N} = 7, N \in [5, 20]$
	F	Bo'Bo'[c-f]   Co'Co'[c-f]	90 km/h	T + B + J	$\hat{N} = 25, N \in [10, 50]$

B( $P$ ,  $a$ ,  $b$ ,  $c$ ) indicates a bogie wagon with axle load  $P$  and geometric parameters  $a$ ,  $b$ ,  $c$ ; see fig. 2.7.

$\hat{N}$  – Overall average number of wagons in a train.

LS – Local suburban, F – Freight and P – Passenger

Wagon load and geometry										
Type	Period	Axle load [tn]	Two-axle (T)		Bogie (B)			Jacobs (J)		
			a [m]	b[m]	a [m]	b [m]	c [m]	a [m]	b [m]	c [m]
Passenger	-1900	5.0-9.0	2.3-2.8	4.2	3.0-3.2	11.2-11.9	2.0-2.1	-	-	-
	1900-30	5.0-11.0	2.3-2.8	4.4-8.5	2.4-3.1	11.6-14.4	1.9-2.3	-	-	-
	1930-60	6.0-12.0	2.7	8.5	1.9-4.3	9.1-16.0	2.0-3.0	-	-	-
	1960-85	7.5-13.0	-	-	3.0-4.2	16.0-20.4	2.2-2.7	-	-	-
	1985-	8.5-14.0	-	-	3.2-4.3	16.5-20.4	2.5-2.7	1.6-5.6	15.3-18.2	2.5
Freight	-1900	2.3-9.0	1.5-2.5	2.5-4.0	2.0-2.6	6.5-11.0	1.6	-	-	-
	1900-30	3.0-12.0	1.5-2.5	2.5-5.0	2.2-2.7	6.5-11.5	1.6-1.9	-	-	-
	1930-60	3.7-15.0	1.5-3.0	3.5-7.0	2.4-2.7	8.0-12.0	2.0	-	-	-
	1960-85	5.0-20.0	2.0-4.1	5.5-9.0	2.5-3.2	9.0-15.7	1.8	-	-	-
	1985-	5.6-22.5	2.3-4.1	7.5-11.0	2.5	9.0-15.7	1.8	2.5-2.8	14.2-14.9	1.8

Axle loads are limited by the infrastructure for certain lines; see fig. 2.4



### **Load conditions due to infrastructure and rolling stock**

Comparing the maximum axle loads of locomotives, shown in fig. 2.1a, to permissible axle loads on a track, fig. 2.4, it is clear that the heaviest locomotives are limited to certain lines of the railway network during their respective periods of service.

Furthermore, a comparison of permissible axle loads and the axle load capacity of freight wagons shows that both factors have governed the limits on freight train axle loads. For instance, prior to 1930, several lines had permissible axle loads of 15 tn, as shown in fig. 2.4a, while the maximum axle load of freight wagons used in regular service was only 12 tn for most of the period, as shown in fig. 2.2a. On the other hand, fig. 2.4c shows that axle loads were track-limited to 18 tn for most of the railway network until 1984, while the capacity of freight wagons was at 20 tn since the beginning of 1960.

As the use of passenger wagons has not been restricted by the permissible axle loads on tracks, passenger wagons have been used freely in passenger trains. This freedom does not, however, extend to motorised wagons in multiple units, as certain motorised wagons have levels of axle loads comparable to those of locomotives. Multiple units are therefore also limited to certain lines due to the axle loads of motorised wagons.

Regarding the train speed, fig. 2.5 and table 2.1 show that the regulations of the infrastructure owner have limited the speed of both passenger and freight trains during most of the railways' history. Prior to 1950, no representative data on the speed limits on infrastructure has been found. During this period, the maximum speed of locomotives is suggested as the upper limit on the speed of passenger trains, i.e., 70 km/h until 1910 and 90 km/h after 1910. We take into account that locomotives used for freight trains have generally had smaller wheels than those used for passenger trains, i.e., freight locomotives run in a lower gear than passenger locomotives. The maximum speed of freight trains can be assumed at 50 km/h until 1910 and 65 km/h from 1910.

The capacities of both rolling stock and infrastructure influence the load conditions in a railway network and should therefore be considered when establishing a load model for service life assessment.

### **Differences between passenger and freight trains**

Section 2.2 showed that the axle loads of passenger wagons prior to 1900 were comparable in magnitude to those of freight wagons at 9 tn per axle; however, after 1900, the axle loads of freight wagons were considerably larger, with the difference between maximum axle loads of passenger and freight wagons continuing to grow during the railways' history. Figure 2.2c and fig. 2.3c show that the range of axle loads, i.e., the difference between the minimum and maximum axle loads, is much

smaller for passenger than for freight wagons. The magnitude and the variation of axle loads have therefore been smaller for passenger than for freight wagons.

The passenger wagons have a design and geometry different from those of freight wagons. Passenger trains have primarily consisted of bogie wagons, while freight trains have historically been composed of two-axle wagons and more recently a mix of all three designs. All dimensions,  $a$ ,  $b$ ,  $c$ , and  $L$ , are generally larger for passenger wagons than for freight wagons, i.e., the geometry of passenger wagons generally differs from that of freight wagons. The number of wagons in passenger trains has been lower than that in freight trains, while the speeds of passenger trains have been higher than those of freight trains.

The two types of trains also use different locomotives; although many locomotives have been used with both freight and passenger wagons, the locomotives used in the heaviest freight trains have generally had more driving axles than passenger locomotives. Typically, locomotives used in passenger trains have fewer driving axles due to a lower demand for tractive effort. Furthermore, passenger locomotives have favoured axle arrangements that allow higher speeds, e.g., steam locomotives with larger driving wheels and two leading axles for stability [16].

Since passenger and freight trains differ in axle loads, geometry, design and operation, the response in a structural detail from passenger trains will be different from the response from freight trains. The effect of the difference in response from the two train types on the fatigue damage introduced in the structure will depend on both the specific detail under investigation and the rolling stock of the period. First consider a structural detail with a relatively short influence length compared to the axle distance in wagons. This structural detail will be loaded and unloaded by each passing axle, and each axle introduces a stress range proportional in size to the axle load magnitude. A freight train will then tend to introduce more fatigue damage in this detail than a passenger train because of higher axle loads and axle count. Next consider fig. 2.13, which shows the moment at midspan of a simply supported beam with length 13 m to a sequence of freight and passenger wagons from the period 1930-60, see table 2.3.

This structural detail has a longer influence length that allow two bogies in adjacent passenger wagons to load the structure, but at the same time is shorter than the distance between bogies in one wagon. The structural detail is then loaded and completely unloaded, producing large loading cycles, for each adjacent bogie in the wagon sequence.

The two-axle freight wagons from this period cannot achieve the same stress range as the bogie passenger wagons for this structural detail. Although the two-axle wagons have higher axle loads, and four axles can load the structure at any one time, the axles are more spread apart such that the local load intensity is lower compared to the four axles from bogies in the passenger wagons. The freight wagons from this period will also never be able to completely unload the structure,

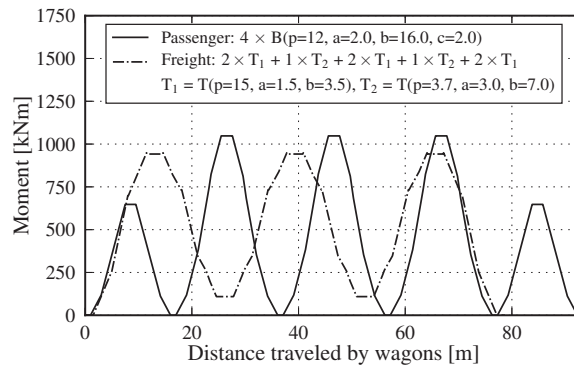


Figure 2.13: Bending moment at midspan of a simply supported beam with length 13 m to a sequence of wagons from the passenger and freight rolling stock 1930-60. B and T denotes bogie and two axle wagons, respectively.

because the longest distance between axles in these wagons is shorter than the influence length of the structure. The maximum stress range from freight traffic will therefore be smaller in magnitude than from passenger traffic for this period.

The number of cycles produced by the different wagon types is obviously linked with the number of wagons in the train, but from fig. 2.13 we see that each passenger wagon induces one cycle (ignoring boundary effects where only a single bogie loads the structure), while two freight wagons are necessary to load and one to unload the structure for a cycle. Taking into account that freight trains have more wagons than passenger wagons, one can estimate that the number of cycles introduced in this structural detail for the two train types are roughly equal. For this particular structural detail and period of rolling stock, the passenger trains will have a larger fatigue damage potential than the freight trains due to the difference in maximum stress range.

Admittedly, the possibility of passenger trains being more damaging than freight trains diminishes for modern trains where the difference in maximum axle load magnitudes are larger, but as a general rule, both passenger and freight traffic should be included in service life assessment due to the difference in axle load magnitudes, geometry, design and operation of these train types and how these parameters influence the response in different structural details.

### Changes in dynamic loads on bridges

The total load on the infrastructure from the rolling stock is comprised of a static, quasistatic and a dynamic part. The static loads are calculated with the static axle weights and the quasistatic load is determined by the static weight, speed of the

train and geometry of the track. The dynamic loads are due to impact forces at the wheel-rail interface, train-bridge interaction and dynamic characteristics of the rolling stock. The dynamic loads are more difficult to calculate than static and quasi-static loads due to mathematical complexity and random nature of the underlying processes. Dynamic loads are therefore typically included in service life assessment by applying a dynamic amplification factor (DAF) to the static loads [59, 104].

The train speed is a common variable for all dynamic effects and the dynamic loads generally increase with train speed. Section 2.2.5 showed that the train speed has increased over the history of the railways, and one might expect the dynamic forces on the infrastructure to increase as well, but this is not true in general. Steam locomotives has an additional vertical dynamic force known as ‘hammer blow’ that is not present in other rolling stock. Hammer blow is a vertical sinusoidal force that comes from mass added to the driving wheels to counterbalance moving mass (steam cylinders and connecting rods) in the horizontal direction of the locomotive. Hammer blow was studied in 1920s by the British railways and these studies concluded that hammer blow dominated the dynamic loads on bridges [53]. The American Railway Engineering Association (AREA) also investigated dynamic loads on steel bridges. Their work involved 37 bridges and 1800 diesel/electric and 3400 steam locomotive passages [7], and confirmed that dynamic amplification of stresses in bridges is higher from steam locomotives than other rolling stock. Historic steam locomotives may therefore have larger dynamic loads than modern rolling stock despite running at lower speeds.

The impact forces from the wheel-rail interface is governed by the unsprung mass of the wheelset and the continuity and smoothness of the contact surfaces. The evolution of wheelset mass for the different types of rolling stock has not been established for the Norwegian railway network due to lack of relevant data, but the international literature indicates that reducing the unsprung mass has been of increasing importance to researchers and manufacturers since the 1980s [66, 70]. Regardless of the wheelset mass, it is clear that the conditions at the contact surfaces have improved. Historically, rails produced in fixed lengths were joined together by fishplates at the web of the profile, forming a jointed rail [54]. The jointed rail surface is discontinuous and an impact is produced at the joint for each passing wheel. In 1966, welding was introduced as a joining technique in the Norwegian railway network, and the share of welded rail in the Norwegian railways was 20% in 1970, 60% in 1980 and by 1990 the majority of the railway network consisted of welded rail [89]. Welded rail result in a continuous rail surface with lower dynamic forces than the jointed track [36]. The discussion above indicates that the impact forces at the wheel-rail interface has been reduced in the last half of the 20th century through reduced unsprung mass and continuous welded rails.

With regard to practical applications, there are several sources that propose DAFs for service life assessment of steel railway bridges with respect to fatigue

damage, see [60] for an overview. To specifically include the effect of hammer blow in the service life assessment, the reader might consider [8], which presents DAFs for steam locomotives and other rolling stock based on the AREA tests made during the 1950s [7].

### **Influence of historic loads on the service life estimation of bridges**

The load conditions in the Norwegian railway network have generally been characterised by increasing axle loads, train speeds, number of wagons in trains and rolling stock geometry throughout the history of the railway. For many structural details, this means that historic loads can be ignored due to the increased load conditions of modern traffic. For instance, the structural detail with a short influence length and high sensitivity to axle load magnitude discussed in section 2.5.2 will be dominated by fatigue damage from modern traffic due to higher axle load. It is however important to note that such an observation does not hold in general. The proportion of fatigue damage that comes from historic traffic compared to more modern traffic will depend on the detail under investigation, the rolling stock and the amount of traffic in each period. The significance of historic loads will therefore vary from case to case.

One aspect of the loading that has not generally increased is the distributed loading on rolling stock. Section 2.2.1 showed that the distributed loading across buffers was highest for steam locomotives in service in the middle of the previous century, with section 2.3.1 confirming that older steam locomotives had a higher local load intensities than more modern locomotives. Considering the static response in the simply supported beam in fig. 2.13 for instance, several of the steam locomotives have higher maximum stress range than any of the modern electric and diesel locomotives in table 2.2. It should also be noted that the dynamic loads from steam locomotives are generally larger than for other locomotives, see discussion in section 2.5.2.

Furthermore, the distributed loading on passenger wagons have remained relatively constant over the history of the railways, see section 2.2.3. Historic passenger trains may therefore be more damaging than modern passenger trains for structural details that are responsive to distributed loading rather than axle load magnitudes, due to the higher distributed and dynamic loading of steam locomotives. The distributed loading on freight wagons has increased in stages and one might not expect that historic freight trains are more damaging than the modern freight trains, but the stress range induced by the locomotive might mitigate this increase such that historic loads contribute significantly to the fatigue damage.

Since historic loads may have a significant influence on the fatigue damage of railway bridges, and the influence vary from case to case depending on the structural detail, rolling stock and amount of traffic, the historic loads should generally

be included in service life estimation of railway bridges.

### 2.5.3 Nature of the presented data

The data presented in this paper have been derived from sources that consider the railway domain as a whole. For many of the variables, only the limits on variables affecting the train loading have been presented. When available, the relative frequencies for load conditions are also provided, e.g., the design of locomotives and wagons. Having more information and data will clearly yield more accurate service life estimates of bridge details. Ideally, the distribution of variables defining the load conditions at a bridge should be known so that a probabilistic or rational deterministic analysis can be performed.

The challenge posed by the available data for railway loadings is that we cannot readily link the relative frequency of a variable defined for the rolling stock to the probability distribution of such rolling stock being used at a particular bridge. To illustrate this point, consider the traffic at an arbitrary bridge in the year 2000. Figure 2.8 shows that among the freight wagons available at the time, approximately 68% were two-axle wagons, 30% bogie wagons and 2% Jacobs bogie wagons. One might assume that the relative frequencies of two-axle, bogie and Jacobs wagons at the bridge follow the distribution of the rolling stock as a whole. It is, however, entirely possible that all freight wagons that pass the bridge are Jacobs bogie wagons. In the year 2000, there were approximately 100 Jacobs bogie wagons available in the rolling stock; four individual trains, each with 25 Jacobs bogie wagons, could be composed using these wagons. The four trains might also be the only freight traffic that pass the bridge, i.e., each train might pass the bridge multiple times a day, depending on the transport distance required by the train. In short, the trains that pass a certain bridge in the railway network are assembled from a subset of the population presented in this paper.

#### **Can the distribution of variables defining the load conditions for a particular bridge be obtained?**

In principle, the distribution can be determined if the infrastructure owner and/or operator have recorded and archived the appropriate data for the variable and the bridge. In the case of the Norwegian railway, a tremendous quantity of documentation that *might* contain the information needed to determine the variables' distributions is in fact stored at the railway museums and the national archives. For instance, while research was being performed for this paper, documentation on the exact composition of trains, i.e., the specific locomotive, the set of wagons and the number of trains each day, was obtained for certain bridges and periods. Using such data, it is possible to construct the distribution of locomotive and wagon variables for the particular bridge and period.

Unfortunately, most historic documentation is not easily accessible in the sense of not having been digitised; additionally, a given piece of data is typically not specifically obtained from a single data source, i.e., the data are spread across several documents or even archives. Extracting more precise data than what is already presented in this paper, e.g., determining the distribution of each variable, is therefore resource intensive. Although a substantial quantity of documentation exists that might contain the appropriate data to determine the distribution of a variable, one must also be ready to accept that certain information was never recorded. It might therefore be possible to obtain the distribution of each variable; however, additional resources will generally be required to do so for each specific bridge.

In conclusion, the data presented in this paper can define the set of possible values of the load variables for a specific bridge; however, the data cannot be used to establish a precise probabilistic description of the load conditions at a bridge. From a probabilistic perspective the data is characterised as *imprecise* [14, 56].

#### 2.5.4 Use of imprecise data in service life estimation

The service life estimation of a bridge is generally based on a numerical model to predict the response and relevant damage mechanism for the structure. The input variables of such numerical models are all uncertain; service life estimations are based on mathematical frameworks that consider such uncertainty. The way uncertainty is handled is different within each framework and not all frameworks are equally suited for handling imprecise data of the type presented in this paper.

A deterministic analysis generally relies on selecting point estimates for input variables. The point estimates are selected to produce a conservative end result, either by selecting the values directly or by combining nominal values with safety factors. Generally, the probabilistic and non-probabilistic information are treated the same way by selecting the ‘worst’ values. The deterministic approach does not consider the information available for probabilistic variables and typically leads to conclusions that the detail should have failed a long time ago, i.e., overly conservative results are obtained.

The traditional reliability framework incorporates more information than deterministic point estimate values of a variable and requires that the distributions of variables be known. In comparison to the deterministic approach described above, such an approach leads to more realistic results, with the probability of failure determined by including the uncertainty in the input variables during the analysis. The interval variables presented in this paper cannot be incorporated in the traditional reliability analysis without making assumptions about the distribution of the variables over the intervals.

The framework of imprecise probabilities can incorporate both probabilistic and non-probabilistic information [14]. Imprecise probabilities will therefore be less

conservative than a deterministic approach, as probabilistic variables can be handled in a more rational way than simply assuming the worst case. Furthermore, the framework does not require assumptions, as is the case for traditional reliability analysis, since knowledge of the distributions of the variables is not needed.

Imprecise probabilities does not change the fact that available data is imprecise, and does not enable precise determination of the remaining service life of a structure. From the perspective of bridge owners, imprecise probabilities still have practical advantages in comparison to the established frameworks. In cases where the deterministic analysis proves too conservative, the imprecise probability framework may be applied to show that the structure has sufficient remaining service life since the incorporation of available data leads to less conservative results. Compared to the traditional reliability framework, imprecise probabilities make it easier to communicate the consequence of the imprecise data, since the imprecisions are explicitly expressed in the results of the analysis instead of being expressed through the assumptions made about the data [10].

The imprecise probability theory has been applied in reliability analysis to problems with imprecise knowledge [14, 56]; however, there are currently no studies in the literature that apply imprecise probabilities to service life estimation of railway bridges. Demonstrating the use of this framework is outside the scope of the present paper; future work should focus on adapting the methodology to service life estimation of railway bridges due to the nature of available data for such assessments.

In addition to service life estimation, imprecise data can be used in a sensitivity analysis to pinpoint the most important variables affecting the estimated service life. The sensitivity analysis can then be used to identify the variable that should be focused on in further data gathering. A starting point for the sensitivity analysis of imprecise data may be found in [51, 93].

In conclusion, the imprecise data presented in this paper can be used in estimating the remaining service life of a bridge by adopting an imprecise probability framework and in a sensitivity analysis to guide further data gathering and assess the possibility of reducing the uncertainty associated with the estimated service life.

### **2.5.5 Relevance of findings and discussion to foreign railways**

This paper has focused on the evolution of the load conditions and available data for the Norwegian railways. The rolling stock and infrastructure are undoubtedly adapted to Norwegian conditions, with the country's particular topology and climate. Much of the rolling stock has been produced by Norwegian manufacturers, while the infrastructure has been managed and maintained by the Norwegian national railway administration throughout the history of the railways.



It is, however, important to note that the design of the Norwegian rolling stock and infrastructure has been heavily influenced by foreign engineers and practices. For instance, the majority of locomotives have been built by Norwegian manufacturers under licenses from foreign factories, e.g., factories in Sweden, Germany, Switzerland, Britain and the USA [9, 16]. Similarly, the railway infrastructure was built or supervised by English and German companies, while the modernisation of the railways was performed while consulting foreign railway experts [58]. International standardisation, e.g., of freight wagons by UIC, as discussed in section 2.2, and privatisation of the railway infrastructure and operations at the end of the previous century have ensured that the technology of rolling stock and infrastructure were similar across countries during much of the railways' history. A foreign reader may therefore adapt and extend the data presented for the Norwegian conditions by performing a less extensive investigation of available information for railways in another country.

Furthermore, imprecise and missing data for loads in the assessment of the service life of existing structures is a general problem [84]. The need for the simplified equivalent load model [1, 116] and its use [101], as well as the assumptions made in the development of the British historic load model [59, 60], all indicate that information relevant to establishing the distributions of variables for specific bridges is costly to obtain or not available at all for railways outside of Norway.

## 2.6 Conclusions

Data on the geometry, design and axle loads of the rolling stock, together with data on the composition and operation of trains throughout the history of the Norwegian railways, have been presented in this paper.

The data show that the maximum axle loads and geometry of locomotives and freight and passenger wagons, as well as train speeds and the number of wagons in trains, have generally increased during the railways' history. Historic loads may however be more damaging than modern traffic for certain structural details. The capacities of both rolling stock and infrastructure influence the load conditions in a railway network. Passenger trains generally differ from freight trains, not only in axle loads but also in geometry, design and operation. As the influence of the geometry, design and operation of passing trains on the response of a structure depends on the specific detail being examined, both passenger traffic and freight traffic over the railways' history should be considered in a service life assessment.

The data for historic railway loads are imprecise, i.e., the probability distribution of variables is generally unknown for a particular bridge. The possibility of obtaining the distribution of variables has been discussed, and although it might be possible to determine the distribution for certain variables and bridges, one must accept that determining the distribution is not possible in the general case. Fu-

ture work should therefore adapt the mathematical framework of imprecise probabilities to service life estimation of railway bridges to incorporate the available information and improve the accuracy of service life estimates.



## Chapter 3

# Finding the train composition causing greatest fatigue damage in railway bridges

Gunnstein T. Frøseth and Anders Rönnquist,  
*Submitted for journal publication 2018.*

### Abstract

This paper presents a method to identify the most damaging train with respect to fatigue damage in railway bridges. The problem is formulated as a combinatorial optimization problem in which the solution space is the set of possible trains. The exact solution can only be obtained for trivial cases where the train set is small and/or for simple structural details where the most damaging train can be identified manually by analysis. Three different heuristics are considered to solve the problem approximately. The Late Acceptance Hill Climbing heuristic is proposed as a general approach to finding the most damaging train due to its strong performance for different train sets and structural details and simplicity in implementation and application. The proposed methodology can be used in the design of new and in the assessment of existing railway bridges to verify sufficient fatigue endurance.

### 3.1 Introduction

Deterioration of existing infrastructure is of primary concern for countries around the world. Bridges are essential components of the infrastructure that generally have a very long service life. A large portion of the railway bridges in developed

countries, constructed during the large building boom at the beginning of the 20th century, are reaching and exceeding their intended design life [117]. Infrastructure owners manage limited resources for renewal and maintenance of the infrastructure by inspecting the infrastructure components and estimating their remaining service life. Inspections are made to ensure the short-term safe operation of the infrastructure, and service life estimations are performed to keep track of future needs for investments and maintenance.

A large portion of the existing railway bridges are steel bridges, and the primary deterioration mechanism in steel bridges is material fatigue [117]. The fatigue damage mechanism is dependent on the loading history of the material and therefore on the historic loads on the railway infrastructure. A description of the historic railway loads is therefore necessary to predict the remaining service life of railway bridges. Ideally, the exact composition of locomotives and wagons and the loads on each axle of the train should be known for all passages of the bridge. Alternatively, a statistical description of the traffic and rolling stock, i.e., the probability distribution and mass functions of axle loads, locomotives and wagons passing the bridge, can also yield an accurate description of the load conditions and fatigue damage in the bridge within a reliability framework. Unfortunately, neither exact nor statistical historic railway loading data are generally available for use in fatigue assessment of bridges. The lack of data availability arises because the data were never recorded, the data have been lost since their acquisition or the time constraints of a specific project do not permit locating the data [84]. More commonly, the load conditions at a site are known in an *imprecise* sense [42], i.e., the locomotives and wagons present in the rolling stock at a certain time are known, but the specific compositions of the locomotive and wagons in trains that pass the particular bridge cannot be established.

Imprecise data therefore define the domain of the loading variables for fatigue loading at a particular bridge site, and through modeling of the fatigue damage mechanism, they also define the domain of the fatigue damage induced by traffic in a structural detail. With regard to service life estimation of bridges, this means that the imprecise data for traffic loads can be used to determine the minimum and maximum fatigue damage induced in the bridge by the traffic of a particular period. Knowing the minimum and maximum damage induced in a structural detail for a certain period has great practical value to infrastructure owners and practicing engineers for several reasons. First, one can determine whether fatigue is a relevant damage mechanism for a bridge detail. Second, if fatigue is a relevant damage mechanism, then knowledge about the maximum fatigue damage for each period can be used to direct further data gathering in the most cost effective and efficient manner, e.g., prioritizing the search for those periods with maximum damage. Traffic loads have changed significantly over the history of the railways [42, 53], which means that traffic from certain periods can likely be ignored because it induced neg-

ligible fatigue damage in the structural detail compared to the traffic from another period. Finally, service life assessment of railway bridges is generally conducted by applying simplified load models meant to represent the traffic over the history of the railways [1, 60]. The load models consist of a few trains for each period selected by a group of experts from historical records [61]. These simplified load models may yield reasonable and conservative service life estimates for some structural details and bridge sites. There is, however, a risk that load models based on a few select trains are biased in identifying damage in one particular group of bridge details, i.e., the load model introduces systematic error and bias into the estimated service life of bridge components. Identifying the maximum damage induced by the rolling stock for each bridge detail avoids this systematic error and therefore allows better management of the infrastructure.

It is possible to manually identify the train composition that maximizes the fatigue damage in the structural detail via analysis and trial and error; see, e.g., Imam and Salter [59] and Frøseth and Rönquist [42]. This manual approach is both difficult and time consuming for cases with complex influence lines and multiple periods with different locomotives and wagons. To be able to utilize the available data on traffic for the large number of different structural details in bridges, it is necessary to employ computers to identify the most damaging train for each structural detail. There are currently no methods in the literature that solve the problem of finding the most damaging train with respect to fatigue damage in railway bridges.

This paper proposes a method to find the train that maximizes the fatigue damage in an arbitrary structural detail. The problem is formulated as a combinatorial optimization problem with the objective of maximizing fatigue damage in a structural detail due to train passage. The solution space is represented by a train set, established from locomotives and wagons available in the rolling stock for the railways in the specific period. The train set is generally too large to solve the problem exactly, and three different search heuristics are considered to solve the problem approximately. The search heuristics are evaluated by considering forty different structural details and two different train sets.

The outline of this paper is as follows: The theory behind the fatigue damage model and response generation for train passage by an influence line (IL) is given in section 3.2. The formulation, notation and optimization problem are given in section 3.3, and the approaches to solve the optimization problem are discussed in section 3.4. Section 3.5 presents ILs and train sets used to evaluate the heuristics and examples with an application of the different heuristics to find the most damaging train for the different train sets and structural details. Section 3.6 provides a discussion of the results, suggestions for selection of the train sets and the use of the heuristics.

## 3.2 Theory

### 3.2.1 Fatigue damage

Fatigue in steel structures is a damage mechanism in which cracks initiate and propagate under cyclic stress. The fatigue endurance of a material or structural detail is determined by a fatigue endurance law. Basquin's relation is expressed as the number of cycles  $N$  a material can endure at cyclic stress  $S$ , i.e.,

$$N(S) = CS^{-m} \quad (3.1)$$

where  $C$  and  $m$  are the fatigue resistance parameters. Bridges are subjected to loads that induce varying stress histories and therefore stress ranges of varying amplitude. To account for the varying stress ranges, Miner's linear damage accumulation rule states that the fatigue damage from each stress range  $S_i$  yields fatigue damage equal to  $D_i = \frac{1}{N(S_i)}$  and that the total fatigue damage from a stress range spectrum is determined by the sum of the damage contributions from each of them. Combining Miner's linear damage accumulation rule with Basquin's relation eq. (3.1) yields

$$D = \frac{1}{C} \sum S_i^m \quad (3.2)$$

where the fatigue stress ranges  $S_i$  can be extracted from an arbitrary stress history by cycle counting. Rainflow cycle counting is the *de facto standard* method for cycle counting in service life estimation of bridges [28, 61, 78], and the implementation in [5] is adopted herein.

Further simplification of the fatigue damage can be made when the purpose is to find the most damaging train. The material parameter  $m$  is commonly assumed to be deterministic [63, 75], with a value of  $m = 5$  for a single slope fatigue endurance law [119]. The material parameter  $C$  only scales the fatigue damage; therefore, for the purpose of comparing fatigue damage due to different trains, the pseudo-damage  $d$  can be defined:

$$d = CD = \sum S_i^5 \quad (3.3)$$

Finding the most damaging train is therefore an optimization problem where the objective is to find the train composition that maximizes the pseudo-damage in eq. (3.3).

Note that other definitions of the fatigue endurance, e.g., the tri-linear fatigue endurance model [28], and damage accumulation rules, e.g., a sequential damage accumulation rule [112], can be easily adapted to the methodology presented in this paper.

### 3.2.2 Response generation by influence lines

Liu et al. [79] demonstrated that fatigue analysis utilizing a static solution method with a dynamic amplification factor yielded similar results to a full dynamic analysis except for the case in which the geometry and speed of the train imposed resonance loading on the structure. In practice, such conditions are only likely for high speed lines. Static analysis is therefore generally sufficient for fatigue assessment of existing railway bridges. Static analysis by the IL approach is most commonly used to predict the stress histories in evaluations of existing railway bridges [32, 33, 59, 61, 62].

An IL  $l(x)$  is the response of a structure of some measurable quantity to a unit load located at  $x$ ; see fig. 3.1a. In practice, the IL can be obtained either numerically [15, 30, 68, 95] or from measurements of real structures [47, 94].

The load is defined by a load function  $f(x)$ , and for a train, the load function is defined by

$$f(x) = \sum_{i=1}^{N_p} p_j \delta(x - x_j) \quad (3.4)$$

where  $\delta(x)$  is the Dirac delta function,  $N_p$  is the number of axles,  $p_j$  are the axle load magnitudes, and  $x_j$  are the axle load positions; see fig. 3.1b.

The static response  $z_s(u)$  of the structure is then a convolution of the load function  $f(x)$  and the IL  $l(x)$ :

$$z_s(u) = (f * l)(u) = \sum_{j=1}^{N_p} p_j l(u - x_j) \quad (3.5)$$

where  $u$  is the shift variable, i.e., the distance the load is shifted along the load path of the IL.

The dynamic response is determined by applying a dynamic amplification factor  $\Phi$  to the static response; see Imam et al. [60] for a thorough discussion on the topic. In the present paper, the dynamic load effect is adapted from CEN/TC250 [27] for fatigue loads, which is determined by train speed  $v$  and IL length  $L_\Phi$ , i.e.,

$$\phi = \phi(v, L_\Phi) \quad (3.6)$$

The dynamic response  $z(u)$  is then obtained by multiplying the static response by a dynamic amplification factor,  $\Phi = 1 + \phi(v, L_\Phi)$ , i.e.,

$$z(u) = \Phi z_s(u) \quad (3.7)$$



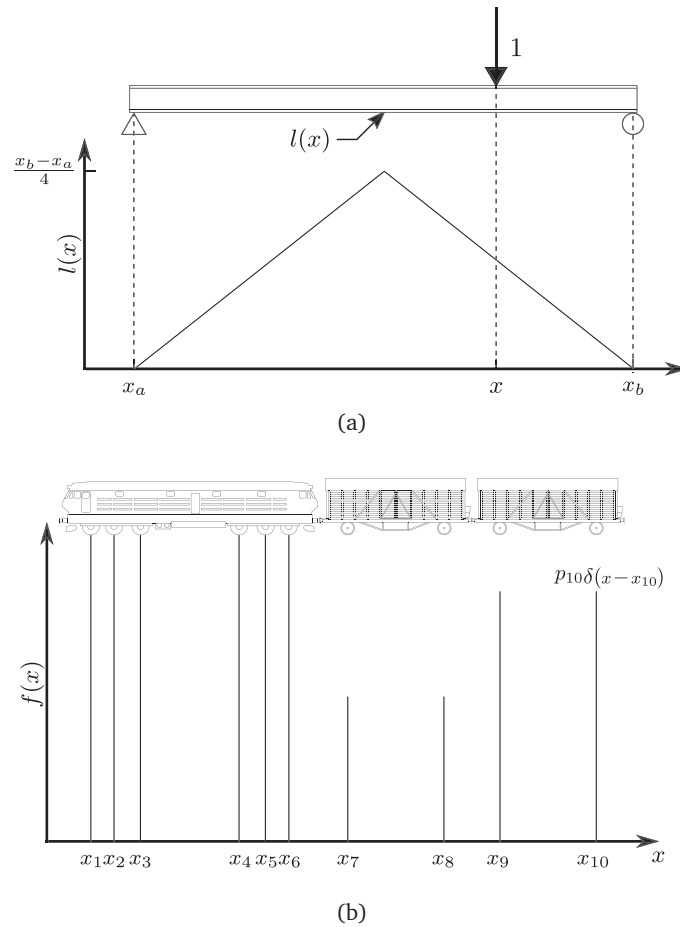


Figure 3.1: (a) illustrates the influence line for the moment in the midspan of a simply supported beam. The coordinate  $x$  defines the position of the unit load. (b) shows an example of a load function eq. (3.4) for a train.

### 3.3 Formulation, notation and problem statement

#### 3.3.1 Trains, locomotives and wagons instead of axle position and load magnitudes

The problem is simple: determine the train that produces the most fatigue damage in a structural detail when it crosses the structure.

The unknowns related to finding the fatigue damage are  $x_j$  and  $p_j$  from eq. (3.5) and  $v$  from eq. (3.6).

These unknowns are subject to constraints from reality, which limit the pos-

sible load functions  $f(x)$ . If these constraints are not properly described and incorporated into the solution process, then we risk identifying a function  $f(x)$  that maximizes the fatigue damage rather than *the train* with load function  $f(x)$  that maximizes the fatigue damage.

Unfortunately, the constraints are awkward to describe in terms of axle position  $x_j$  and load magnitude  $p_j$ . Considering fig. 3.1b, the constraints on the distance between the axles between two wagons (e.g.,  $x_9 - x_8$ ) is different from the constraints on the axle distance within a wagon (e.g.,  $x_8 - x_7$ ) or between axles in a bogie of a locomotive (e.g.,  $x_6 - x_5$ ). The issue becomes even more challenging when different locomotive and wagon designs are introduced, e.g., four axle wagons or locomotives, and when the number of wagons vary. Formulating the problem by axle positions and axle load magnitudes therefore means that our optimization problem changes during the solution process, as the number of parameters and their constraints will be altered as the solution space is explored.

It is easier to describe and implement the load function and the relevant constraints properly if they are directly related to their parent objects, i.e., a train is defined by locomotives and wagons instead of axle magnitudes and axle positions. The notation and definitions of trains, locomotives and wagons are therefore introduced below to break down and concisely describe the problem. The notation will also aid in describing our approach to solving the problem and analyzing the results.

### 3.3.2 Notation, solution space and problem statement

A train  $T$  is an element of the train set  $\mathcal{T}$  and consists of a locomotive  $L$  and  $N \in \mathbb{N}[N^\downarrow, N^\uparrow]$  wagons  $W_1, W_2, \dots, W_N$ . Each locomotive  $L$  drives the train at speed  $v \in \mathbb{R}[v^\downarrow, v^\uparrow]$  and is an element of the locomotive set  $\mathcal{L}$ . Each wagon  $W$  has a varying axle load  $p \in \mathbb{R}[p^\downarrow, p^\uparrow]$  and is an element of the wagon set  $\mathcal{W}$ . The wagon set is sampled with replacement, i.e., a train can consist of multiple instances of the same wagon.

Train  $T$  has a load function  $f(x; T)$  and speed  $v$  that can be used to generate the response  $z(u; T)$  via eq. (3.7). The fatigue damage  $d(T)$  produced by train  $T$  can be determined from the response  $z(u; T)$  by extracting the stress cycles in accordance with section 3.2.1 and by applying eq. (3.3). Furthermore, the number of elements (cardinality) of a set  $\mathcal{S}$  is denoted by  $|\mathcal{S}|$ .

Finding the most damaging train is an optimization problem in which the set of possible trains  $\mathcal{T}$  is searched to find the train  $T^*$  that maximizes the fatigue damage  $d$ , i.e.,

$$T^* = \arg \max_{T \in \mathcal{T}} d(T) \quad (3.8)$$

### 3.4 Solving the problem – Finding the most damaging train

This section considers exact methods and approximate methods, i.e., heuristics, to identify the most damaging train. The purpose is to establish a general approach that is independent of the train set and the IL.

#### 3.4.1 Exact solution

The exact solution can be obtained by checking the fatigue damage introduced by every train in the train set. The most efficient way to do this is by checking each train once, i.e., each train is enumerated or marked and checked against the objective function. Unfortunately, enumerating the solution space is only possible in trivial cases where the train set is small. The number of different trains with  $N$  wagons is  $|\mathcal{L}| \cdot |\mathcal{W}|^N$  (the wagons can be selected from the wagon set with repetition). The size of the train set is therefore

$$|\mathcal{T}| = |\mathcal{L}| \sum_{N=N^\downarrow}^{N^\uparrow} |\mathcal{W}|^N \geq |\mathcal{W}|^{N^\uparrow} \quad (3.9)$$

that is, at least in the same order of magnitude as the maximum number of wagons in a train. For comparison, Norwegian freight trains in regular traffic have on average approximately 20 wagons [42]. Solving eq. (3.8) by exploring the entire solution space is infeasible since modern CPUs can perform on the order of  $\approx 10^{10}$  operations per second, and the number of operations necessary to evaluate eq. (3.8) is much greater than one. Alternative and approximate methods must therefore be adapted to solve eq. (3.8) in a reasonable time.

#### 3.4.2 Approximate solution

Skiena [113] suggests three different search strategies that can be used to obtain an approximate solution for the combinatorial optimization problem in eq. (3.8): random sampling, local search and a meta-heuristic that combines the two. In the following subsections, these strategies are discussed in relation to our specific problem.

##### Random sampling

The simplest approach to solving eq. (3.8) is to perform random sampling (RS) of the solution space. This heuristic proceeds as follows: randomly sample trains from the solution space  $\mathcal{T}$ , and select the train  $T_{\max}$  that introduces the highest fatigue damage as an approximation to the most damaging train  $T^* \approx T_{\max}$ .

How well RS performs depends on the probability of drawing the most damaging train from the train set. We have already argued that the train set is unduly large for the general case, but how many acceptable solutions are there in the train set? This depends on the structural detail under investigation and the train set itself. Consider the IL shown in fig. 3.1a, and let the support of the function be shorter than any of the axle distances of trains in the train set such that the structure is only loaded by a single axle at any one time. The most damaging train  $T^*$  will then have the highest number of axles possible and each axle maximally loaded. Any combination of wagons from the wagon set with maximum axle load and maximum number of axles is then an optimum train. In this case, the number of optimal trains is large. On the other hand, in cases with longer and more complicated ILs and more diverse wagon and train sets, where both the geometry and load magnitudes are important, there might be only one optimal train in the entire train set.

For the general case, the probability of drawing the optimal train by RS is therefore as low as  $p \leq \frac{1}{|W|N^T}$ , i.e., this process is slower than direct enumeration of the solution space. Due to the simplicity of RS and the fact that it is not obvious how many optimal trains there are in a typical train set, RS is applied to an example in section 3.5 to confirm the analysis above and to provide a reference for the performance of the other approximate methods presented below.

### Hill Climbing

The previous sections concluded that an exhaustive search of the solution space is infeasible and that finding the optimal train by random sampling is unlikely for the general case. Hill climbing (HC) is a *local search* strategy that focuses on improving a given solution by searching around the currently best known solution in the solution space.

For our application, the local search is performed by considering the *neighbor train*. The neighbor train is obtained by performing one of the four following operations on the train: *swap locomotive*, *swap wagon*, *insert wagon* or *remove wagon*.

The HC heuristic is similar to RS, but instead of comparing a randomly selected train from the train set to the best known solution  $T_{\max}$ , a neighbor  $T = \text{neighbor}(T_{\max})$  is compared against the best known solution. If  $d(T) \geq d(T_{\max})$ , then the neighbor is accepted as the new best known solution, and the search continues from there.

Local search heuristics generally outperform random sampling heuristics if the solution space is coherent [113], i.e., if a better solution can be expected to lead us in the direction of the best solution. We will show by example that the problem of finding the most damaging train is coherent, and the neighbor and neighborhood of the optimal train will generally be more damaging than a random train in the

train set.

Hill Climbing performs best in cases where the solution space is convex, meaning that there is only one optimum, and moving “uphill” will eventually lead us to the top. The fact that HC only allows accepting better solutions is an issue if the solution space contains local maxima. HC will then find an optimum depending on the initial starting point in the solution space but generally not the true global optimum.

Again, the solution space in the problem in eq. (3.8) changes depending on the specific train set and IL. Generally, there are several local maxima present in the solution space, and the HC heuristic will therefore fail in these instances.

One approach to overcoming the issue of local maxima is to restart the HC with different starting points and compare the new solution to a previous solution. The performance of such an approach deteriorates as the number of local maxima increases; in the limit, it performs as random sampling, so finding the global maxima becomes unlikely. Unfortunately, the number of local maxima typically increases with the size of the solution space, i.e., more elements in the train set means more local maxima. There are also certain ILs that induce more local maxima in the solution space than others. The inability of HC to escape local maxima is therefore an issue for larger train sets and certain ILs. For the general case, there is a need for a heuristic that is able to escape local maxima.

### Late Acceptance Hill Climbing

The previous sections argued that there is a need for a heuristic that is able to escape local maxima to obtain the most damaging train for the general case. It has also been argued that the underlying structure of the solution space for the problem in eq. (3.8) varies with the IL and train set. Since the solution space varies from case to case, it is important that the meta-heuristic applied to our problem is as simple as possible to avoid excessive calibration for each case of application.

Late Acceptance Hill Climbing (LAHC) is a general purpose meta-heuristic with the ability to escape local maxima [25]. LAHC uses a local search that can accept “worse” neighbor solutions over the best known solution depending on recent parts of the solution history. In comparison to the HC heuristic, LAHC compares the candidate solution to the neighborhood rather than to the single best known solution. The size of the neighborhood or the *history length*  $\lambda$  determines the ability to escape local maxima in favor of the global one and is the only parameter that needs to be determined for the LAHC meta-heuristic. Note that the simple greedy HC heuristic described in section 3.4.2 is obtained from the LAHC heuristic when the solution history has length one, i.e.,  $\lambda = 1$ .

Algorithm 1 shows the pseudocode for the LAHC heuristic; it is largely adopted from [25] except for one minor change incorporated at lines 5, 15 and 16, where

the most damaging train  $T_{\max}$  is stored and kept separate from the currently accepted train  $T$ . For the majority of cases, these two states will be the same, but in certain circumstances, we found that the accepted solution diverged from the maximum after accepting a worse solution. The change makes the algorithm more robust and accurate at very little cost.

The termination criteria at line 6 is appropriate for larger (realistic) sized train sets; for smaller train sets, the algorithm may converge within a few hundred iterations such that the criterion becomes unreasonably conservative. A few test runs with a train set quickly reveal whether the termination criterion should be adjusted or left as in algorithm 1. For more discussion on alternative termination criteria, see [24, 25]. The details of algorithm 1 should be self-explanatory, perhaps with the exception of  $h$  and  $j$ , which implement the history buffer and virtual beginning of the history buffer, respectively.

The implementation of the *getNeighbor* function assigns a probability<sup>1</sup> of  $\frac{1}{N+3}$  to the occurrence of removing a wagon, inserting a wagon, swapping the locomotive and swapping any of the  $N$  wagons at each step. This means that the probability of performing the operation of swapping out a wagon is  $\frac{N}{N+3}$ , compared to  $\frac{1}{N+3}$  for the other basic operations. This probability assignment was selected early in the development of the methodology after a comparison with other probability assignments indicated that it performed well for a large range of influence lines and train sets. Other probability assignments are also possible and will affect the characteristic behavior of the algorithm; for instance, in a case where the number of wagons in trains and in the wagon set is small and the locomotive set is comparatively large, increasing the probability of replacing the locomotive will allow faster exploration of the locomotive set and might enhance the convergence characteristics of the algorithm.

## 3.5 Examples

### 3.5.1 Train sets and influence lines to evaluate heuristics

Table 3.1 shows different ILs used in the assessment of the proposed heuristics. These ILs have been selected from the literature that assesses fatigue load models [22, 107] because they represent a wide range of structural details found in railway bridges.

Table 3.2 shows the train sets used in the investigations of this paper. The selected locomotives and wagons are representative of the rolling stock that were in service in the Norwegian railways for the period from 1930–60; see Frøseth and Rønnquist [42].

---

<sup>1</sup>The probability for inserting or removing a wagon is doubled ( $\frac{2}{N+3}$ ) when removing or inserting a wagon is prohibited by the restrictions on train length, i.e., when  $N = N^\downarrow$  or  $N = N^\uparrow$

**Algorithm 1** Most damaging train according to Late Acceptance Hill Climbing**Input:**  $\mathcal{T}, \mathcal{L}, \mathcal{W}, \lambda$ **Output:**  $T_{\max}$ 


---

```

1: procedure LATEACCEPTANCEHILLCLIMBING
2:    $T \leftarrow \text{chooseOne}(\mathcal{T})$ 
3:   For all  $k \in \{0, \dots, \lambda - 1\}$ :  $h_k \leftarrow d(T)$ 
4:    $i \leftarrow 0$ ;  $i_{\text{idle}} \leftarrow 0$ 
5:    $T_{\max} \leftarrow T$ 
6:   while  $i_{\text{idle}} \leq \max(5000, \frac{i}{50})$  do
7:      $T_{\text{cand}} \leftarrow \text{getNeighbor}(T)$ 
8:     if  $d(T_{\text{cand}}) \leq d(T)$  then
9:        $i_{\text{idle}} \leftarrow i_{\text{idle}} + 1$ 
10:    else
11:       $i_{\text{idle}} \leftarrow 0$ 
12:       $j \leftarrow i \bmod \lambda$ 
13:      if  $d(T_{\text{cand}}) > h_j$  or  $d(T_{\text{cand}}) \geq d(T)$  then
14:         $T \leftarrow T_{\text{cand}}$ 
15:        if  $d(T_{\text{cand}}) > T_{\max}$  then
16:           $T_{\max} \leftarrow T_{\text{cand}}$ 
17:        if  $d(T) > h_j$  then
18:           $h_j \leftarrow d(T)$ 
19:       $i \leftarrow i + 1$ 

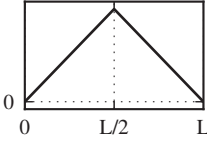
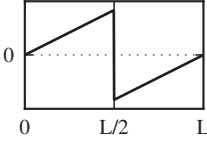
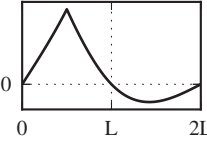
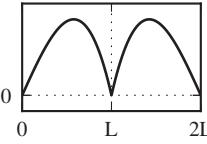
1: function getNeighbor( $T$ )
2:    $N \leftarrow \text{getNumberOfWagons}(T)$ 
3:    $n \leftarrow \text{randomInt}(0, N + 2)$ 
4:   if  $n = 0$  then
5:      $L \leftarrow \text{chooseOne}(\mathcal{L})$ 
6:      $T_{\text{out}} \leftarrow \text{swapLocomotive}(T, L)$ 
7:   else if  $1 \leq n \leq N$  then
8:      $W \leftarrow \text{chooseOne}(\mathcal{W})$ 
9:      $T_{\text{out}} \leftarrow \text{swapRandomWagon}(T, W)$ 
10:  else if  $(n = N + 1 \text{ and } N > N^{\downarrow}) \text{ or } (N = N^{\uparrow})$  then
11:     $T_{\text{out}} \leftarrow \text{removeRandomWagon}(T)$ 
12:  else
13:     $W \leftarrow \text{chooseOne}(\mathcal{W})$ 
14:     $T_{\text{out}} \leftarrow \text{insertRandomWagon}(T, W)$ 
15:  return  $T_{\text{out}}$ 

```

---

Train set 1 is established from three different locomotives and a wagon set with twelve two-axle wagons generated from three different geometries and four different axle load magnitudes. The trains in train set 1 are restricted to have between three and five wagons. Train set 1 therefore consists of  $|\mathcal{T}_1| = 813888$  unique trains. Due to the relatively small size of train set 1, it is possible to explore

Table 3.1: Influence lines used in the evaluation of the different heuristics. These influence lines represent examples for typical fatigue critical details in steel railway bridges, e.g., stringer, cross girder and stringer-cross girder connections. In this paper, the length  $L$  of the influence line is varied within  $\{3.0, 5.0, 7.0, 11.0, 17.0, 23.0, 29.0, 37.0, 53.0, 101.0\}$ .

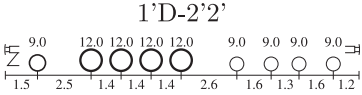
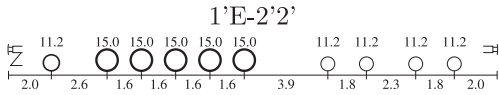
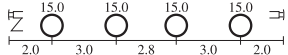
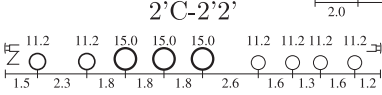
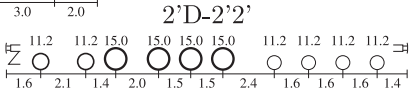
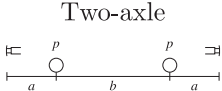
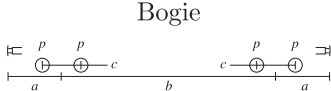
Id	Structural detail	Influence line
1	Midspan of a simply supported beam (moment). Cross girder, vertical and lower chord of truss bridge.	
2	Midspan of a simply supported beam (shear). Diagonal of truss bridge.	
3	Midspan of a continuous two-span simply supported beam. Stringer of truss bridge.	
4	Support of a continuous two-span simply supported beam. Stringer-cross girder connection in truss bridge.	

the entire solution space by enumeration in a reasonable time. The most damaging train(s) can therefore be determined for this train set for all of the considered ILs.

Train set 2 is much larger, with  $|\mathcal{T}_2| \geq 10^{105}$  trains consisting of a locomotive and between ten and fifty wagons. The trains are established from five different locomotives and a wagon set with 65 two-axle wagons and 65 bogie wagons. The two-axle wagons and bogie wagons are generated from thirteen different geometries each,  $\mathcal{G}_{\text{two-axle}}$  and  $\mathcal{G}_{\text{bogie}}$ , respectively, and five different axle load magnitudes  $\mathcal{P}$ . The size of train set 2 does not permit complete exploration of the solution space, and it is therefore necessary to rely on heuristics to obtain an approximate solution to the problem.



Table 3.2: Definition of the train sets used to investigate the different approaches to finding the most damaging train.

Train set 1, $\mathcal{T}_1$	
$\mathcal{L} = \{B'B', 2'C-2'2', 1'D-2'2'\}$ , $N = \mathbb{N}[3, 5]$	
$\mathcal{W} = \{(a, b, p) \mid (a, b) \in \{(1.5, 3.5), (2.3, 5.3), (3.0, 7.0)\} \wedge p \in \{3.8, 7.5, 11.3, 15.0\}\}$	
Train set 2, $\mathcal{T}_2$	
$\mathcal{L} = \{B'B', 2'C-2'2', 1'D-2'2', 2'D-2'2', 1'E-2'2'\}$ , $N = \mathbb{N}[10, 50]$	
$\mathcal{W} = \{(a, b, p) \mid (a, b) \in \mathcal{G}_{\text{two-axle}} \wedge p \in \mathcal{P}\} \cup \{(a, b, c, p) \mid (a, b, c) \in \mathcal{G}_{\text{bogie}} \wedge p \in \mathcal{P}\}$	
$\mathcal{G}_{\text{two-axle}} = \{(1.5, 3.5), (3.0, 3.5), (3.0, 7.0), (1.5, 7.0), (2.2, 5.2), (2.2, 3.5), (3.0, 5.2), (2.2, 7.0), (1.5, 5.2), (1.9, 4.4), (2.6, 4.4), (2.6, 6.1), (1.9, 6.1)\}$	
$\mathcal{G}_{\text{bogie}} = \{(2.3, 8.0, 2.0), (2.7, 8.0, 2.0), (2.7, 12.0, 2.0), (2.3, 12.0, 2.0), (2.5, 10.0, 2.0), (2.5, 8.0, 2.0), (2.7, 10.0, 2.0), (2.5, 12.0, 2.0), (2.3, 10.0, 2.0), (2.4, 9.0, 2.0), (2.6, 9.0, 2.0), (2.6, 11.0, 2.0), (2.4, 11.0, 2.0)\}$	
$\mathcal{P} = \{3.8, 6.6, 9.4, 12.2, 15.0\}$	
Locomotives	
	
$B'B'$	
	
	
Speed: (1'D-2'2'= 50.0 km/h), (B'B', 2'D-2'2', 1'E-2'2'=70.0 km/h), (2'C-2'2'=90.0 km/h)	
Wagons	
	

### 3.5.2 Performance of random sampling and Hill Climbing

This section investigates how well local search performs in identifying the most damaging train in train set 1; the random sampling approach is also included to confirm the analysis in section 3.4.2. Algorithm 1 with  $\lambda = 1$  and an implementation of the RS algorithm outlined in section 3.4.2 were applied 1000 times to train set 1 ( $\mathcal{T}_1$ ) and all forty variations of the ILs in table 3.1. Both the HC algorithm and the RS algorithm were terminated at 1000 iterations, i.e., the termination criteria in algorithm 1 was altered for this particular investigation. Figure 3.2 shows the results from these simulations.

First, considering the performance of the RS heuristic, fig. 3.2 shows that the success rate for RS is generally poor. The only case where the RS heuristic performs reasonably well is for IL 1 with  $L = 29.0$ , the reason being that for this IL, any train with locomotive 2'C-2'2' followed by two wagons with configuration (1.5, 3.5, 15.0) maximizes the damage. The probability of sampling one of these trains from the

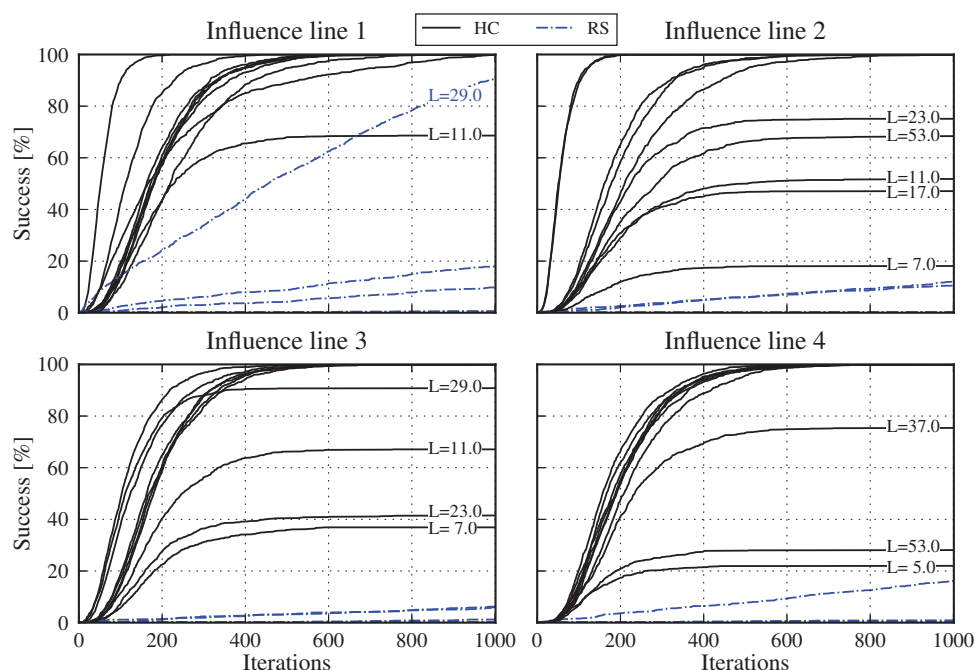


Figure 3.2: The cumulative distribution of the number of iterations until the RS and HC heuristics converged to the most damaging train for the train set and influence lines. Less than 100% success means that the heuristic did not identify the true optimum in each of the 1000 trials.

train set is then  $\frac{1}{3} \cdot \frac{1}{12} \cdot \frac{1}{12} \approx 0.2\%$  for each trial, and the probability of sampling at least one of these trains in 1000 trials is 90%, as shown in the figure.

The HC heuristic generally performs better than the RS heuristic for all forty different ILs. Figure 3.2 also shows that thirteen of the forty cases have a success rate lower than 100%, i.e., the HC heuristic does not converge to the global maxima. This indicates that the problem is nonconvex for the general case and motivates the introduction of a heuristic that can traverse local maxima.

The figure also shows that the success rate of the HC heuristic depends on both the shape and length of the IL, e.g. IL 1, 2, and 3 with  $L = 5.0$  have a 100% success rate, while this rate is only approximately 25% for IL 4, and IL 1 has a 100% success rate for all lengths except  $L = 11.0$ . The worst performance for the HC heuristic is found for IL 2 with a length of  $L = 7.0$ , with a success rate of 20%. For other train sets, different either in size or in the locomotive and wagon sets, the success rate can be even smaller than the worst case presented here.

Figure 3.2 also shows that HC generally converges in less than 1000 iterations, which is a significant improvement over the number of evaluations necessary by enumeration. The local search is therefore effective in finding an optimal or near optimal solution to the problem.

### 3.5.3 Influence of the history length on the performance of the LAHC heuristic

This section investigates how the history length affects the performance of the LAHC heuristic. Train set 1 and the ILs that did not achieve a 100% success rate in the previous section are considered in the analysis. The history length was varied within  $\lambda \in \{100, 250, 500, 1000, 2000\}$ , and 1000 trials at each history length were performed with algorithm 1. The same initial trains were used in these simulations as in the simulations for HC in the previous section.

Figure 3.3 shows that increasing the history length generally increases the success rate of the LAHC heuristic. The figure also shows that the relationship between the success rate and history length is dependent on the IL itself. IL 2 with  $L = 7.0$  and IL 3 with  $L = 23.0$  have a smaller slope between the history length and success than the other ILs considered. While the other ILs all achieve a 100% success rate with  $\lambda < 500$ , a history length of  $\lambda = 2000$  is necessary to achieve a 100% success for IL 2 with  $L = 7.0$ , and an even higher length is necessary for IL 3 with  $L = 23.0$ . Again, the reason for the difference between the improvements in the success rate for different ILs is that the solution space changes with different ILs. The average number of iterations required before the algorithm terminates also increases with the history length, as shown by fig. 3.4a.

The increase in the number of iterations is approximately proportional to the history length, which is a typical characteristic for the LAHC algorithm [25]. This linear characteristic can be used to predict the run time to convergence for the algorithm and can be used to select the appropriate history length for simulations within a specified time allocated for the analysis.

The computational efficiency of the heuristic is expressed in fig. 3.4b as the number of iterations per success. The optimal history length is different for the various ILs, which implies that one cannot select a single optimal history length for a train set that can be applied to all influence lines. A further discussion on selecting the optimal history length will be given below.

In conclusion, this section has shown that increasing the history length of the LAHC heuristic increases the likelihood of finding the most damaging train and the number of iterations to termination of the algorithm. The history length therefore also determines the computational efficiency of the LAHC heuristic.

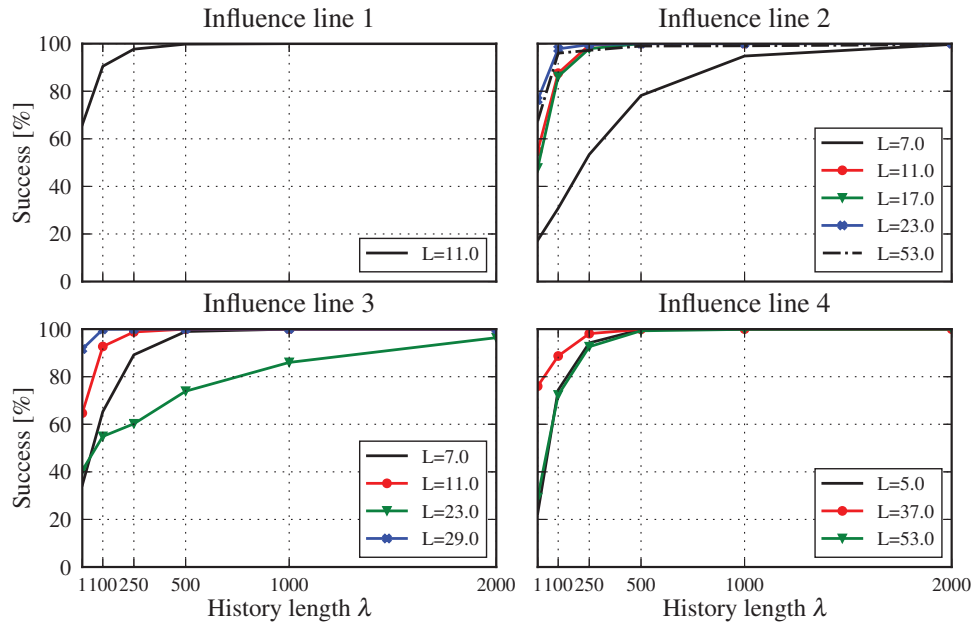


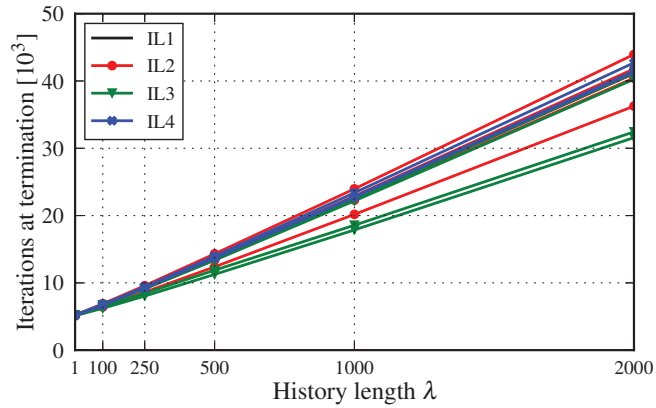
Figure 3.3: Success rate of the LAHC heuristic in finding the most damaging train in train set 1 for different history lengths.

### 3.5.4 Behavior and performance of LAHC with larger train sets

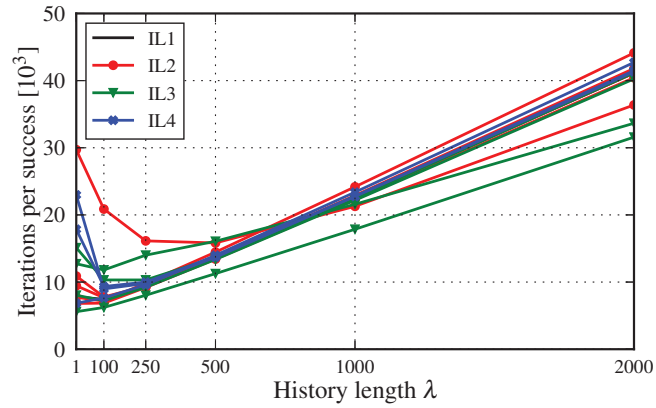
The previous sections demonstrated that the LAHC heuristic successfully and efficiently identified the most damaging train in train sets of small size for all considered influence lines. In this section, the behavior and performance of LAHC in finding the most damaging train in train set 2 are considered. Figure 3.5 shows the normalized damage from HC and LAHC for 144 trials with train set 2 for each of the forty ILs. The box shows the first, second (median) and third quartiles, the whiskers extend to the 2nd and 98th percentiles of the distribution, and the outliers signify trials that fall outside these percentiles. All damage is scaled against the maximally known damage for each IL.

LAHC performs equally or better than HC in terms of maximum damage for all ILs, i.e., the most damaging train identified by LAHC has the same damage or is more damaging than the most damaging train identified by HC. The worst performance for HC is a normalized damage of 92% of that obtained with LAHC for IL 4 with  $L = 17.0$ . The response  $z(u)$  and the load functions  $f(x)$  for the most damaging trains obtained by the two heuristics for this IL are shown in fig. 3.6.

Figure 3.6 shows that both heuristics find the same locomotive, the steam loco-



(a)



(b)

Figure 3.4: Average number of iterations at termination of the algorithm (a) and iterations per success (b).

motive with label 2'C-2'2'. The most damaging train for the LAHC heuristic consists of a repeated sequence of the same two empty and four full wagons throughout the entire train; the loaded wagons at  $x \approx 600$  are in reverse order compared to the other load cycles. This wagon sequence induces a response with large fatigue cycles that range from approximately  $z = 0.10$  to  $z = 0.85$ . The most damaging train from HC also displays the same overall structure with the same number of unload/load cycles as the most damaging train obtained by LAHC, but the particular wagons used in empty and loaded sequences are different and irregular. The response is therefore also more irregular, and the peaks do not consistently reach  $z = 0.85$ , e.g., compare the responses  $z(u)$  at  $u \approx 120$  and  $300$ . In terms of fatigue

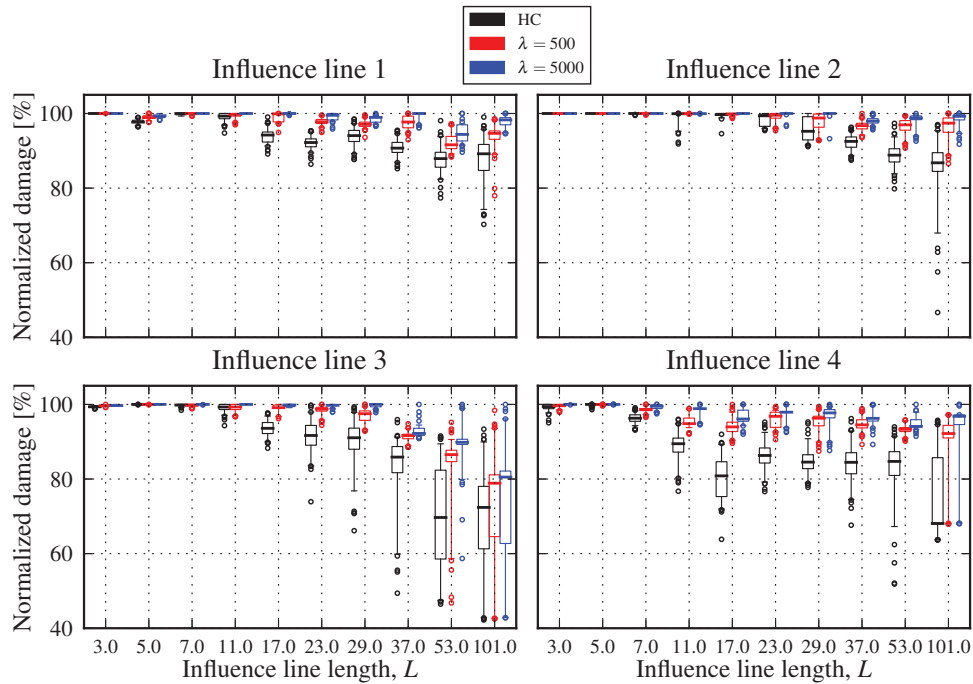


Figure 3.5: Distribution of normalized damage induced by trains identified with algorithm 1 for train set 2.

loads and damage, the LAHC train produces a number of fatigue load cycles with slightly higher magnitudes than the HC train, which induces more fatigue damage under the damage rule in eq. (3.3).

Figure 3.5 also shows that the range of or variation in the estimated damage decreases and the estimate converges to a single value for the normalized damage in cases where the history length is sufficiently large. Consider, for instance, IL 3 with  $L = 17.0$  in fig. 3.5. For HC, the results range from 88 to 97% of the maximum damage known for the IL, with a median of 93%; for larger history lengths, the range decreases, and the median converges towards 100% normalized damage. For this IL and a particular train set, a history length of  $\lambda = 5000$  means that all 144 trials identify the same normalized damage within one percent, i.e., the same train or trains that are equally damaging are identified in each trial. The reason that increasing the history length reduces the variance in the results is that the number of local maxima that can ‘trap’ the local search is reduced by increasing the history length, i.e., when the history length is sufficiently large, the global maximum is the only place where the algorithm can terminate.

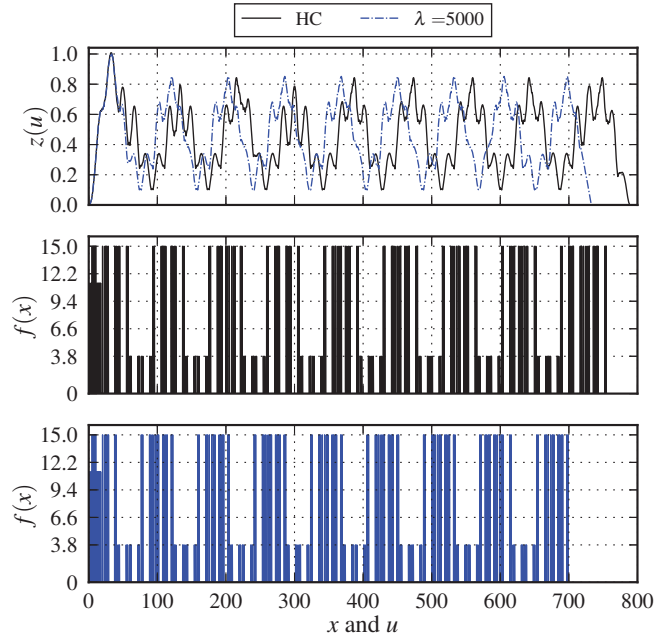
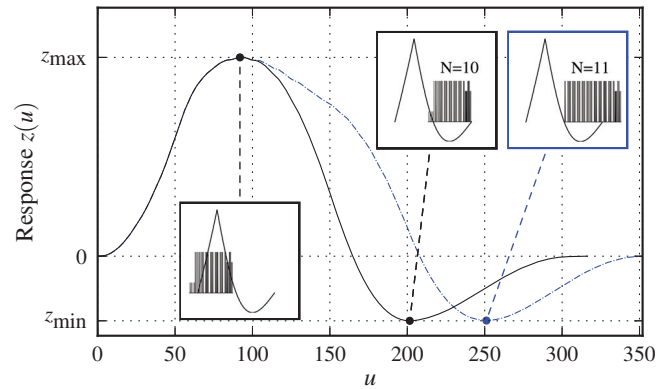


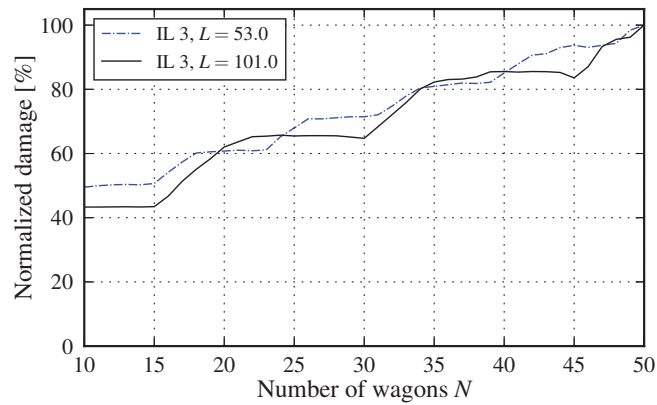
Figure 3.6: Response for influence line 4 with  $L = 17.0$  and the load functions from the most damaging trains identified by HC and LAHC ( $\lambda = 5000$ ). The fatigue damage induced by the HC train is 92% of the damage induced by the LAHC train.

Furthermore, fig. 3.5 shows a tendency that the results have greater variation in normalized damage for longer IL lengths. The reason is that loading and unloading of longer structures depends on several wagons at a time, i.e., one has to change several wagons in a train to make a significant change to the fatigue response in the structure. Consider fig. 3.7a, which shows the most damaging train identified by LAHC ( $\lambda = 500$ ) for  $N = 10$  and  $N = 11$  wagons for IL 3 with  $L = 101.0$ .

The locomotive and first six wagons are the same for both trains, and the maximum response  $z_{\max}$  is the same for the two trains. The minimum response  $z_{\min}$  for the two trains is also practically the same, and from the perspective of fatigue damage, the response for the two trains is almost identical. Figure 3.7b shows that at least six wagons must be added to the most damaging train with  $N = 10$  wagons to make a significant change to the fatigue response to trains in train set 2 for IL 3 with  $L = 101.0$ . Note also that the majority of trains with  $N = 11$  wagons are significantly less damaging than the most damaging train with  $N = 10$  and that the most damaging train with  $N = 11$  is not obtained from a single change of the train with  $N = 10$  wagons, i.e., a new wagon must be added and the last four wagons must be swapped out to find the most damaging train with  $N = 11$ . The figure also



(a)



(b)

Figure 3.7: (a) shows the response to the most damaging train identified for trains with 10 and 11 wagons for IL 3 with  $L = 101.0$ . (b) shows the maximum damage identified in train set 2 for different train lengths  $N$  with LAHC ( $\lambda = 500$ ) and 144 trials.

shows that there are two other plateaus with similar damage for the most damaging train with different  $N$ ; each of these corresponds to the addition of another cycle to the response while maintaining the minimum and maximum responses observed for  $N = 10$ . The most damaging train with  $N = 50$  wagons has the same minimum and maximum responses as  $N = 10$ , but with three additional loading cycles; see fig. 3.8.

Figure 3.7 also shows that the damage for the most damaging trains for IL 3 with  $L = 53.0$  displays the same characteristic plateaus as for IL 3 with  $L = 101.0$ .



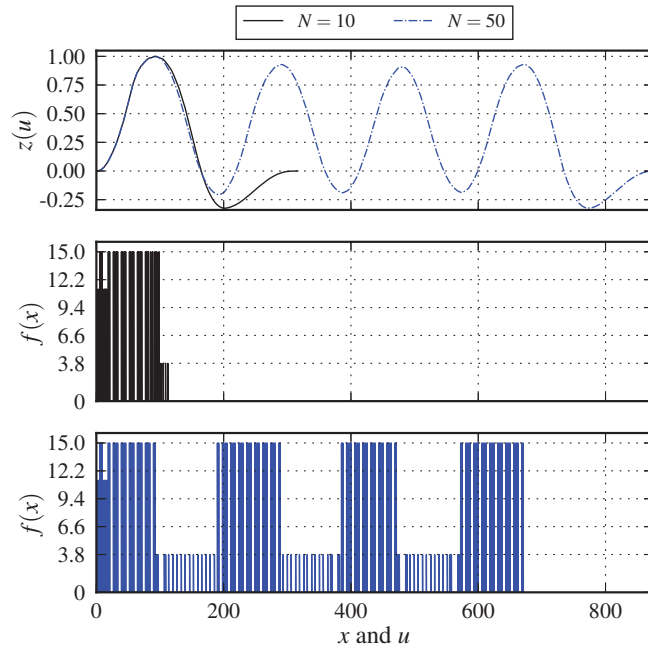


Figure 3.8: Response for influence line 3 with  $L = 101.0$  and the load functions from the most damaging trains with  $N = 10$  and  $N = 50$  wagons identified by LAHC ( $\lambda = 5000$ ). The fatigue damage induced by the train with  $N = 10$  wagons is 43% of the damage induced by the train with  $N = 50$  wagons.

The length of the plateaus is related to the number of wagons necessary to span the length of the structure, i.e., wagons in train set 2 are between 6.5 and 17.4, and at least 6 and 12 are necessary to span IL 3 with  $L = 53.0$  and  $L = 101.0$ , respectively.

The history length in the LAHC algorithm should therefore be increased for longer influence lines to escape local maxima reliably because more changes to the train are necessary to significantly alter the response in the structure.

## 3.6 Discussion

### 3.6.1 Selecting the history length and number of trials

Section 3.5 demonstrated that the history length parameter  $\lambda$  in the LAHC heuristic determines the likelihood of obtaining the most damaging train and the time to convergence of the algorithm. Selecting the optimal history length must therefore be based on requirements for accuracy in the estimate of the most damaging train and resources available for computation and analysis of the results.

One cannot know a priori what the optimal history length is, but section 3.5 revealed several features of the solution that can be used to assess the quality of the estimated solution and determine the computational cost of obtaining a solution. The number of iterations to obtain a solution is proportional to the history length. Simulations at two different history lengths can therefore be used to estimate the computational time for other history lengths. Furthermore, the variation in the estimated damage induced by trains can be used as an indicator of the accuracy of the solution. Section 3.5.4 demonstrated that when the history length was sufficiently large, the variation in the damage induced by the estimated train diminished and tended towards the maximally known damage for the IL. Additionally, for many of the ILs considered in section 3.5, a history length of  $\lambda = 1$  was the most efficient history length since it converged at fewer iterations and identified the most damaging train with the same success rate as longer history lengths.

Following the discussion above, we suggest that the history length be initially set to  $\lambda = 1$  and then increased if the variation in the estimated damage is large. The increase in history length continues until the variation in the estimated results is satisfactory or when time and resources do not permit increasing the history length further. A simple measure of the variation is the ratio  $\rho$  between the minimum and maximum damages identified at the history length,

$$\rho = \frac{\min d}{\max d} \Big|_{\lambda} \quad (3.10)$$

The criterion for increasing the history length can then be defined by a threshold value for  $\rho$ .

The number of trials at a history length determines the variability or range of the normalized damage obtained by the heuristics, i.e., the probability of obtaining ‘extreme’ values of normalized damage for the converged train increases with the number of trials. Let  $d_{\gamma}$  and  $d_{1-\gamma}$  denote the percentile point values for the  $\gamma$ th and  $(1-\gamma)$ th percentiles of the probability distribution for normalized damage, respectively. The probability  $p_{\gamma}$  of sampling at least one value of normalized damage below the lower percentile point ( $d < d_{\gamma}$ ) and at least one value of normalized damage above the upper percentile point ( $d > d_{1-\gamma}$ ) in  $n$  random and independent trials is

$$p_{\gamma} = 1 - (1 - 2\gamma)^n - 2 \sum_{k=1}^n \binom{n}{k} \gamma^k (1 - 2\gamma)^{n-k} \quad (3.11)$$

where  $\binom{n}{k} = \frac{n!}{k!(n-k)!}$  is the binomial coefficient. Table 3.3 provides the solution of eq. (3.11) for  $n$  at different percentiles  $\gamma$  and probabilities  $p_{\gamma}$ .

Many different combinations of  $n$ ,  $p_{\gamma}$  and the threshold value for  $\rho$  are viable to create a criterion for either accepting the solution or increasing the history length.

Table 3.3: Number of random and independent trials  $n$  necessary to obtain at least one sample below the  $\gamma$ th percentile and one sample above the  $(1-\gamma)$ th percentile with a probability of  $p_\gamma$ .

$\gamma$ [%]	Trials $n$		
	$p_\gamma = 90\%$	$p_\gamma = 95\%$	$p_\gamma = 99\%$
1.0	296	366	527
2.5	118	146	210
5.0	58	72	104
10.0	29	35	51
25.0	11	13	19

The table shows that the interquartile range ( $\gamma = 25\%$ ) is found with high confidence with as few as  $n = 13$  trials. Unfortunately, fig. 3.5 also shows that the interquartile range (indicated by the box in the boxplot) is comparable for different history lengths, regardless of the difference in range between the minimum and maximum and the most damaging train for different history lengths. For example, the interquartile range for IL 1 with  $L = 23.0$  yields  $\rho = 98\%$  for both HC and LAHC with  $\lambda = 5000$ , but the most damaging train for HC is only 95% of the most damaging train for LAHC. The interquartile range is therefore not a reliable indicator for the variation and for the quality of the obtained train.

The ranges presented in fig. 3.5 are given for 144 trials, which give approximately a 95% confidence in spanning over the 2.5% and 97.5% percentile points of the damage distribution. We suggest that the number of iteration be set to  $n \approx 150$  and that the solution and history length be accepted if  $\rho \geq 95\%$ . This criterion means that many of the solutions in fig. 3.5 for HC that do not achieve the same maximum damage as LAHC will be rejected [see the results for IL 1 ( $L = 17.0, 23.0, 19.0, 37.0$ ), IL 2 ( $L = 37.0$ ), IL 3 ( $L = 17.0, 23.0, 29.0$ ) and IL 4 ( $L = 7.0$ ) and accepted if the same damage as with LAHC is achieved.

### 3.6.2 Defining the train set

#### Selecting the number of wagons in trains

For many ILs, the most damaging train will be the train with the maximum number of wagons, i.e.,  $N = N^\uparrow$ , because adding another wagon either means adding another cycle or increasing the stress range of an existing cycle. One might therefore consider selecting a train set where all trains have the maximum number of trains  $N^\downarrow = N^\uparrow$ . There are, however, cases where adding another wagon will reduce the magnitude of a stress range. Figure 3.7a shows the response in IL 4 with  $L = 101.0$

for the most damaging trains with 10 and 11 wagons. From a practical standpoint, these two trains induce identical fatigue damage, but the train with only 10 wagons is slightly more damaging. The reason is that the locomotive, which has a higher load intensity than any of the wagons, can load the negative coefficients of the influence line to minimize the response in the structure. Additionally, if the train set is restricted to only include trains with the maximum number of wagons, then the size of the train set is not reduced considerably since  $|\mathcal{W}^{N^\uparrow}|$  completely dominates the other lower order terms in eq. (3.9).

The train set should therefore be selected to include the range of possible train lengths since reducing the range of the number of wagons in trains is both ineffective and potentially excludes the most damaging train from the search.

### Selecting the wagons in the wagon set

A wagon is defined by load variables  $p_j$  and geometric variables  $a$ ,  $b$  and  $c$ . While the geometric variables are discrete variables, the load variables are continuous over an interval  $p \in \mathbb{R}[p^\downarrow, p^\uparrow]$ , which means that there are an infinite number of different wagons in a real wagon set.

In practice, this issue is solved by discretizing the continuous domain, and in section 3.5, the axle load interval  $p$  was discretized into equally spaced levels of axle load for the train sets. The effect of this discretization is evidently nonexistent. Section 3.5 showed that none of the most damaging trains for the ILs in table 3.1 have wagons with axle loads other than the minimum  $p^\downarrow$  or maximum axle load  $p^\uparrow$ , except in cases where the axle load magnitude of certain wagons in the train does not affect the fatigue loading. Note that for all these exceptions, there exists an equally damaging train with min/max axle load. Other IL lengths have also been considered in an attempt to find a single instance where the most damaging train must include intermediate load levels for certain wagons, but no such instance has been found.

The experience from the work on this paper is therefore that the most damaging train will be a combination of fully loaded ( $p^\uparrow$ ) and empty ( $p^\downarrow$ ) wagons. However, since only a selection of the infinite number of possible ILs and train set combinations has been considered, there might still be cases where the most damaging train includes wagons with intermediate levels of axle load. Until more experience with other types of ILs and train sets has been gained or a proof is established that shows that the most damaging train will only consist of wagons with min/max axle loads, we suggest that the axle load interval be discretized into five equally spaced levels of axle loads to ensure that the most damaging train is included in the search and to enable discovery of cases in which intermediate axle load levels are part of the most damaging train.

Real wagon stock generally consist of a large number of different geometries.

For the problem of finding the most damaging train, it is important to select wagons that represent the geometry of wagons in service and, at the same time, to limit the size of the wagon set to keep the problem computationally tractable. This is most efficiently done by selecting wagons that are significantly different from each other, i.e., distributed over the entire domain of the parameters. In section 3.5, the geometry of the wagons was selected from thirteen evenly distributed points in the domain of the geometric parameters  $a$  and  $b$  for both the two-axle and bogie wagons; see fig. 3.9.

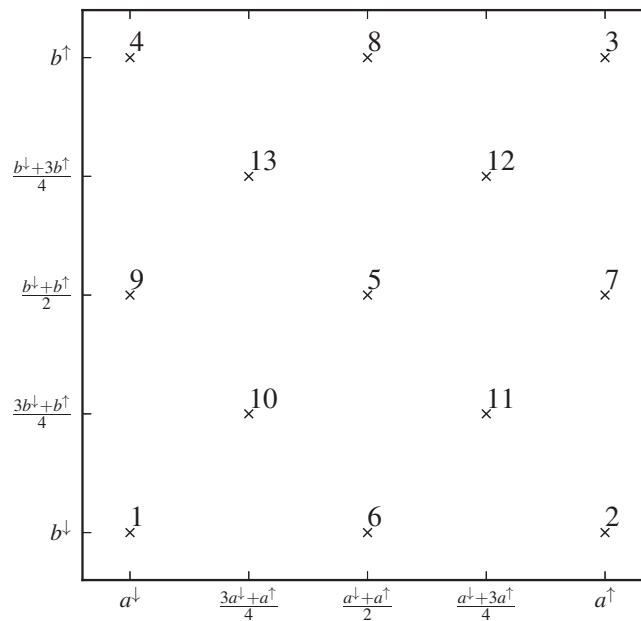


Figure 3.9: Selection of the geometric variables  $a$  and  $b$  for wagons.

The reader might not want to use the ‘artificial’ distributed points in fig. 3.9, but the figure can be used to select wagons from available data that lie close to the distributed wagons in the figure.

In light of the findings on intermediate levels of axle loads, one might question the necessity of the central point in geometric variables. The simulations in section 3.5, however, showed that the most damaging train for several of the ILs included wagons where the central geometry wagon was necessary. The explanation is that central points allow alignment of the axle loads with the optimal points of the influence line to maximize/minimize the response. Central geometry points should therefore be included in the wagon set to ensure that the most damaging train is included in the search.

### Influence of train set parameters on computational cost of obtaining the most damaging train

Section 3.4 presented approaches to obtaining exact and approximate solutions to the most damaging train. The computational cost of obtaining the exact solution by enumeration is determined by the train set size. Equation (3.9) shows that the train set size grows exponentially with the number of wagons with the wagon set as the base, and from this perspective, it is desirable to limit both the number of wagons in trains and the wagon set size. Fortunately, the computational effort required to obtain the most damaging train by LAHC is not directly determined by the size of the train set but rather by the size of the neighborhood of a train, the number of changes that must be made to the initial train and the number of paths from a train to the optimal train.

The number of neighbors a train with  $N$  wagons has is determined by the following:

- $|\mathcal{L}| - 1$  neighbors obtained by swapping the locomotive.
- $N(|\mathcal{W}| - 1)$  neighbors obtained by swapping any of the wagons.
- $N$  neighbors obtained by removing any of the wagons.
- $(N + 1)|\mathcal{W}|$  neighbors obtained by inserting a wagon.

The total number of neighbors is therefore  $|\mathcal{L}| + (2N + 1)|\mathcal{W}| - 1$ .

The number of changes that must be made to a train with  $N$  wagons to obtain the optimal train with  $N^*$  wagons is in the worst case one change for the locomotive, one change for  $\min(N, N^*)$  wagons and either insert or remove  $|N - N^*|$  wagons. The number of changes that must be made to any suboptimal train to obtain the optimal train is therefore at most  $1 + \max(N, N^*) \approx N^\uparrow$ . The locomotive and wagon set size influence the number of changes that must be made to a train in an average sense; e.g., if the locomotive and wagon sets are large, then the probability that several components of a randomly selected initial train are wrong is larger than if the these sets are small.

The number of paths from a train to the optimal train, i.e., the number of neighbors that leads to the optimal train, is difficult to estimate because it depends on several of the problem parameters. First, it depends on how close the train is to the optimum train. Consider a train where the locomotive and the wagons are all sub-optimal. Initially, any wagon can be selected and swapped out for an optimal one, which means that there are a large number of paths that will lead to the optimal train. As the solution progresses, the number of wagons that can be swapped out to bring the suboptimal train closer to the optimal train decreases. Eventually, the

suboptimal train is one wagon replacement away from obtaining the most damaging train, and the number of paths to the optimal train is limited to the wagons in the wagon set that yields an optimal train. The number of paths also depends on the characteristics of the influence line, locomotive set and wagon set and the interaction between them. For instance, if the wagon set has a large number of different wagon geometries but the differences in the wagon geometries are such that the response with respect to fatigue loading does not change, then the number of paths will be large. However, if the geometries are significantly different such that only one or a few wagons can be swapped in at each step, then the number of paths is small.

From the analysis above, one can conclude that the least influential parameter is the size of the locomotive set  $|\mathcal{L}|$  because of its small size compared to the size of the wagon set and because it only influences one out of  $N + 1$  components of the train. It is difficult to give a general answer to which parameter is most influential on the computational cost of obtaining the most damaging train by analysis due to the uncertainty surrounding the number of paths. A numerical experiment was therefore performed in which the maximum number of wagons in a train  $N^\uparrow$  and the wagon set size  $|\mathcal{W}|$  were changed, while all other parameters for train set 2 were fixed as in table 3.2. The wagon set size was altered by using geometries 1 to 5 and 1 to 9 instead of geometries 1 to 13 for both two-axle and bogie wagons; see fig. 3.9 for a definition of the geometric points. Figure 3.10 shows the average number of iterations to termination with LAHC ( $\lambda = 500$ ) and 144 trials.

The figure confirms that the computational effort required to obtain a solution by LAHC is not directly determined by the train set size. Figure 3.10 shows a linear relation between the maximum number of wagons in a train and the average number of iterations to termination; e.g., if the maximum number of wagons is reduced to  $\frac{10}{50} = 20\%$  or  $\frac{30}{50} = 60\%$ , then the average number of iterations generally reduces by 20% or 60%. The effect of reducing the wagon size set on the average number of iterations to termination is smaller and nonlinear; see, e.g., IL 2 with  $L = 17.0$ , where no reduction in the number of iterations is found when reducing the wagon set size by  $\frac{90}{130} \approx 69\%$ , while a 85% reduction is obtained by reducing the wagon set size to  $|\mathcal{W}| = 50$  wagons. These results indicate that one should prioritize reducing the number of wagons in a train rather than the wagon set size because the effect is more significant and predictable.

### 3.7 Conclusions

This paper has presented a methodology to find the train that induces the highest fatigue damage in structural details of railway bridges. The exact solution can only be obtained for trivial cases, and heuristics must be applied to solve the problem approximately in reasonable time. Three different heuristics have been considered

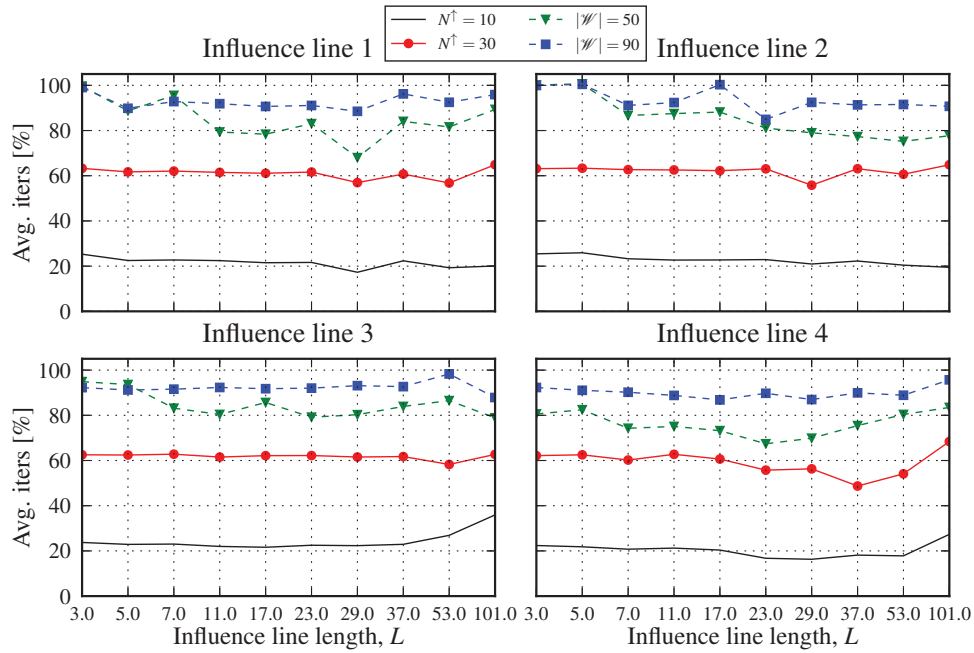


Figure 3.10: Average number of iterations at termination for different  $N^\dagger$  and wagon set sizes  $|\mathcal{W}|$  in train set 2, while all other parameters are fixed. The results are normalized against the average number of iterations with train set 2 and are obtained by LAHC ( $\lambda = 500$ ) with 144 trials at each IL.

to obtain a solution. Random sampling of the solution space can only identify the most damaging train reliably if the proportion of most damaging trains in the train set is high, i.e., in special combinations of structural detail and rolling stock. A local search strategy performs well in many cases but fails in the general case with a large number of local maxima. Late Acceptance Hill Climbing is therefore proposed as a method for the general case due to its ability to escape local maxima and its simplicity in implementation and use. The heuristic relies on a single algorithmic parameter, the history length, which determines the likelihood of finding the most damaging train and the time to convergence. Selection of the history length and the solution space has been discussed.





## Chapter 4

# Load model of historic traffic for fatigue life estimation of Norwegian railway bridges

Gunnstein T. Frøseth and Anders Rönquist,  
*Submitted for journal publication 2019.*

### Abstract

This article presents a load model of historic traffic for fatigue life estimation of Norwegian railway bridges. A general framework for the calibration of a fatigue load model is established. The load model is calibrated to the maximum fatigue damage induced by passenger and freight traffic and is guaranteed to be conservative for a wide range of structural components. The significance of historic traffic to fatigue damage development is considered. Modern freight trains after 1985 have the highest fatigue damage potential of all rolling stock. The fatigue damage contribution from historic passenger and freight trains after 1900 is significant for certain lines due to the moderate fatigue damage potential and high number of train passages. The fatigue damage contribution of passenger and freight trains from the period prior to 1900 is shown to be insignificant and can be neglected in fatigue life estimation of Norwegian railway bridges. Structural components that are not considered in the calibration of the load model are demonstrated to yield a load model that is neither consistent nor conservative. Alternative approaches to assess structural components that are not considered in load model calibration are suggested.

## 4.1 Introduction

Aging and deterioration of railway infrastructure is an issue of paramount importance to industrialized countries around the world. Bridges are essential components of the infrastructure that cannot be replaced without considerable investment cost or interruption to operation of the railways. The infrastructure owner must document that the bridges are safe to operate and determine the remaining service life of the bridges, such that maintenance and renewal of the bridge stock is achieved in the most economic, social and environmentally sustainable and efficient way.

There are a large number of steel railway bridges in the Norwegian and European railway network that are approaching and exceeding one hundred years in service, due to the rapid expansion and technological advancements in the 19th and early 20th century [52, 117]. Concerns about the remaining service life of these bridges have been raised by infrastructure owners because of the considerable change in loads over the lifespan of these bridges and the deterioration of load bearing capacity due to corrosion and material fatigue. Material fatigue is the primary damage mechanism of steel railway bridges and may cause component failure and even bridge collapse if the fatigue cracks are not identified and repaired before they develop to critical length. Fatigue crack initiation and growth is governed by the loading history of the material, and it is therefore necessary to describe the historic traffic conditions at a bridge site to be able to estimate the remaining fatigue life of railway bridges [61, 72].

Traffic conditions that are used to estimate the fatigue damage in a bridge are commonly represented by a fatigue load model. Fatigue load models generally consist of a reference load and a corresponding set of calibration factors [57]. The fundamental idea of fatigue load models is to introduce the same fatigue damage as the fatigue damage introduced by actual past traffic. To achieve this, it is necessary to calibrate the fatigue load model with relevant data on the actual past traffic conditions.

Frøseth and Rönnquist [42] gives an account of the available data for the historical loads in the Norwegian railway network. The conclusion from that work is that direct measurements of the traffic loads in the railway network are generally not available and that there are not sufficient data from other sources to determine the exact realization or precise probabilistic description of traffic conditions at a bridge site. This means that there are generally not enough relevant traffic data available to calibrate a load model to the exact past traffic conditions.

Case studies and other literature on fatigue life estimation of railway bridges also indicate that lack of data on past traffic is not only an issue for Norwegian railways; see assumptions and discussion on past loads for Canada [33], Germany [100], Sweden [1], Italy [101, 104], Portugal [82], U.S.A [19], Greece [114]

and England [61]. To the best of our knowledge, there is currently only one example in the literature that claims to know the loading history of the entire life of a bridge; see Grundy [49]. It is therefore generally necessary to estimate past traffic loads with limited data. Limited data means that the exact past loading history cannot be established, and according to good engineering practice, lack of data is addressed assuming the “worst” possible value, i.e., making a conservative assumption about the loads.

Åkesson [1] presents the concept of an equivalent freight train as a general approach to make a conservative estimate of past traffic with limited data. The idea is to use a train that has axle loads equal to the maximum permissible axle loads in the current railway infrastructure to represent all past traffic. The number of passages from this equivalent train is estimated by statistical data on transported goods and transport capacity of the equivalent train. In the project Sustainable Bridges [117], an extension of the concept is presented to allow changes to geometry of wagons and axle loads based on additional historic information of permissible axle loads on the line. This general framework allows an estimate of the past traffic loads to be obtained with information about development of permissible axle loads on a line, statistical traffic data on past transported goods and development of the geometry of wagons.

There are both practical and theoretical issues associated with the use of the equivalent freight train concept in fatigue life assessment. First, the claim that the simplest version described by Åkesson [1] is conservative has recently been questioned because the axle position of the train has a significant influence on fatigue loading for certain structural details [59]. Furthermore, the equivalent freight train concept describes a general approach to obtain a conservative estimate of past traffic with limited data, but it is not a readily available load model for practical use. For instance, the axle position of wagons should be selected from a range of possible values for each specific structural detail to represent the maximum fatigue load case. Although methodology has recently been developed to find the most damaging train composition for an arbitrary structural detail [41], it is impractical to apply this methodology for each structural detail that must undergo fatigue life assessment. A load model with a set of representative load cases and a set of calibration factors that is applicable to a wide range of different structural details is needed to efficiently evaluate the large number of components in the railway infrastructure.

Several important contributions to the field of fatigue life estimation and load modeling are presented in this paper. First, a discussion of the important properties of a fatigue load model for efficient and reliable estimation of remaining service life of steel railway bridges is provided. Second, a general framework for fatigue load model calibration is established, which is guaranteed to be conservative for all structural components that are considered in the calibration. Third, a load model of

historic traffic for fatigue life estimation of Norwegian railway bridges is presented, which demonstrates the use of the general calibration framework and has great practical value in fatigue life assessment of Norwegian railway bridges.

This paper is organized as follows. Section 4.2 discusses the philosophy and desired properties of a load model for fatigue life estimation. Section 4.3 presents the methodology for the development of the load model and establishes a general framework for load model calibration based on the formulation of an optimization problem. The structural components and the historic traffic conditions in the Norwegian railway network are also defined. Section 4.4 considers the significance of historical loads to fatigue life estimation of Norwegian railway bridges, presents the proposed load model and discusses the consequences of applying the load model to structural components not considered in load model calibration.

## 4.2 Properties of the proposed fatigue load model

The aim of this paper is to establish a load model with the following three properties. The load model should be

- Simple
- Conservative
- Consistent

The two last properties will be discussed in more detail in the subsections below. The first property, *the load model should be simple*, refers to the implementation and usage of the load model. A complex load model increases the possibility of making errors in the service life assessment, such that the service life is grossly overestimated or underestimated. Both complex load modeling and the increased possibility of making errors increase the resource usage associated with the service life assessment and should therefore be avoided. The load model is therefore established with as few reference loads and conditionals as possible.

### 4.2.1 The load model should be conservative

A fatigue load model is conservative if it induces the same or more fatigue damage in a structural component than the actual traffic on the bridge site. It is important that the load model is conservative because it ensures that the estimated remaining service life of a structural component is as long or longer than the actual remaining service life of the component, i.e., a conservative load model ensures that the bridge is safe to operate within the estimated time interval.

Unfortunately, an accurate description of the traffic at a bridge site is generally missing [42], i.e., the exact fatigue damage induced by the traffic is unknown. There is, however, a good description of the locomotives and wagons that existed during a period of the infrastructure and rules for operating the trains on the infrastructure. This means that there are data on the trains that existed during a specific period of time and how these trains operated, i.e., the set of possible trains are known from available data. The actual traffic conditions at a bridge site are then some unknown combination of trains from the possible train set.

Knowing all trains that existed during a period obviously does not permit exact determination of the fatigue damage that has been induced by past traffic. It is, however, possible to determine the fatigue damage introduced by any train in the possible train set, including the train that causes the maximum fatigue damage in a component for a specific period. Frøseth and Rönnquist [41] developed methodology to find the train that causes the greatest fatigue damage in a structural component. A conservative prediction of traffic loads can then be made by assuming that all trains that passed the bridge in a specific period introduce fatigue damage equivalent to the most damaging train from that period.

The load model is made conservative by calibrating it to the most damaging trains for structural components in the infrastructure. It is also important that the load model is not made more conservative than necessary since this leads to unnecessary use of more advanced and resource intensive assessment methodology, strengthening and repair of bridge components or even decommissioning of an adequate and safe bridge. More discussion on the topic of overconservatism is given in the following subsection on consistency in the load model.

#### 4.2.2 The load model should be consistent

A fatigue life assessment has multiple purposes for the infrastructure owner. It asserts and documents that the bridge is safe to operate within a time interval, and it guides the regular inspections towards structural details that are susceptible to fatigue damage and helps the decision maker allocate resources for maintenance and renewal in the most effective way, i.e., a fatigue life assessment provides a ranking of the components in the infrastructure by severity of fatigue damage. This aspect is important in the development of a load model for fatigue life assessment; if the load model is not carefully designed, it may be conservative for all structural details, but the level of fatigue damage may be more conservative for some of the components. An inconsistent load model will indicate inconsistent levels of fatigue damage in structural details and a bias in the ranking among them.

To illustrate this point and the consequences of an inconsistent load model further, consider fig. 4.1, which shows the fatigue damage introduced by an arbitrarily selected load model in two different structural details of a three-span simply sup-

ported beam at different lengths  $L$ . The fatigue damage is normalized against the maximum fatigue damage introduced by Norwegian freight trains in the period between 1985 and 2000, and the true fatigue damage introduced by any train from this period will therefore lie in the interval  $[0, 1]$  of normalized damage.

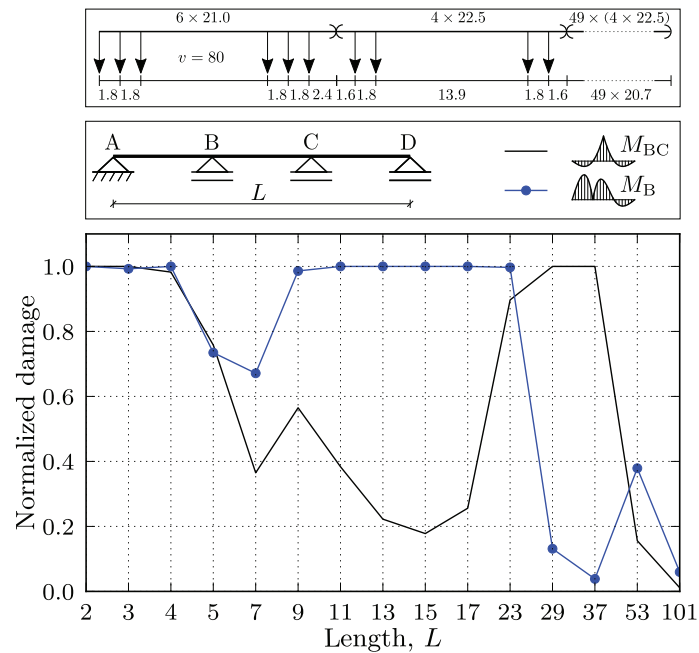


Figure 4.1: Fatigue damage introduced by the load at the top of the figure in two different structural details of a three-span simply supported beam.

First, consider the fatigue damage introduced due to the bending moment  $M_B$  at the support (B). The load model introduces the same fatigue damage as the most damaging freight train in the infrastructure for lengths between 2.0 and 4.0 and lengths between 9.0 and 23.0. At other lengths, the fatigue damage from the load model is less than the most damaging train, e.g., the normalized fatigue damage is only  $\approx 5\%$  for  $L = 37.0$ . This means that the load model is unconservative for these structural details; however, the issue of unconservatism can be addressed by simply scaling the fatigue damage obtained by the load model with a factor, e.g., twenty passages of the train presented in fig. 4.1 for every real train is sufficient for the structural detail at (B) to make the load model conservative at all lengths. Assume in the continuation that the load model in fig. 4.1 is calibrated with a scaling factor such that it is conservative for all structural details in the infrastructure.

A more subtle issue is that the load model does not introduce consistent levels of fatigue damage in all components. Consider a case where a three-span simply supported bridge with length  $L = 37.0$  is to be assessed for fatigue damage with

the load model in fig. 4.1 and assume that the fatigue detail category and cross-sectional properties at the midsupport (B) and midspan (BC) are roughly equal. The fatigue assessment will then conclude that detail (BC) is much more critical than the detail at (B), i.e., the fatigue damage at (BC) is shown to be approximately 20 times higher than that at (B).

The danger in this scenario is that detail (BC) is prioritized *over* detail (B) in subsequent investigations due to the conclusions of the fatigue life assessment. For instance, if the actual fatigue damage in the components is close to critical level, e.g., 80%, both components have a relatively high fatigue damage and should be monitored or at the very least, closely inspected during periodic inspections. However, due to the inconsistent load model, the fatigue life assessment indicates (BC) at 1600% over the critical level, while (B) is still only at 80%. A decision maker with a limited budget or an inspector with limited time would be correct to prioritize component (BC) over (B) in light of the result from the fatigue life assessment. An inconsistent load model may therefore reduce the overall safety and reliability of the infrastructure by overestimating the fatigue damage in certain components.

Another problem associated with an inconsistent load model is that components that are in no danger of fatigue failure are indicated as critical by fatigue life assessment. For instance, if the actual fatigue damage in component (BC) is 5% of the critical fatigue damage, a fatigue life analysis with the inconsistent load model will indicate the component at the critical level. The infrastructure owner would then order subsequent assessment of the noncritical component simply because of the inconsistent load model. This problem grows with decreasing consistency, i.e., the number of components that are falsely indicated as critical to fatigue failure increases with decreasing consistency. A more consistent load therefore facilitates more efficient assessment of the infrastructure.

In conclusion, a load model should be consistent to ensure that the infrastructure is managed in the most efficient, safe and reliable way.

### 4.3 Methodology

This section describes the methodology used to develop a load model that fulfills the properties described in the previous section. The problem is formulated as an optimization problem, where the objective is to find a set of reference trains with a corresponding traffic mix to represent the most damaging passenger and freight trains for the six periods of train traffic identified in [42].



### 4.3.1 Formulation of the optimization problem

Let  $T$  denote a train and be a member of the train set  $\mathcal{T}$ , i.e.,  $T \in \mathcal{T}$ , and let  $S$  denote a structural component and let  $\mathcal{S}$  be the set of all structural components in the railway infrastructure such that  $S \in \mathcal{S}$ . The fatigue damage induced in a structural component by a train is defined by the fatigue damage function  $d : \mathcal{S} \times \mathcal{T} \rightarrow \mathbb{R}_{>0}$ , where  $\mathbb{R}_{>0}$  is the set of positive real numbers. The train that causes the greatest fatigue damage to a structural component  $S$  is denoted  $T^\uparrow(S)$  and is defined by

$$T^\uparrow(S) = \arg \max_{T \in \mathcal{T}} d(S, T) \quad (4.1)$$

and the maximum fatigue damage induced in a component  $S$  is denoted  $d^\uparrow(S)$  and is defined by

$$d^\uparrow(S) = d(S, T^\uparrow(S)) \quad (4.2)$$

The purpose of this paper is to establish a simple, consistent and conservative fatigue load model for the structural components in the railway infrastructure. In this context, let the load model be defined by  $n$  reference trains  $(T_1, T_2, \dots, T_n) \in \mathcal{T}^n$  together with the corresponding traffic mix  $(a_1, a_2, \dots, a_n) \in \mathbb{N}^n$ , where  $\mathbb{N}$  is the set of nonnegative integers,  $T_i$  and  $a_i$  is reference train  $i$  and the number of times reference train  $i$  is applied to a structural component, respectively. The total fatigue damage induced in a structural component  $S$  by the load model is the sum of the contributions from each train passage

$$\sum_{i=1}^n a_i \cdot d(S, T_i) \quad (4.3)$$

The fatigue load model is conservative if the fatigue damage induced in any of the structural components in the infrastructure is greater or equal to the fatigue damage induced by the most damaging train; with eq. (4.2) and eq. (4.3), the conservative property of the fatigue load model can be expressed as

$$\sum_{i=1}^n a_i d(S, T_i) \geq d^\uparrow(S), \forall S \in \mathcal{S} \quad (4.4)$$

The fatigue load model is consistent if the level of fatigue damage, relative to the maximum fatigue damage by real traffic, is the same for all structural components in the infrastructure. The consistency  $\zeta \in \mathbb{R}(0, 1]$  of a load model can be expressed by the ratio between the minimum and maximum relative fatigue damage in all structural components, i.e.,

$$\zeta(T_1, \dots, T_n, a_1, \dots, a_n) = \frac{\min_{\forall S \in \mathcal{S}} \left\{ \frac{\sum_{i=1}^n a_i d(S, T_i)}{d^\uparrow(S)} \right\}}{\max_{\forall S \in \mathcal{S}} \left\{ \frac{\sum_{i=1}^n a_i d(S, T_i)}{d^\uparrow(S)} \right\}} \quad (4.5)$$

which means that a completely consistent load model will have a consistency equal to one ( $\zeta = 1$ ) and that a decreasingly consistent load model is obtained towards zero.

The fatigue load model is simple if it is applicable to any structural component in the infrastructure without any condition. Another aspect of simplicity is the number of reference trains and size of the traffic mix. Ideally, a load model is based on a single reference train and is applicable to both freight and passenger trains from all periods of the infrastructure.

As mentioned in section section 4.2.2, the conservative property of a fatigue load model is easily obtained by scaling the traffic mix, i.e., each of the traffic mix coefficients  $a_i$  are scaled with the same factor such that eq. (4.4) is satisfied. Unfortunately, the consistency property is much more difficult to satisfy. Selecting a consistent load model is not trivial because of the dependence on the many different structural components in the infrastructure as well as the characteristics of the traffic that has passed the bridge. Furthermore, the simple and consistent properties of the fatigue load model are conflicting, i.e., a simple load model is generally not consistent and vice versa; for instance, a load model with a reference train (the most damaging train) for each structural component is consistent, but it is not simple, as it consists of an infinite number of reference trains. Finding a simple, conservative and consistent fatigue load model for the infrastructure is therefore an optimization problem whose objective is to make the load model as consistent as possible under the constraint of being conservative and keeping the number of reference trains low. A concise formulation of this optimization problem is given below:

$$\underset{\substack{a_i, T_i \\ i=1,2,\dots,n}}{\text{maximize}} \quad \zeta(T_1, \dots, T_n, a_1, \dots, a_n) \quad (4.6a)$$

$$\text{subject to} \quad \min_{\forall S \in \mathcal{S}} \left\{ \frac{\sum_{j=1}^n a_j d(S, T_j)}{d^\uparrow(S)} \right\} = 1 \quad (4.6b)$$

where the objective eq. (4.6a) is to maximize the consistency of the load model and the constraint eq. (4.6b) is a rewritten version of eq. (4.4), which ensures that the load model is just conservative, i.e., the least conservative component is exactly conservative.

### Solving the optimization problem

The optimization problem is solved by adapting the late acceptance hill climbing (LAHC) algorithm [25] to adjust the train composition and traffic mix from an initial state. A new state is created by randomly selecting one of the trains or a traffic mix coefficient. The train composition is adjusted by considering the neighbor train, see [41]. The solution space for the optimization problem is discussed further in section 4.4.3. Each load model is established by accepting the best of twelve trials, and with a history length of 500 for the LAHC algorithm.

### 4.3.2 Fatigue damage calculation

The procedure to calculate the fatigue damage exactly follows the procedure that is described in detail in [41]. The stress response induced in a structural component by a train is calculated with the static influence line of the structural component and the dynamic amplification factor according to appendix D in [27]. Stress ranges are then extracted from the stress response by rainflow cycle counting [5]. A single slope linear fatigue endurance curve with slope parameter  $b = 5$  is adapted in the fatigue calculations. Note that the intercept parameter of the fatigue endurance curve is not necessary for the purpose of comparing one train to another as it only scales the fatigue damage. Finally, the fatigue damage is calculated by adopting Miner's damage accumulation rule.




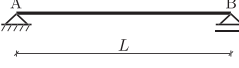


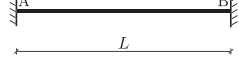
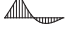

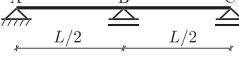

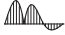
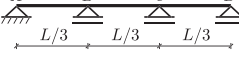
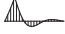
### 4.3.3 Representing structural components in the infrastructure

There are a large number of structural components in the infrastructure that need to be assessed for fatigue damage, for example, there may be several hundred different components in a single bridge. Fortunately, many of the structural components are similar in boundary conditions and loading pattern such that the characteristic response to a load moving over the bridge is the same, i.e., the influence line of many critical details is the same. Table 4.1 shows fourteen different influence lines parameterized by the length  $L$ , the majority of which are chosen from the literature on fatigue load effects and calibration of fatigue load models [22, 31, 107].

These influence lines represent a large range of different fatigue critical components in old railway bridges, in addition to the base systems shown in table 4.1. For instance, consider an open deck truss railway bridge: IL 2 can be found in the upper and lower chord, verticals and cross girder; IL 3 is representative of the response in a diagonal close to the mid span; and IL 6–10 are representative of influence lines found in the stringer and the connection between the stringer and cross girders.

In the development of the load model, the influence lines in table 4.1 with  $L = \{2.0, 3.0, 4.0, 5.0, 7.0, 9.0, 11.0, 13.0, 15.0, 17.0, 23.0, 29.0, 37.0, 53.0,$

Table 4.1: Influence lines used in the development of the load model.

IL	Shape	Base system	Description
1		–	Total load effect
2			$M_{AB}$
3			$V_{AB}$
4			$M_{AB}$
5,5r			$M_A, M_B$
6,6r			$M_{AB}, M_{BC}$
7			$M_B$
8			$M_{BC}$
9,9r			$M_B, M_C$
10,10r			$M_{AB}, M_{CD}$

101.0} are proposed to represent the infrastructure, i.e., the structural component set  $\mathcal{S}$  is defined by

$$\begin{aligned} \mathcal{S} &= \{ \text{IL}(n, L) \mid n = (1, 2, \dots, 10, 10r) \wedge L \in \ell \} \\ \ell &= \{ 2.0, 3.0, 4.0, 5.0, 7.0, 9.0, 11.0, 13.0, \\ &\quad 15.0, 17.0, 23.0, 29.0, 37.0, 53.0, 101.0 \} \end{aligned} \quad (4.7)$$

where  $\text{IL}(n, L)$  refers to influence line  $n$  with length  $L$ , see table 4.1. The lengths  $\ell$  are selected such that there is a higher density of them at shorter influence line lengths, where the overall response is more sensitive to load positioning, and low density at the longest lengths, where the response is more sensitive to changes in the group of loads rather than the exact positioning of a single load.

It is important to acknowledge that, although the influence lines in table 4.1 represent many components, a much greater set of influence lines in the infras-

structure exists. For instance, IL 2 is the moment at the midspan of a simply supported beam, but the influence line at the quarterspan or any other fraction of the beam length is different from that given for IL 2. This is also the case for all the other beams and possible quantities. Additionally, the length parameter  $L$  varies from structural component to structural component and can practically take on any value on the real number line between the shortest bridges at 2.0 m and the longest continuous structures at approximately 100.0 m. Unfortunately, it is impossible to include all structural details in the infrastructure in the development of a load model due to the computational demand of such a task. The structural component set  $\mathcal{S}$  defined above will therefore always be incomplete in comparison to the actual structural component set. The issue of an incomplete structural component set and the consequences to the applicability of load models based on an incomplete structural component set is studied and discussed further in section 4.4.5 below.

#### 4.3.4 Historic traffic conditions in the Norwegian railway network

As discussed in the introduction to this paper, the exact realization of the historic traffic cannot be established from the available data; however, data on each individual locomotive and wagon as well as when and how trains were operated during the history of the railways provide a definition of the trains that were available during a particular period [42]. Table 4.2 shows a summary of the rolling stock over the history of the Norwegian railways.

Table 4.2: Summary of the rolling stock in the Norwegian railway network

	Period	Locos.	Wagons		Train operation	
			cls.	Axle loads	Wagons	Speed
Passenger	-1900	3	8	5.0-9.0	1-20	55-70
	1900-30	7	22	5.0-11.0	1-20	55-90
	1930-60	6	16	6.0-12.0	2-20	65-90
	1960-85	6	18	7.5-13.0	3-20	70-120
	1985-00	12	6	8.5-14.0	5-20	105-160
	2000-	8	6	8.5-14.0	5-20	120-160
Freight	-1900	3	14	2.3-9.0		50
	1900-30	7	15	3.0-12.0		40-60
	1930-60	7	10	3.7-15.0	10-50	40-65
	1960-85	6	16	5.0-18.0		70-80
	1985-00	12	18	5.6-22.5		80
	2000-	8	23	5.6-22.5		90

For instance, the passenger trains in the period 1930-60 were composed of one out of six possible locomotives and a combination of between two and twenty wagons out of sixteen different wagon classes, each with an axle load between 6.0 and 12.0 tonnes. These trains operated at a maximum speed between 65 km/h to

90 km/h, depending on the maximum speed of the locomotive and the allowable speed on the infrastructure.

Section 4.A defines the trains and train sets  $\mathcal{T}$  in more detail, with the specific locomotives and wagons available in each period and the speed of each train and number of wagons used in passenger and freight trains throughout the history of the railways.

The most damaging train for each of the train sets and for each of the influence lines is determined with the method described in [41], with 150 trials in each train set and influence line with a history length of 500.

## 4.4 Results and discussion

### 4.4.1 Fatigue damage potential and significance of historical loads

This section compares the fatigue damage potential of the traffic from each traffic type and period with the objective of establishing the period during which the traffic has the highest fatigue damage potential and the significance of historical loads in fatigue life assessment. The most damaging train and maximum fatigue damage of any train for all structural components described in section 4.3.3 are shown in fig. 4.2.

The figure shows that freight traffic after 1960 and especially 1985 generally has the highest fatigue damage potential of all historic traffic. This is due to high axle loads and distributed loading of the freight wagons from this period, which means that the higher stress magnitudes and the relatively large number of wagons in these freight trains facilitated a high number of stress cycles [42].

Overall, more modern traffic has a higher fatigue damage potential than older traffic, although there are important exceptions to this general conclusion. Passenger trains in the period 1900–1960 have a slightly higher fatigue damage potential for longer structures than more modern passenger trains, see e.g., results for influence line 4, 5, 6 at lengths longer than 23.0 m. Historical loads have a higher fatigue damage potential for longer influence lines due to the high distributed loading of steam locomotives from this period compared to more modern traffic, where distributed loading rather than axle load magnitudes determine the stress cycle magnitude for longer influence lines [42].

Another general conclusion that can be drawn from the figure is that freight traffic has a higher fatigue damage potential than passenger traffic. This is clear for traffic after 1960 but also true for the majority of structural components prior to 1960. Again, there are exceptions to this general conclusion; for example, compare the fatigue damage potential of freight and passenger traffic between 1900–1960 for structural components 4, 5, 6 at lengths between 7.0 and 17.0.

Regarding the significance of historical loads to the fatigue life assessment, both

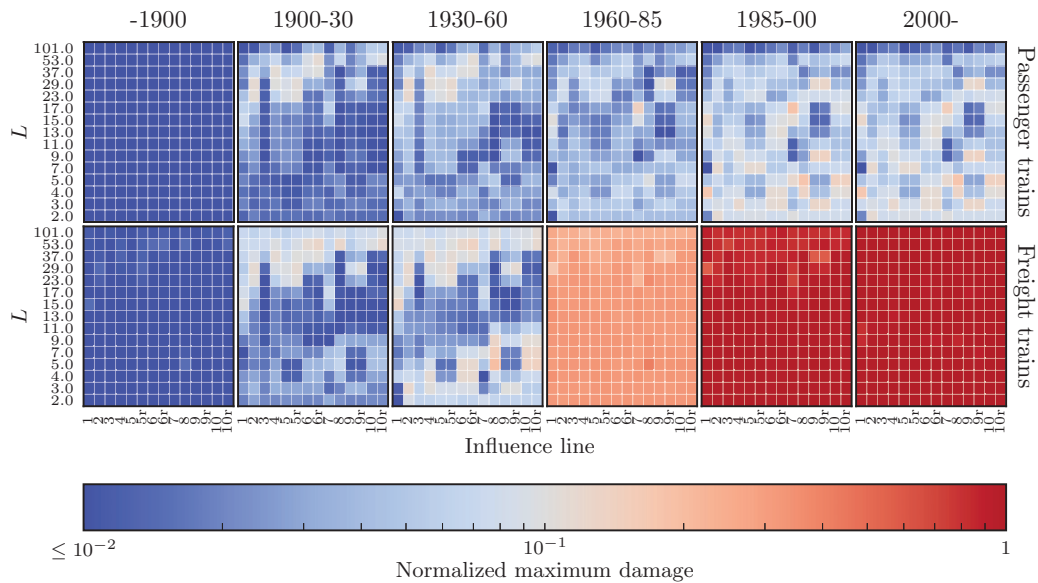


Figure 4.2: Comparison of the maximum fatigue damage induced by passenger and freight trains over the entire history of the railways. Damage is normalized against the maximum fatigue damage known for each influence line.

the fatigue damage potential and the number of trains that have traveled on the bridge must be considered. Figure 4.3 shows the number of train passages over the history of the railways for different sublines of the railway network. The number of train passages are normalized against the number of freight trains in 2000 for each subline, except for subline 25 and 37 which are normalized against the number of freight trains in 1980 and 1960, respectively, due to zero freight trains in 2000.

Consider first the significance to fatigue life of trains from the period prior to 1900. Figure 4.3 shows that there were generally a fewer number of passenger or freight trains in 1900 than there were freight trains in 2000. However, for subline 15, there were 4 times as many passenger trains in 1900, and for subline 23, there were twice the number of freight trains in 1900 than there were freight trains in 2000. Figure 4.2 shows that the fatigue damage potential of trains from the period prior to 1900 is two orders of magnitude lower than modern freight traffic after 1985. This means that the fatigue damage contribution from trains from the period prior to 1900 is less than 4% of the contribution from modern freight trains.

Next, consider the significance of trains from the period 1900–1930 to fatigue life of railway bridges. Figure 4.2 shows that the fatigue damage potential of passenger or freight trains from this period for the influence lines of longer lengths is

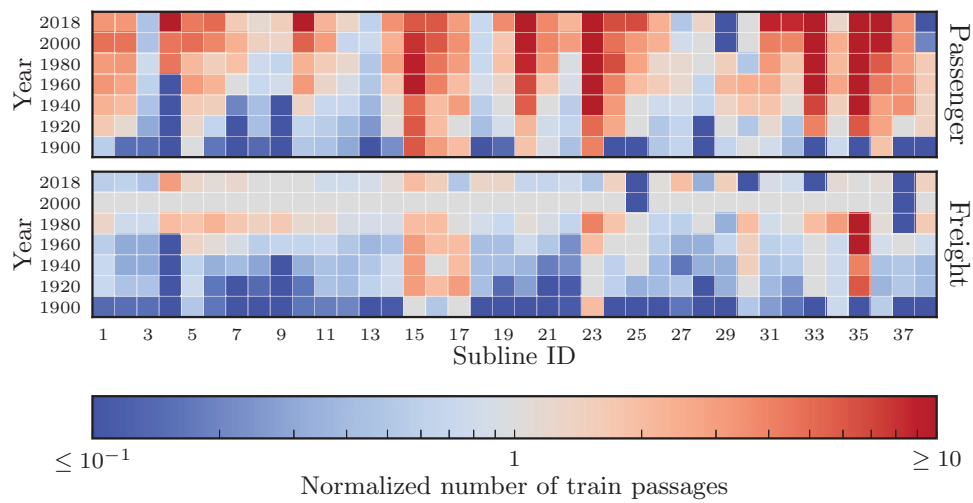


Figure 4.3: Number of train passages over the history of the railways for different lines in the Norwegian railway network normalized against the number of freight trains in 2000, see table 4.B.3 for subline ID.

approximately 10% of the fatigue damage potential of modern freight trains. Figure 4.3 shows that there are a number of sublines that have an equal or higher number of passenger or freight trains in 1900 than modern freight trains. The fatigue damage contribution of trains from the period 1900–1930 is therefore upwards of 10% of the fatigue damage contribution for structural components with longer length.

For the periods after 1930, both the fatigue damage potential and the number of train passages increases even further for both freight and passenger traffic, and an even greater contribution to fatigue damage can be expected from historic traffic than that of the period 1900–1930. For instance, fig. 4.3 shows that the number of passenger trains for many of the sublines is much greater than the number of modern freight trains, such that the contribution from passenger traffic may be greater than that for freight traffic, despite the lower fatigue damage potential of passenger trains.

Based on the discussion above, one can conclude that the fatigue damage contribution of passenger and freight trains from the period prior to 1900 is insignificant compared to modern train traffic and that the significance of both passenger and freight trains from 1900 onward will increase and be significant to the fatigue life estimation of Norwegian railway bridges. Since the fatigue damage contribution from trains prior to 1900 is insignificant and considering the fact that the number



of bridges that were built prior to 1900 are relatively few, a load model for trains prior to 1900 will not be established.

#### 4.4.2 Load model based on existing reference trains

A fatigue load model consists of a collection of reference trains and a corresponding traffic mix that should ideally induce the same fatigue damage as the most damaging train for each of the train types. There exists a number of different load models in the literature that already define reference trains [23, 27, 59, 60, 123]. Using an existing set of reference trains would greatly simplify the optimization problem in eq. (4.6) as the dimensionality of the problem is reduced.

In this section, the reference trains defined by the UIC [123] and the Eurocode (EC) [27] are used to establish a load model by adjusting the traffic mix of the pre-defined reference trains. All reference trains in either UIC or EC that are described as freight trains are used to establish a load model for the most damaging freight train in traffic. The other reference trains, i.e., those not described as freight trains, are used to establish a load model for the most damaging passenger trains. For EC, this means that trains 5, 6, 7, 8, 11 and 12 are the reference trains for freight traffic, while 1, 2, 3, 4, 9 and 10 are reference trains for passenger traffic.

Note that EC provides train speeds for each individual train for calculation of the dynamic response, while UIC does not define the speed of the reference trains. In the search for new load models, the solution space includes trains that allow train speeds between 5 and 200 km/h, see section 4.4.3. To allow a fair comparison between the load models based on existing reference trains from EC and UIC with other load models presented later in this paper, the train speed of each existing reference train in EC and UIC is allowed to vary between 5 and 200 km/h.

Figure 4.4 shows the consistency of load models based on the freight and passenger reference trains from UIC [123] and the Eurocode [27].

Consider first the results for the load models of freight trains. The load model based on the freight reference trains in the UIC standard provides a better consistency with the traffic in the period up to 1960 than for the period after 1960 and until today. Conversely, the consistency of the load model based on the freight reference trains in the Eurocode is better with modern traffic after 1960 and worse with historic traffic prior to 1960. Overall, a load model based on the UIC reference trains prior to 1960 and the Eurocode reference trains in the period after 1960 yields a load model for freight traffic with a consistency of approximately 20% over the entire history of the railways.

Regarding the passenger traffic, the load model based on EC reference trains shows similar characteristic to that of freight traffic, with higher consistency in modern traffic after 1960. The load model for passenger traffic based on UIC reference trains has the best consistency with traffic in the period 1900–1930 and

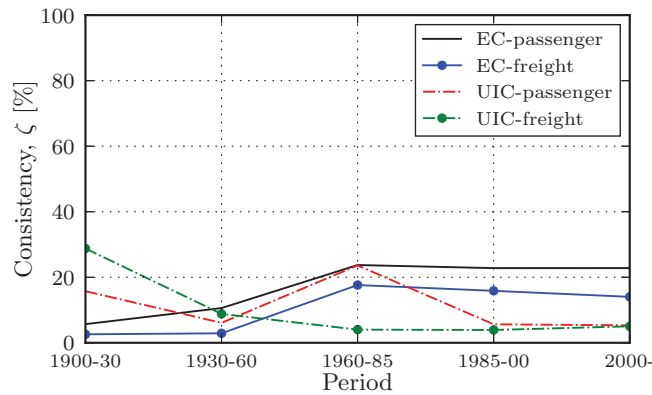


Figure 4.4: Consistency of load models for freight and passenger trains in the Norwegian railway network with optimized traffic mix of reference trains from the Eurocode [27] and the UIC leaflet 778-2 [123].

1960–1985. The consistency of the load models for passenger traffic is slightly more variable overall, with a consistency of approximately 15% prior to 1960 and 20% for the period from 1960 and until today.

One might ask why a load model based on a particular set of reference trains yields better consistency with traffic from one period than from another. This outcome is seemingly because the locomotives and wagons in the reference trains are more similar to the actual rolling stock for some periods over others. For instance, the locomotives used in the UIC reference trains are more similar in design and geometry to the steam locomotives of the older rolling stock, while the locomotives and wagons of EC trains are similar to the modern rolling stock. Thus, a load model with better overall consistency than a load model based on the reference trains from UIC and EC can be obtained if the reference trains are selected from the actual rolling stock; more discussion on this topic is provided in the next section.

Overall, load models based on the existing reference trains in EC and UIC provide a consistency of approximately 20%. As mentioned in section 4.2.2, the number of components that are *falsely* flagged as critical to fatigue failure is inversely proportional to the consistency of the load model. For instance, assuming that a load model has an overall consistency of 20% means that all components that in reality are only at 20% of critical damage are flagged as critical if the load model is overly conservative for that component. The higher the consistency of the load model is, the less resources wasted on reassessment and maintenance of components that in reality are perfectly fine.

It is difficult to define an absolute limit on the acceptable level of consistency

of a load model, but given the large number of components in the infrastructure, it is clear that large gains in efficiency and resource usage in maintaining the bridge stock can be made by using a load model with higher consistency. The advantages of higher consistency load models motivates the search for new reference trains.

#### 4.4.3 Which and how many new reference trains?

The optimization problem in eq. (4.6) requires that a solution space is defined for the traffic mix coefficients and the reference trains. The solution space of the traffic mix coefficients is the set of positive integers, but what train set should be used in the search for the new reference trains, and how many reference trains should the load model consist of? This section considers both of these questions to establish the parameters of the optimization problem before the new load model is presented in the next section.

##### Basis for the new reference trains

The results from the previous section indicated that the load models based on trains that were more similar to the actual trains they were representing had a higher consistency. This section investigates this result further; a load model based on one reference train from the train set of a train type and period is established for the most damaging train for each of the train types and periods. Figure 4.5 shows the consistency of load models for the most damaging train for different periods. Note that the speed of each reference train in a load model is allowed to vary between 5 and 200 km/h, i.e., the train set used in the optimization problem and search for new reference trains is modified to include and allow train speeds between 5 and 200 km/h.

Consider, for instance, a load model for the most damaging passenger train for period 1, where the bottom row of the figure shows different load models based on a reference train from the freight and passenger train sets for different periods. The highest consistency load model for the passenger trains of the 1st period is obtained for the load model based on the reference train from this same train type and period, i.e., from the passenger train set of the 1st period. The figure shows that this is also generally true for the other periods and train types, where a load model has high consistency with the actual traffic conditions if it is based on the same trains as in traffic.

There are also cases where other train sets can yield high consistency. For instance, an equally high consistency load model can be obtained for the 4th or 5th period of passenger trains with reference trains from either the 4th or 5th period passenger train sets. Comparing the locomotives and wagons of these periods of passenger trains, see table 4.A.1, it is clear that these train sets are in fact similar

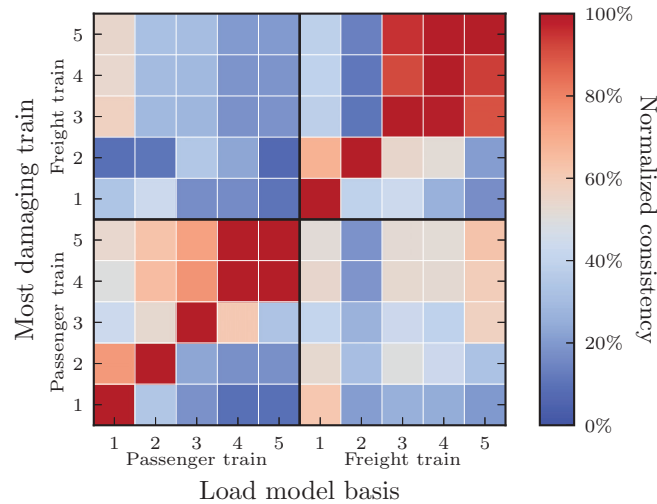


Figure 4.5: Consistency of load models for the most damaging train based on reference trains from different train sets. The consistency is normalized against the maximally known consistency for the most damaging train. The train sets 1–5 refer to the five periods from 1900–1930 to 2000– in increasing order.

and that the only difference is that there are four fewer locomotives for the 5th period than in the 4th period, i.e., the train set for the period 2000– is a subset of the train set for the period 1985–2000. This is also evident in fig. 4.2, which shows a high correlation between the fatigue damage potential for the two last periods and that the overall scale of fatigue damage potential is similar. The train set for freight trains of the 3rd-5th period also shares similarity in both the locomotive set and the wagon set such that a high consistency load model can be achieved by using reference trains from one of the other train sets.

Based on the results in this section and in the previous section, it is concluded that high consistency load models can be established by considering a solution space that is similar to the train sets it is designed to represent.

#### Number of reference trains in the new load model

Load models in the literature generally consist of more than one reference train, e.g., there are six reference freight trains in EC [27]. This section considers the influence of including more reference trains in a load model. Figure 4.6 shows the consistency of load models of the most damaging train for different train sets with between one and five reference trains. All load models are based on reference trains from the train sets of the train type and period they are representing.

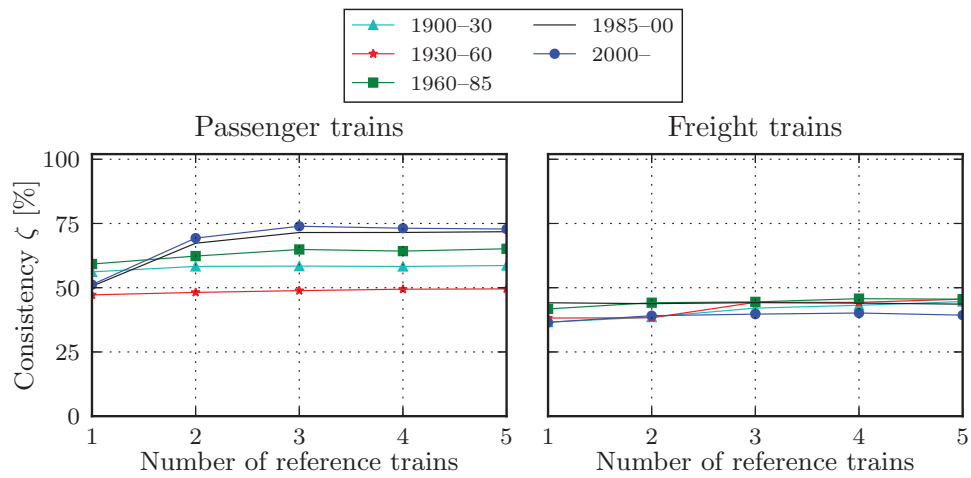


Figure 4.6: Consistency of load model with different number of reference trains

The figure shows that the consistency of load models generally improves with an increasing number of reference trains in the load model. For passenger trains in the period after 1985, the consistency is improved from approximately 50% with one reference train to 75% percent with three or more trains. The improvement is, however, modest for all of the other train sets, with only a slight increase in consistency. For instance, the consistency of a load model for passenger trains of the period 1960–1985 only increases by  $\approx 5\%$  points when the number of reference trains is increased from one to five trains.

Although there is generally an increase in consistency when the number of reference trains increases, the load model also becomes more complex, and more resources are necessary to perform the fatigue life assessment, i.e., the load model becomes less simple. Finding the optimal number of reference trains in a load model therefore becomes a tradeoff between the consistency and simplicity of the load model. For all train sets, except passenger trains for the period after 1985, the slight increase in consistency by increasing the number of reference trains does not outweigh the disadvantages of including more reference trains in the load model. The optimal number of reference trains in all train sets except passenger trains after 1985 is therefore one.

For passenger trains after 1985, there is a significant increase in consistency by increasing the number of reference trains from one to two or three. The consistency level with only one reference train is still better than that of all freight trains and roughly the same as that for the other passenger train sets. Based on these

observations and the desire to keep the load model simple, the load model for the most damaging passenger trains for the two periods after 1985 will also be based on a single reference train. All the proposed load models will therefore be based on a single reference train.

#### 4.4.4 Proposed load model

The proposed load model is defined in detail in section 4.B. The proposed load model consists of four reference trains for passenger traffic, see table 4.B.1, and four reference trains for freight traffic, see table 4.B.2. The reference trains represent traffic for the periods 1900–1930, 1930–1960, 1960–1985 and 1985–present. This means that a single reference train is used to represent traffic for both periods 1985–2000 and 2000–present. Table 4.B.1 and table 4.B.2 also show that the reference trains generally consist of fewer than four different wagon geometries, while the number of wagon geometries in the train sets presented in section 4.A are all greater than six.

The load model is a result of several iterations to simplify the final load model in terms of the number of reference trains and the variety in composition while still retaining the maximum possible consistency. The following steps have been performed to arrive at the proposed load model:

1. A baseline load model with a single reference train for each traffic type and period was established based on the train sets presented in section 4.A.
2. Simplified train sets were established for each traffic type and period by considering the most frequent wagons in the baseline load models and the characteristics of these wagons. A load model based on these simplified train sets achieves approximately the same consistency as the baseline load models.
3. The number of reference trains was reduced by considering a single reference train to represent several periods of the same traffic type and at the same time retaining the consistency of the baseline load model.

The baseline load model from the first step was established to ensure that the simplifications in the second and third step did not reduce the performance of the load model in terms of consistency. The consistency of the baseline model is essentially the same as presented for a load model with one reference train in fig. 4.6.

The second step involved a process of trial and error for each of the simplified train sets. For instance, if the two most frequent wagons in a baseline load model have very similar loads and geometries, adding the second wagon will not increase the consistency of a load model based on the resulting train set because the first

wagon can replace the second wagon without much loss in consistency. Additionally, in some of the train sets, one of the least frequently used wagons was necessary to achieve the desired consistency.

The third step resulted in a reduction from five to four reference trains for each traffic type, i.e., a single reference train is used to represent the traffic for the two train sets from 1985–2000 and 2000–present for both passenger and freight traffic. This is a result of the similarity in the train sets, see fig. 4.5 and discussion in section 4.4.3.

Figure 4.7 shows the consistency of the proposed load model with the historic traffic in the Norwegian railways.

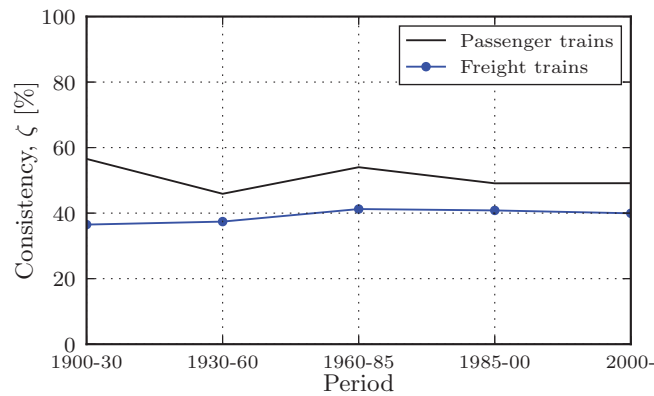


Figure 4.7: Consistency of the proposed load model for freight and passenger trains.

The consistency of the proposed load model is approximately 40% for freight traffic and 50% for passenger traffic. Ideally, the consistency of the load model should be 100% for the most efficient fatigue load model.

There are several reasons for the suboptimal consistency of the proposed load model. Section 4.4.3 showed that the consistency of the load model of the passenger trains for the two last periods could be increased by adding more reference trains to the load model, but it also showed that the improvement was modest beyond three trains and for the other train sets. Higher consistency could be achieved by increasing the number of reference trains, but this would also make the load model less simple.

Another reason for the suboptimal consistency of the load model may be due to the definition of the solution space for both the reference trains and the traffic mix coefficients. Section 4.4.3 showed that among the train sets defined in section 4.A, using the train set that the load model is designed to represent generally resulted in high consistency of the resulting load models. However, it is possible that there

exists a train set that allows for a fully consistent load model. Other possible solution spaces have been considered in the work of this paper but have unfortunately not been successful in improving upon the consistency displayed by the proposed load model. One possible idea to improve the consistency by changing the solution space is to allow nonphysical values for the traffic mix coefficients and the reference trains. For example, allowing negative traffic mix coefficients or negative axle loads on the locomotives and wagons might provide the flexibility necessary for the solution space to make a load model fully consistent. Allowing nonphysical values in the solution space has not been considered in this work, but may be a feasible approach to improve the consistency of a load model in future works.

Regarding the methodology used to solve the optimization problem presented in section 4.3.1, the LAHC heuristic has been shown to be effective in providing good solutions to a wide range of different problems [25, 41]. There is however a vast number of different optimization algorithms in the literature, some of that may be more effective than the LAHC algorithm for the present optimization problem. Future works may therefore explore the possibility of using other optimization heuristics to improve upon the consistency of load models.

The consequence of suboptimal consistency of the load model is that all structural components which are indicated as critical to fatigue failure cannot be ranked among each other because the load model introduces a bias in the ranking. All structural components that are indicated as critical by the load model should therefore be reassessed by finding the maximum fatigue damage by the methodology presented in [41] for each of the train sets presented in section 4.A. The relatively high consistency of the proposed load model does however mean that relatively few components will falsely be indicated as being critical to fatigue failure and therefore facilitates efficient assessment of the bridges in the infrastructure by filtering only the most critical components.

In comparison to the best possible load model based on existing reference trains from EC and UIC with an overall consistency of 20%, the proposed load model has significantly higher consistency. The proposed load model is also simpler due to considerably fewer reference trains overall. The proposed load model will therefore be more efficient in the assessment of railway bridges due to better consistency and simplicity.

#### **4.4.5 Can a load model be used on structural components that it was not calibrated for?**

Section 4.3.3 concluded that there are an infinite number of different structural components in the infrastructure and that it is impossible to include all of them in the load model calibration due to the computational demand of such a task. The structural set that is used to calibrate the load model will therefore always be



an incomplete structural set, i.e., a subset of all the structural components in the infrastructure.

To study the consequences of an incomplete structural set, new structural component sets  $\mathcal{S}_u \subseteq \mathcal{S}$  are established by bootstrapping the structural component set  $\mathcal{S}$  defined in eq. (4.7), i.e., a new structural component set with the same size as the original set is established by random sampling with replacement from the structural component set  $\mathcal{S}$ . A load model for each train type and period is then established by calibrating it against the most damaging train for all structural components in  $\mathcal{S}_u$ . The consistency and minimum relative fatigue damage of these load models are then determined for the complete structural component set  $\mathcal{S}$ . Figure 4.8 shows the consistency of 1000 different load models<sup>1</sup> calibrated on  $\mathcal{S}_u$  when applied to the superset  $\mathcal{S}$ .

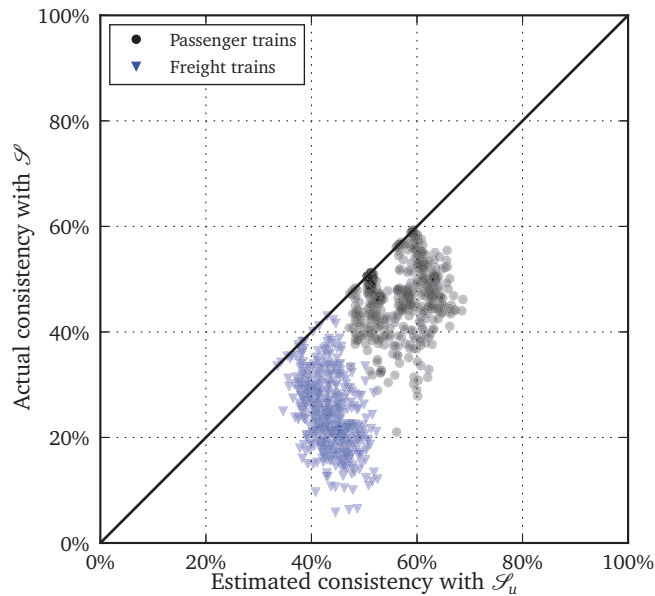


Figure 4.8: Consistency of load models calibrated with structural components  $\mathcal{S}_u \subseteq \mathcal{S}$ , when applied to structural components in  $\mathcal{S}$

The figure shows that the consistency of a load model when applied to structural components outside of the structural component set it was calibrated for will always have equal or lower consistency than what was predicted for the subset. The difference in the estimated and actual consistency can be significant, e.g., a load model for freight trains with an estimated consistency of approximately 50% can have as low as 5% consistency when applied to structural components outside

<sup>1</sup>100 load models for each train type and period

of the calibration set.

A more important question is whether the load model is still conservative when applied to structural components outside of the calibrated structural component set. Figure 4.9 shows the minimum relative fatigue damage of subset calibrated load models when applied to the superset.

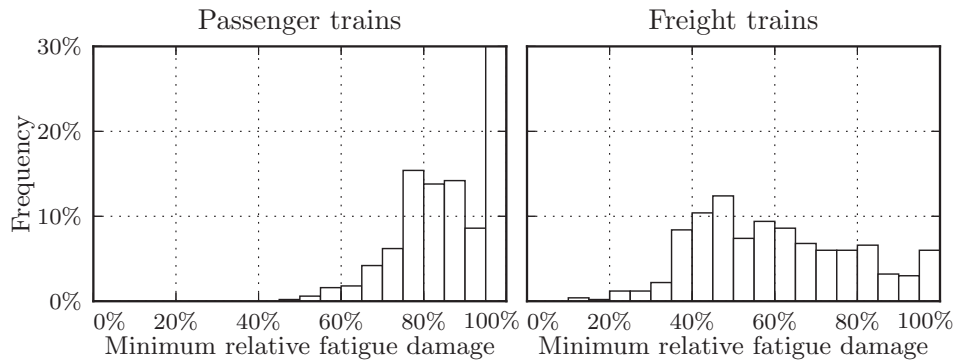


Figure 4.9: Minimum fatigue damage relative to the maximum fatigue damage for each structural component of load models calibrated with structural components  $\mathcal{S}_u \subseteq \mathcal{S}$  when applied to structural components in  $\mathcal{S}$

The minimum relative fatigue damage should be equal or greater than 100% for a conservative load model. Figure 4.9 shows that only 30% of the load models for passenger trains and 7% of load models for freight trains are conservative when applied to structural components outside of the calibration set, i.e., the majority of load models are unconservative for both passenger and freight trains.

A load model is therefore generally neither conservative nor consistent when it is applied to structural components that it was not calibrated for. The load model should therefore not be used to assess the remaining fatigue life of structural components that are not included in the calibration of the load model. This raises a new question: *How should structural components not included in the calibration set be assessed?*

#### Assessing structural components not considered in load model calibration

A typical approach to address the unconservative issues is to apply a ‘safety factor’ to the fatigue assessment, i.e., a common scaling factor is applied to the traffic mix. Considering the load models of trains in fig. 4.9, a safety factor of two would make all the passenger train load models conservative, while a safety factor of ten would be necessary for the load models for freight trains. The advantage of this approach

is that it requires little modification to the load model and additional resources to perform the assessment. Unfortunately, one cannot know what an appropriate safety factor is before the maximum fatigue damage induced by trains in the unknown structural component is established; therefore, it is always possible that the end result after applying the safety factor is unconservative. Additionally, this approach does not address the issue with decreased consistency. The fatigue life of a structural component that is assessed by adapting the load model with a safety factor can therefore not be compared to the fatigue life of structural components in the calibration set of the load model. A structural component assessed with an adapted load model that indicates critical fatigue damage must therefore always be reassessed, regardless of the criticality compared to other components.

A more rigorous approach is to determine the maximum fatigue damage from trains by the method presented in [41] and the train sets defined in table 4.A.1 and table 4.A.2. This step ensures that the overall assessment is conservative and that the expected consistency of the assessment is retained. Furthermore, the fatigue life of a structural component assessed by such an approach can be compared to the fatigue life of structural components in the calibration set determined by the load model. The disadvantage of finding the maximum damage for each structural component not in the calibration set is that it requires considerably more time and computing resources than adapting the load model with a safety factor.

To obtain the best of both approaches, we suggest that structural components that are not included in the calibration set are assessed with the proposed load model with a safety factor of two for the passenger trains and ten for the freight trains. If the fatigue life assessment shows that there is no danger of fatigue damage, e.g., the fatigue damage level is 10% or less of critical fatigue damage, the component is safe and no further assessment of the component is necessary. However, if the fatigue life assessment indicates significant fatigue damage, the component is reassessed by finding the maximum fatigue damage for each train set and influence line.

## **4.5 Conclusion**

This paper has presented a load model of historic traffic for fatigue life estimation of Norwegian railway bridges. A general framework for load model calibration has been established. The significance of historic traffic to fatigue life of Norwegian railway bridges has been considered. Traffic from the period prior to 1900 can be neglected for all lines in the railway network due to insignificant fatigue damage contribution in comparison to modern freight traffic. Freight trains from the period after 1985 have the highest fatigue damage potential, but due to a higher number of passenger trains on many of the lines in the network, the overall fatigue damage contribution from passenger trains may be larger than that from freight

trains. The presented load model is conservative for structural components that have been used in the calibration of the load model. The load model has a consistency of 40% for freight trains and a consistency of 50% for passenger trains. It has been demonstrated that a load model applied to a structural component for which it was not calibrated will generally not retain its consistency and will not be conservative. The proposed load model with a safety factor and/or identification of the most damaging train can be used to assess structural components outside of the structural component calibration set.

## Appendices

### 4.A Definition of train sets

Table 4.A.1 and table 4.A.2 define the train sets for passenger and freight trains, respectively, for each of the six periods: prior to 1900, 1900–1930, 1930–1960, 1960–1985, 1985–2000, and 2000 to present. Each train type and period has a set of locomotives  $L$  belonging to the locomotive set  $\mathcal{L}$  and a wagon set of wagons  $W$  belonging to a wagon set  $\mathcal{W}$ . The wagon set  $\mathcal{W}$  is generated from the geometry set of two-axle wagons  $\mathcal{G}_T \subset \mathbb{R}_{>0}^2$ , bogie wagons  $\mathcal{G}_B \subset \mathbb{R}_{>0}^3$  and jacobs bogie wagons  $\mathcal{G}_J \subset \mathbb{R}_{>0}^3$  and axle loads  $p \in \mathcal{P} \subset \mathbb{R}_{>0}$ ; see table 4.A.1 and table 4.A.2. Figure 4.A.1 shows the definition of the geometry and loads of the three different types of design used in the Norwegian railway network.

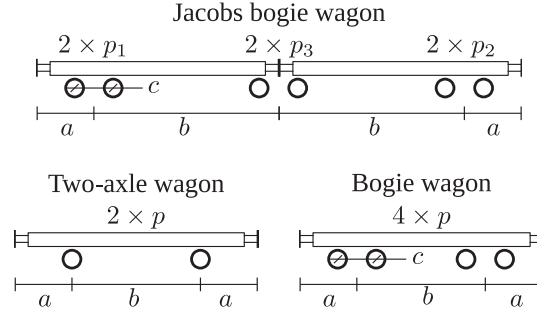


Figure 4.A.1: Design of wagons and variables defining the geometry and load of different wagon designs

The wagon set is more concisely given by:

$$\begin{aligned} \mathcal{W} &= \mathcal{W}_T \cup \mathcal{W}_B \cup \mathcal{W}_J & (4.8) \\ \mathcal{W}_T &= \{(a, b, p) \mid (a, b) \in \mathcal{G}_T \wedge p \in \mathcal{P}\} \\ \mathcal{W}_B &= \{(a, b, c, p) \mid (a, b, c) \in \mathcal{G}_B \wedge p \in \mathcal{P}\} \\ \mathcal{W}_J &= \{(a, b, c, p_1, p_2, p_3) \mid (a, b, c) \in \mathcal{G}_J \wedge p_1 \in \mathcal{P} \wedge p_2 \in \mathcal{P}, \\ &\quad p_3 = \min(p_1 + p_2, \max(\mathcal{P}))\} \end{aligned}$$

where the definition of  $p_3$  of the jacobs bogie wagon ensures that the axle loads of the middle bogie do not exceed the maximum permitted axle load on the wagon and that the two bodies of the jacobs bogie wagon can be loaded independently.

From the locomotive and wagon set, a train set  $\mathcal{T}$  can be defined as follows:

$$\mathcal{T} = \bigcup_{N=N^\downarrow}^{N^\uparrow} \mathcal{L} \times \mathcal{W}^N \quad (4.9)$$

where  $N^\downarrow \in \mathbb{N}$  and  $N^\uparrow \in \mathbb{N}$  are the minimum and maximum number of wagons in a train, respectively; see table 4.A.1 and table 4.A.2. In other words, each train  $T \in \mathcal{T}$  has one locomotive  $L \in \mathcal{L}$  followed by  $N \in \mathbb{N}[N^\downarrow, N^\uparrow]$  wagons  $W \in \mathcal{W}$ .

The speed  $v_T \in \mathbb{R}_{>0}$  of the train  $T$  is restricted by either the maximum possible speed of the locomotive  $v_L \in \mathbb{R}_{>0}$  or the maximum allowable speed  $v^\uparrow \in \mathbb{R}_{>0}$  for the train type, i.e.,

$$v_T = \min(v_L, v^\uparrow) \quad (4.10)$$

where  $v^\uparrow$  is given in table 4.A.1 and table 4.A.2 and  $v_L$  is given in table 4.A.3.

Table 4.A.1: Definition of the rolling stock for passenger trains

-1900
$N \in [1, 20]$ , $v^\uparrow = 70.0$ $\mathcal{L} = \{2'B-2[a, c]\}$ , $\mathcal{P} = \{5.0, 6.0, 7.0, 8.0, 9.0\}$ $\mathcal{G}_T = \{(2.3, 4.2), (2.6, 4.2), (2.8, 4.2)\}$ $\mathcal{G}_B = \{(3.1, 11.3, 2.0), (3.1, 11.8, 2.0), (3.1, 11.3, 2.1), (3.2, 11.2, 2.1), (3.2, 12.0, 2.1)\}$
1900-1930
$N \in [1, 20]$ , $v^\uparrow = 90.0$ $\mathcal{L} = \{2'D-2'2[a, b], 2'C-2'2[a, b], 2'B-2[a, c]\}$ , $\mathcal{P} = \{5.0, 6.5, 8.0, 9.5, 11.0\}$ $\mathcal{G}_B = \{(2.4, 13.4, 2.1), (2.8, 13.2, 2.1), (2.8, 14.4, 2.1), (2.9, 12.5, 2.1), (2.9, 13.5, 2.1), (2.9, 13.7, 2.1), (2.9, 13.8, 2.1), (2.9, 13.8, 2.3), (2.9, 11.6, 1.9), (2.9, 13.1, 2.1), (2.9, 13.4, 2.1), (2.9, 13.6, 2.1), (2.9, 14.1, 2.3), (2.9, 14.4, 2.1), (2.9, 14.4, 2.3), (3.0, 13.6, 2.1), (3.0, 14.4, 2.3), (3.0, 14.1, 2.3), (3.1, 14.0, 2.3), (3.1, 14.2, 2.3), (3.1, 14.1, 2.3), (3.1, 14.4, 2.3)\}$
1930-1960
$N \in [2, 20]$ , $v^\uparrow = 90.0$ $\mathcal{L} = \{B'B[a, b], 2'C-2'2[a, b], 2'D-2'2[a, b]\}$ , $\mathcal{P} = \{6.0, 7.5, 9.0, 10.5, 12.0\}$ $\mathcal{G}_B = \{(2.0, 16.0, 2.6), (3.0, 14.4, 2.3), (3.1, 13.4, 2.3), (3.2, 11.8, 2.1), (3.3, 14.4, 2.5), (3.4, 14.4, 2.5), (3.5, 14.5, 2.6), (3.7, 16.0, 2.6), (3.8, 15.0, 2.6), (3.8, 15.5, 2.5), (3.8, 15.5, 2.6), (3.8, 16.0, 2.6), (3.8, 16.0, 2.5), (3.8, 13.2, 3.0), (3.8, 13.2, 2.5), (3.8, 13.4, 3.0)\}$
1960-1985
$N \in [3, 20]$ , $v^\uparrow = 120.0$ $\mathcal{L} = \{B'B[a, b], Co'Co[a, b], Bo'Bo[a, b]\}$ , $\mathcal{P} = \{7.5, 8.9, 10.2, 11.6, 13.0\}$ $\mathcal{G}_B = \{(3.1, 13.4, 2.3), (3.2, 11.8, 2.1), (3.3, 14.4, 2.5), (3.4, 14.4, 2.5), (3.5, 14.5, 2.6), (3.7, 16.0, 2.6), (3.8, 15.0, 2.6), (3.8, 15.5, 2.5), (3.8, 15.5, 2.6), (3.8, 16.0, 2.3), (3.8, 16.0, 2.5), (3.8, 16.0, 2.6), (3.8, 13.2, 3.0), (3.8, 13.2, 2.5), (3.8, 13.4, 3.0), (4.0, 16.0, 2.5), (4.0, 17.4, 2.5), (4.0, 18.2, 2.5)\}$
1985-2000
$N \in [5, 20]$ , $v^\uparrow = 160.0$ $\mathcal{L} = \{Co'Co[a, f], Bo'Bo[a, f]\}$ , $\mathcal{P} = \{8.5, 9.9, 11.2, 12.6, 14.0\}$ $\mathcal{G}_B = \{(3.8, 16.0, 2.5), (3.8, 16.0, 2.6), (4.0, 16.0, 2.5), (4.0, 19.1, 2.5), (4.0, 17.4, 2.5), (4.0, 18.2, 2.5)\}$
2000-
$N \in [5, 20]$ , $v^\uparrow = 160.0$ $\mathcal{L} = \{Co'Co[c, f], Bo'Bo[c, f]\}$ , $\mathcal{P} = \{8.5, 9.9, 11.2, 12.6, 14.0\}$ $\mathcal{G}_B = \{(3.8, 16.0, 2.5), (3.8, 16.0, 2.6), (4.0, 16.0, 2.5), (4.0, 19.1, 2.5), (4.0, 17.4, 2.5), (4.0, 18.2, 2.5)\}$

Table 4.A.2: Definition of the rolling stock for freight trains

-1900		
$N \in [10, 50]$ , $v^\dagger = 50.0$	$\mathcal{L} = \{1'C-3[a, c]\}$ , $\mathcal{P} = \{2.3, 4.0, 5.6, 7.3, 9.0\}$	
$\mathcal{G}_T = \{(1.5, 2.9), (1.6, 3.7), (1.8, 2.8), (1.9, 3.1), (1.9, 3.0), (1.9, 3.7), (2.0, 3.7), (2.0, 3.2), (2.1, 3.8), (2.2, 4.0), (2.2, 3.8), (2.3, 3.7), (2.5, 4.0), (2.5, 3.9)\}$		
1900-1930		
$N \in [10, 50]$ , $v^\dagger = 65.0$	$\mathcal{L} = \{1'D-2'2'[a, d], 1'C-3[a, c]\}$ , $\mathcal{P} = \{3.0, 5.2, 7.5, 9.8, 12.0\}$	
$\mathcal{G}_T = \{(1.4, 2.8), (1.5, 2.9), (1.6, 3.7), (1.8, 3.2), (1.8, 2.0), (1.9, 3.4), (2.0, 3.7), (2.1, 4.0), (2.1, 3.7), (2.3, 3.7), (2.3, 4.0), (2.4, 4.0), (2.4, 4.4), (2.5, 3.9), (2.6, 4.5)\}$		
1930-1960		
$N \in [10, 50]$ , $v^\dagger = 65.0$	$\mathcal{L} = \{B'B'[a, b], 1'D-2'2'[a, d], 1'E-2'2'[a]\}$ , $\mathcal{P} = \{3.7, 6.5, 9.4, 12.2, 15.0\}$	
$\mathcal{G}_T = \{(1.6, 3.7), (1.9, 3.2), (1.9, 6.0), (2.0, 3.2), (2.1, 7.2), (2.2, 5.3), (2.4, 4.0), (2.5, 5.9), (2.7, 4.0), (2.7, 6.0)\}$		
1960-1985		
$N \in [10, 50]$ , $v^\dagger = 80.0$	$\mathcal{L} = \{B'B'[a, b], Co'Co'[a, b], Bo'Bo'[a, b]\}$ , $\mathcal{P} = \{5.0, 8.2, 11.5, 14.8, 18.0\}$	
$\mathcal{G}_T = \{(1.6, 9.0), (2.0, 7.5), (2.3, 6.5), (2.3, 9.0), (2.4, 5.7), (2.5, 9.0), (2.6, 5.7), (2.6, 9.0), (2.7, 5.7), (2.9, 8.0), (3.0, 8.0), (3.1, 8.0)\}$		
$\mathcal{G}_B = \{(2.5, 9.0, 1.8), (2.5, 10.7, 1.8), (2.5, 15.7, 1.8), (3.2, 10.3, 1.8)\}$		
1985-2000		
$N \in [10, 50]$ , $v^\dagger = 80.0$	$\mathcal{L} = \{Co'Co'[a, f], Bo'Bo'[a, f]\}$ , $\mathcal{P} = \{5.6, 9.8, 14.0, 18.3, 22.5\}$	
$\mathcal{G}_T = \{(2.0, 7.5), (2.0, 8.5), (2.4, 5.7), (2.5, 9.0), (2.6, 9.0), (2.7, 9.3), (2.9, 8.0), (3.0, 8.0), (3.1, 9.0), (3.1, 8.0), (3.3, 9.0), (3.6, 10.0), (3.8, 9.0), (4.1, 9.0)\}$		
$\mathcal{G}_B = \{(2.5, 9.0, 1.8), (2.5, 10.7, 1.8), (2.5, 15.7, 1.8), (3.2, 10.3, 1.8)\}$		
2000-		
$N \in [10, 50]$ , $v^\dagger = 90.0$	$\mathcal{L} = \{Co'Co'[c, f], Bo'Bo'[c, f]\}$ , $\mathcal{P} = \{5.6, 9.8, 14.0, 18.3, 22.5\}$	
$\mathcal{G}_T = \{(2.0, 7.5), (2.0, 8.5), (2.3, 9.0), (2.5, 9.0), (2.6, 9.0), (2.7, 9.3), (2.9, 8.0), (3.0, 8.0), (3.1, 9.0), (3.1, 8.0), (3.3, 9.0), (3.6, 10.0), (3.8, 9.0), (4.1, 9.0)\}$		
$\mathcal{G}_B = \{(2.5, 8.5, 1.8), (2.5, 9.0, 1.8), (2.5, 15.7, 1.8), (2.5, 9.9, 1.8), (2.5, 10.7, 1.8), (3.2, 10.3, 1.8)\}$		
$\mathcal{G}_J = \{(2.5, 14.9, 1.8), (2.8, 14.2, 1.8), (2.8, 14.4, 1.8)\}$		

Table 4.A.3: Maximum speed of the locomotives  $v_L$ .

Class	Subclass	Maximum speed $v_L$ [km/h]
1'C-3	(a,b,c)	(60.0, 60.0, 60.0)
1'D-2'2'	(a,b,c,d)	(45.0, 45.0, 40.0, 45.0)
1'E-2'2'	(a)	(70.0)
2'B-2	(a,b,c)	(60.0, 55.0, 70.0)
2'C-2'2'	(a,b)	(90.0, 65.0)
2'D-2'2'	(a,b)	(70.0, 70.0)
B'B'	(a,b)	(70.0, 70.0)
Bo'Bo'	(a,b,c,d,e,f)	(105.0, 115.0, 200.0, 120.0, 140.0, 140.0)
Co'Co'	(a,b,c,d,e,f)	(143.0, 120.0, 160.0, 120.0, 120.0, 140.0)

## 4.B Load model of historic traffic for fatigue life estimation of Norwegian railway bridges

Table 4.B.1 and table 4.B.2 presents the reference trains and traffic mix coefficients of the proposed load model for passenger and freight traffic, respectively. Each of the reference trains are defined by a locomotive (L) and between two and four base wagons (A, B, C, D). The composition of the locomotive and the base wagons into a reference train is given by the loop shown below the locomotives and base wagons. The load of the base wagons is modified by the load modifier given above the wagon identifier in the loop. As an example, the locomotive and the first two wagons of reference train 8 is given below:

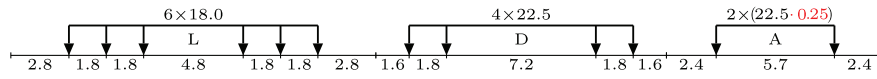


Figure 4.B.1: The locomotive and two first wagons of reference train 8. Note the modifier applied to the load of the second wagon.

Table 4.B.3 presents the yearly number of freight and passenger train for the Norwegian railways in the years 1900, 1920, 1940, 1960, 1980, 2000 and 2018. The total number of train passages  $n_0$  for a subline during a particular period can be determined by integration of table 4.B.3. Note that the traffic mix coefficient  $a_i$  for reference train  $i$  together with the number of train passages  $n_0$  must be used to determine the total number of passages  $n_i$  by reference train  $T_i$  in fatigue assessment, i.e.,

$$n_i = a_i n_0 \quad (4.11)$$

The total fatigue damage  $D$  induced by the load model in a structural component  $S$  is determined by

$$D = \sum_{i=1}^8 n_i d(S, T_i) \quad (4.12)$$

where  $d(S, T_i)$  is the fatigue damage function. If the fatigue load model is not applicable, e.g., if  $S$  is a structural component not included in the calibration set and/or the safety factor approach suggested in section 4.4.5 is not satisfactory, the total fatigue damage can be determined by finding the maximum fatigue damage  $d^{\uparrow}(S)$  for each traffic type and period in section 4.A, the corresponding number of train passages  $n_0$  from table 4.B.3 and summing over all traffic types and periods.



Table 4.B.1: Reference trains for passenger traffic. Axle loads are given in tonnes and axle pitch is given in metres.

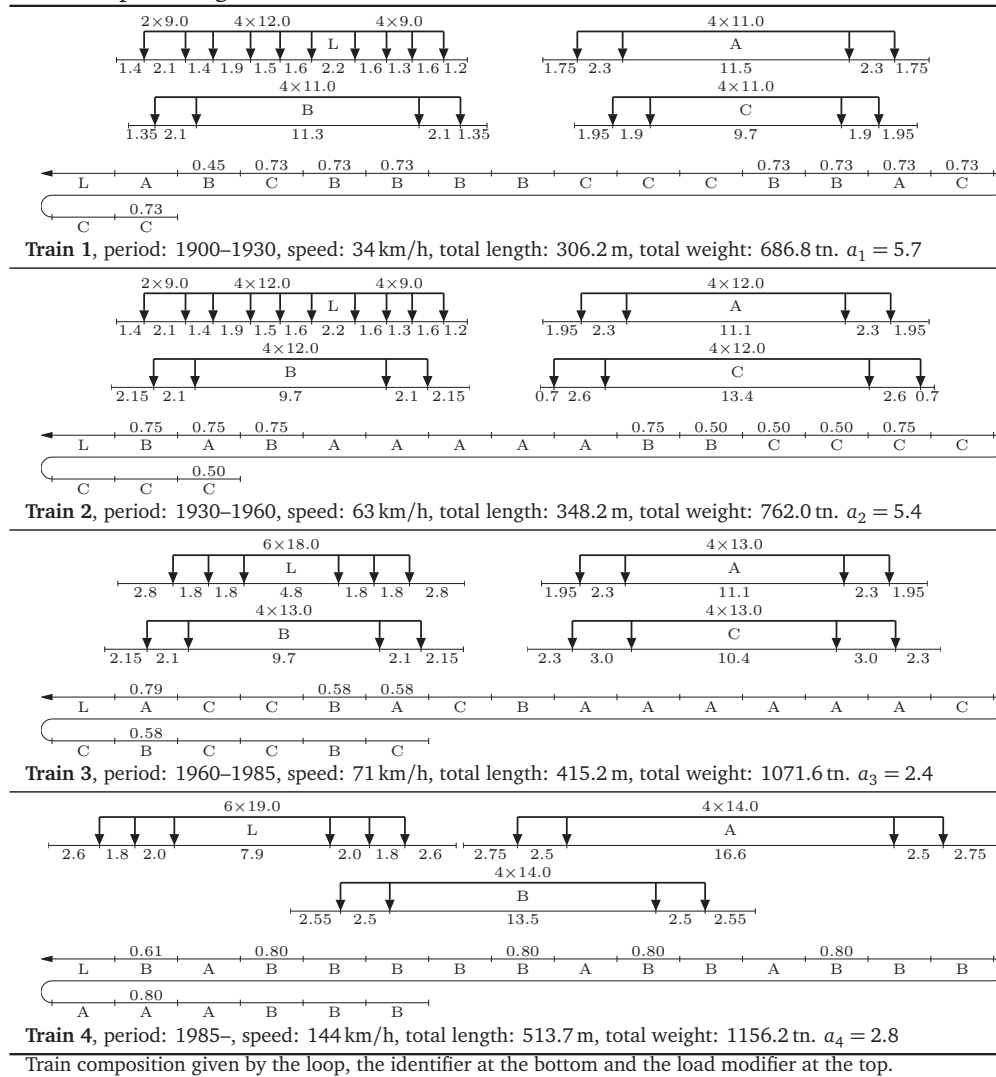


Table 4.B.2: Reference trains for freight traffic. Axle loads are given in tonnes and axle pitch is given in metres.

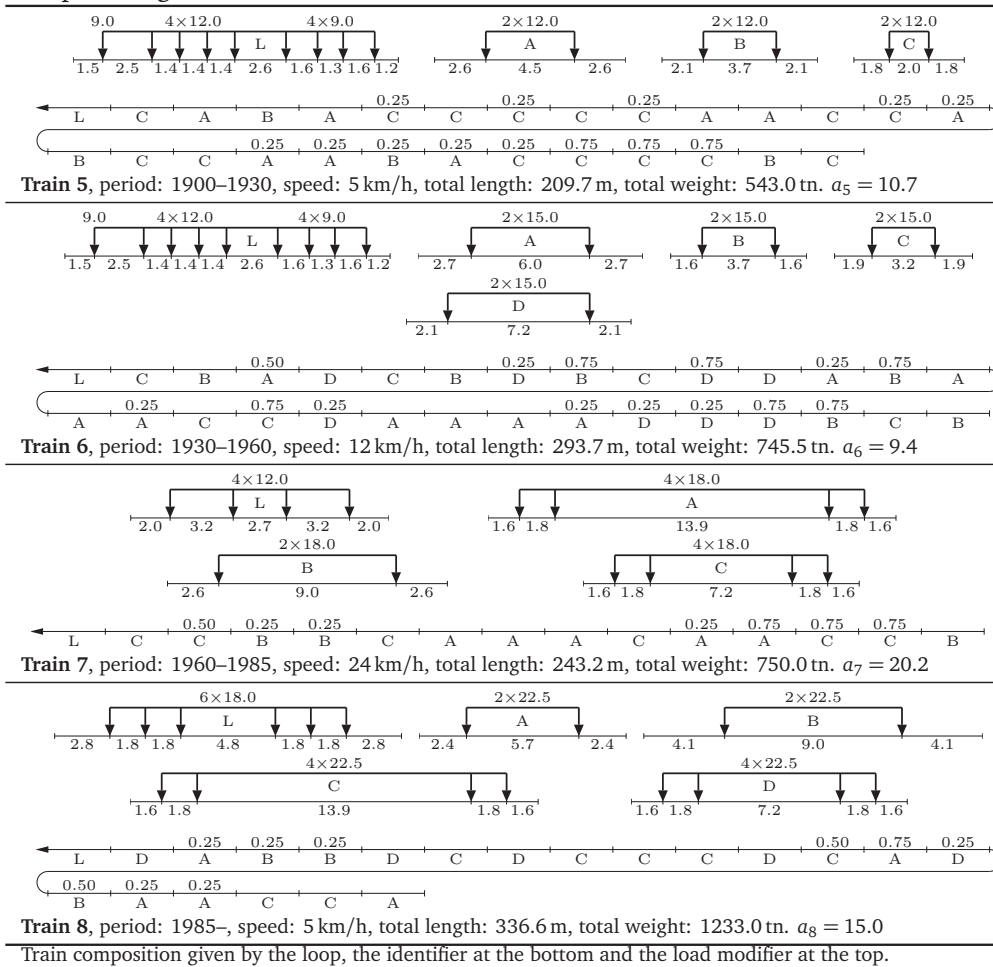


Table 4.B.3: Yearly number of freight and passenger train passages on sublines in the Norwegian railway network.

Line	ID	Subline		Freight trains										Passenger trains									
		Terminal A	Terminal B	1900	1920	1940	1960	1980	2000	2018	1900	1920	1940	1960	1980	2000	2018						
Nordlandsbanen	01	Trondheim	Hell	730	3650	3650	2920	6570	5110	2920	2920	8995	12045	16790	16060	24455	16790						
	02	Hell	Steinkjer	730	2190	1460	1460	3650	4745	2920	730	5475	9490	13140	15330	21900	15330						
	03	Steinkjer	Mo i Rana	730	2190	1460	1460	3650	4745	2190	730	1460	2190	2920	3650	2190	2190						
	04	Mo i Rana	Bodø	0	0	0	0	1460	730	2190	0	0	0	0	3285	3285	7300						
Søtlandsbanen	05	Drammen	Hokksund	2920	4380	3650	7665	10220	5840	7300	5840	7300	9490	17885	12045	28470	25550						
	06	Hokksund	Nordagutu	730	730	1460	4745	9855	4380	4745	730	2920	6570	9855	6570	16790	21900						
	07	Nordagutu	Nelau	0	1460	3285	6205	3650	4380	0	0	730	3650	6935	8760	5840	5840						
	08	Nelau	Kristiansand	365	730	1460	2920	7300	5110	5110	730	2190	2190	3650	4015	7300	5840						
	09	Kristiansand	Egersund	0	0	0	2920	7300	4380	4380	0	0	0	3650	2920	5840	6570						
Dovrebanen	11	Eidsvoll	Hamar	1460	3650	3650	5840	9490	8030	6570	3650	4380	5840	10220	12410	24820	18250						
	12	Hamar	Dombås	1460	2920	2920	3650	6570	7300	5840	2190	2920	5110	6570	8760	5110	9490						
	13	Dombås	Støren	0	3650	2920	2190	5110	5840	5110	0	1460	2190	2920	2920	4380	3650						
	14	Støren	Trondheim	730	5110	5110	2920	5840	6570	6935	1460	6935	7300	11315	18980	15695	22630						
Rørosbanen	15	Hamar	Elverum	730	2190	2190	1460	1460	730	1460	4380	4380	3650	8030	6570	5840	4380						
	16	Elverum	Røros	365	1460	730	1460	1460	730	1095	2190	1460	1460	2920	3285	4380	4380						
	17	Røros	Støren	730	2190	1460	1460	730	730	365	1460	730	2190	1460	2190	2555	2190						
Bergensbanen	18	Hønefoss	Myrdal	365	730	2190	2190	4380	5110	6570	0	2190	2920	4380	3650	3650	3650						
	19	Myrdal	Bergen	365	730	2190	2190	3650	5110	6570	730	4380	5110	6570	9490	8760	18980						
Østfoldsbanen w.	20	Oslo S	Ski	730	2190	2920	6205	8760	8030	5475	14600	17520	45260	54385	68620	74460	81760						
	21	Ski	Sarpsborg	730	730	1460	4015	7300	8030	5475	7300	6570	8030	13870	26280	30660	29930						
	22	Sarpsborg	Kornsjø	730	730	1460	1460	4380	6570	5110	2920	4380	3650	5840	6205	19710	14600						
Vestfoldsbanen	23	Drammen	Eidanger	1460	730	730	1460	2920	730	365	2920	2920	3650	7300	8760	16060	18250						
	24	Oslo S	Roa	0	2190	2190	3650	6570	3650	5110	0	9490	11680	14600	23725	17520	24090						
Kongsvingerbanen	25	Roa	Gjøvik	0	730	2190	2190	2190	0	0	0	2190	2190	4380	6205	6935	14600						
	26	Lillestrøm	Kongsvinger	730	2920	2920	4015	4745	7300	7665	3650	3650	5840	11315	8760	17520	17520						
Raumabanen	27	Kongsvinger	Ch.berg	730	2190	730	1460	2555	4380	8395	2920	2920	3650	5110	5110	3650	2190						
	28	Dombås	Åndalsnes	0	0	730	730	2190	2190	730	0	0	1460	1460	2190	2190	2920						
Meråkerbanen	29	Kongsvinger	Elverum	0	730	730	1460	730	2190	3285	1460	2190	2920	4745	3285	0	0						
	30	Hell	Storlien	730	1460	2190	2190	2920	1460	0	1460	730	2555	3650	730	1460	1460						
Hovedbanen	31	Oslo S	Lillestrøm	4380	6570	8030	9855	14235	16790	14965	13870	19710	29930	43070	54020	70080	146730						
	32	Lillestrøm	Eidsvoll	1460	2190	4745	5840	8760	8760	6935	3650	3650	4380	9490	12775	16060	33580						
Østfoldsbanen e.	33	Ski	Sarpsborg	0	730	730	730	1460	730	0	0	2920	5110	7300	9490	12410	15330						
	34	Hokksund	Hønefoss	2190	2190	2190	2190	8760	2920	3285	2190	2920	4380	8030	6205	7300	3650						
Bratsbergbanen	35	Eidanger	Nordagutu	0	2190	1460	3650	4015	365	365	0	2190	6570	4380	4380	6570	7300						
	36	Oslo S	Drammen	4380	2920	3650	6935	8760	8030	8760	14600	22630	23360	34675	47450	75190	173010						
Arendalsbanen	37	Nelau	Arendal	0	730	730	1460	0	0	0	0	1460	5110	5110	4380	5110	5110						
	38	Roa	Hønefoss	0	1460	1460	2920	5840	3650	5110	0	5110	5110	5840	5840	730	0						

## Chapter 5

# Conclusion

### 5.1 Concluding remarks

**Available historic load data for estimation of remaining fatigue life of steel railway bridges** The available load data for estimation of remaining fatigue life of steel railway bridges in the Norwegian railway network has been presented in chapter 2. Characteristics of rolling stock, permissible loads and speed on the infrastructure and regulation of operation of trains are considered for the railways between 1852 and present. It is shown that the capacities of both rolling stock and infrastructure limit the load conditions in the railway infrastructure. The available data does not permit that the exact realization of the load condition at a bridge site to be determined, but all trains that possibly operated the railway infrastructure during a particular time can be established by data on loads and geometry of locomotives and wagons together with documentation on how the trains were operated. The trains that operated the infrastructure can therefore be determined, but not which of them passed a particular bridge.

**Methodology to determine the conservative load case given the available load data for the Norwegian railways** Chapter 3 presented a methodology to find the most damaging train composition for an arbitrary structural component given the possible trains in the infrastructure during a period. The methodology therefore determines the conservative load case for passenger and freight traffic over the history of the Norwegian railways.

**Significance of historic loads in fatigue life estimation** Chapter 2 showed that the axle loads, geometry, design, composition and operation of both passenger and freight trains has changed multiple times over the railways history. Axle loads on all rolling stock as well as permissible axle loads on infrastructure have generally

increased since the initial construction of the railways. Similarly, the maximum possible speed of locomotives and the permissible speed on the infrastructure have increased. The distributed loading of locomotives was highest for steam locomotives from the period 1900 to 1960 and the distributed on passenger wagons have remained largely unchanged since 1900, while the distributed loading of freight trains have increased moderately. This indicates that the fatigue damage contribution of historical loads to structural components which are sensitive to distributed loading rather than axle loads will be significant.

Chapter 4 considers both the fatigue damage potential of passenger and freight trains as well as the number of train passages on different lines in the railway network over the history of the railways. The fatigue damage potential is greatest for freight trains for the period after 1985. Generally, the fatigue damage potential of freight trains is greater than passenger trains and the fatigue damage potential of modern trains is greater than historical trains. There are however structural components where passenger trains and historic trains have a higher damage potential than freight and modern trains, respectively. The fatigue damage contribution from both passenger and freight traffic after 1900 are therefore significant to the fatigue life of Norwegian railway bridges, and the fatigue damage contribution of passenger trains may be greater than that from freight trains due to considerably higher number of train passages.

It is concluded that the fatigue damage of traffic prior to 1900 is insignificant to the fatigue life of Norwegian railway bridges, while both passenger and freight trains from after 1900 have a significant fatigue damage contribution for certain lines and structural components in the infrastructure and must be included in fatigue life assessment of Norwegian railway bridges.

#### **Conservative fatigue load model based on the available Norwegian traffic data**

Chapter 4 presents a general framework for establishing and calibrating a load model to the conservative load case for structural components in the infrastructure. The framework is used to establish a conservative load model of historic traffic based on the available data for the Norwegian railway network. The load model is calibrated considering a limited, but extensive set of influence lines of different shape and lengths. It is demonstrated that the fatigue load model is not conservative when applied to structural components not considered in the calibration of the load model. Using a safety factor with the proposed load model or using the methodology to establish the conservative load case is suggested as approaches to make a conservative assessment of fatigue life of structural components not considered in the calibration of the load model.

## 5.2 Suggestions for further work

### **Develop and implement a load monitoring system for the Norwegian railway network**

This thesis has shown that modern freight trains have a fatigue damage potential that are orders of magnitude higher than historic passenger and freight trains. Some bridges in the infrastructure will fail a verification with the most damaging train assumption. Many more bridges are likely to fail under the assumption of most damaging train if this load is projected into the future, it will therefore be impossible to verify and document sufficient fatigue life of these bridges by the assumption of most damaging train and the data available in the literature.

It has also been established that direct measurements of the basic variables of a train, i.e. the axle loads, axle spacing and train speed, is necessary to obtain an accurate load model of the traffic and thereby an accurate estimate of the fatigue damage induced in bridges in the infrastructure. Field measurements in the Norwegian railway network [47] and other countries [67, 83] indicate that the actual traffic loads are less severe than those of the most damaging train.

Future research should therefore focus on developing a traffic load monitoring system that gives a precise description of the actual traffic loads in the railway network such that the safety of bridges in the railway network can also be verified in the future.

### **Present a case study with the proposed load model**

A case study on a bridge in the Norwegian railway network should be conducted to demonstrate the use of the proposed load model. The case study should include a structural component which was not considered in the calibration of the load model and the case study should demonstrate the suggested alternative approach to assess this structural component. The case study can be used to establish a best practice for conducting a fatigue assessment of Norwegian railway bridges with the presented load model and a standard format of reporting fatigue life assessment of Norwegian railway bridges. Establishing best practice and a standardized format for reporting fatigue life analysis allows that a portfolio of bridges can be assessed effectively and that assessment reports on one bridge can easily be compared to that from another bridge.

### **Adapt the imprecise probability framework in service life assessment of railway bridges**

Chapter 2 concluded that the available data on traffic loads in the Norwegian railway network could not be used to establish neither a deterministic or a precise prob-

abilistic description of the load conditions in the railway network. The available load data is imprecise and cannot be included in a traditional probabilistic reliability framework without making assumptions about the probability distribution of the loads. The framework of imprecise probabilities can combine both probabilistic and non-probabilistic information in the assessment of remaining fatigue life. Probabilistic information on the other basic variables of a fatigue life assessment, e.g. the fatigue endurance, can then be included in the analysis together with the available data on load conditions to fully utilize all the available information and maximize the precision of fatigue life estimates.

Furthermore, the imprecise probability framework can be used in a sensitivity analysis to identify the most important variables of a fatigue life assessment. Such sensitivity analysis can therefore be used to direct further data gathering towards the most important variables of the analysis to improve the fatigue life estimates with maximum efficiency.

#### **Consider other heuristics to determine the conservative load case**

A novel methodology to find the conservative load case given the possible trains has been presented in chapter 3. The methodology is based on the Late Acceptance Hill Climbing heuristic and was selected due to its high efficiency in finding the most damaging train compared to other considered methodology and simplicity in both implementation and application. The field of combinatorial optimization is however vast, and there exists a large number of different methods ranging from evolutionary algorithms to neural networks, all of which has different advantages. It is therefore possible that a more efficient heuristic exists that can be used to identify the conservative load case in fatigue life assessment. Improving the efficiency in finding the conservative load case will also improve the efficiency of fatigue life assessment of the infrastructure.

# References

- [1] B. Åkesson. *Fatigue Life of Riveted Steel Bridges*. PhD thesis, 1994.
- [2] H. Abe. Fatigue Strength of Corroded Steel Plates from Old Railway Bridge. In *IABSE Symposium (Lisbon): Durability of Structures*, volume 57/1, pages 205–210, 1989.
- [3] M. Al-Emrani and R. Kliger. FE Analysis of Stringer-to-Floor-Beam Connections in Riveted Railway Bridges. *Journal of Constructional Steel Research*, 59(7):803–818, July 2003.
- [4] A. Almar-Naess. *Fatigue Handbook: Offshore Steel Structures*. Tapir, Trondheim, 1985. ISBN 978-82-519-0662-3.
- [5] C. Amzallag, J. P. Gerey, J. L. Robert, and J. Bahuaud. Standardization of the rainflow counting method for fatigue analysis. *International Journal of Fatigue*, 16(4):287–293, 1994. ISSN 0142-1123. doi: 10.1016/0142-1123(94)90343-3.
- [6] A. Andersson. *Fatigue Assessment of Railway Bridges. [Utmattningsanalys Av Järnvägsbroar, in Swedish]*. Licentiate, Royal Institute of Technology, Stockholm, 2009.
- [7] AREA. Summary of Tests on Steel Girder Spans. In *Proceedings of the Fifty-Ninth Annual Convention of the American Railway Engineering Association*, volume 61, pages 51–78, Chicago, 1960. American Railway Engineering Association.
- [8] AREMA. Manual for Railway Engineering. Technical report, American Railway Engineering and Maintenance of Way Association, Washington D.C, 2008.
- [9] N. C. Aspenberg. *Elektrolok i Norge (In Norwegian)*. Preutz Grafisk AS, Larvik, 2001. ISBN 82-91448-42-6.



- [10] J. M. Aughenbaugh and C. J. J. Paredis. The Value of Using Imprecise Probabilities in Engineering Design. *Journal of Mechanical Design*, 128(4):969–979, 2006.
- [11] K. A. Baker and G. L. Kulak. Fatigue of riveted connections. *Canadian Journal of Civil Engineering*, 12(1):184–191, 1985. doi: 10.1139/I85-087.
- [12] B. Bakht and L. G. Jaeger. Bridge Testing—A Surprise Every Time. *Journal of Structural Engineering*, 116(5):1370–1383, 1990.
- [13] P. Basso, S. Casciati, and L. Faravelli. Fatigue reliability assessment of a historic railway bridge designed by Gustave Eiffel. *Structure and Infrastructure Engineering*, 11(1):27–37, 2015.
- [14] M. Beer, S. Ferson, and V. Kreinovich. Imprecise probabilities in engineering analyses. *Mechanical Systems and Signal Processing*, 37(1-2):4–29, 2013.
- [15] A. D. Belegundu. The Adjoint Method for Determining Influence Lines. *Computers & Structures*, 29(2):345–350, 1988. doi: 10.1016/0045-7949(88)90269-6.
- [16] T. Bjerke, T. B. Hansen, E. W. Johansson, and S. E. Sando. *Damplokomotiver i Norge (In Norwegian)*. Thorsrud AS, Lillehammer, 1987. ISBN 82-90286-09-0.
- [17] T. Bjerke, F. Holom, and O. Tovås. *Banedata Data Om Infrastrukturen Til Jernbanene i Norge (In Norwegian)*. Krona, Moss, [norwegian edition, 2013.
- [18] D. Broek. *The Practical Use of Fracture Mechanics*. Kluwer Academic Publishers, Dordrecht, The Netherlands, 1st edition, 1989. ISBN 0-7923-0223-0.
- [19] K. Bruestle and Z. Prucz. Fatigue of steel bridges. In *Proceedings of the American Railway Engineering Association*, volume 93, pages 177–197, Washington D.C, 1992. AREA.
- [20] E. Brühwiler and P. Kunz. Remaining service life of a riveted railway bridge. In *IABSE Colloquium(Copenhagen): Remaining Structural Capacity*, 1993.
- [21] E. Brühwiler, I. F. C. Smith, and M. A. Hirt. Fatigue and Fracture of Riveted Bridge Members. *Journal of Structural Engineering*, 116(1):198–214, Jan. 1990. doi: 10.1061/(ASCE)0733-9445(1990)116:1(198).
- [22] A. Bruls, J.-A. Calgaro, H. Mathieu, and M. Prat. ENV 1991 Part 3: The main models of traffic loads on road bridges; Background studies. *IABSE Colloquium: Basis of design and actions on structures; Background and application of Eurocode 1*, pages 215–228, 1996.

- [23] BSI. BS 5400: Steel, concrete and composite bridges - Part 10: Code of practice for fatigue. 1980.
- [24] E. K. Burke and Y. Bykov. The Late Acceptance Hill-Climbing Heuristic. Technical CSM-192, University of Stirling, UK, June 2012.
- [25] E. K. Burke and Y. Bykov. The late acceptance Hill-Climbing heuristic. *European Journal of Operational Research*, 258(1):70–78, 2017. doi: 10.1016/j.ejor.2016.07.012.
- [26] B. Caglayan, K. Ozakgul, and O. Tezer. Fatigue life evaluation of a through-girder steel railway bridge. *Engineering Failure Analysis*, 16(3):765–774, 2009. doi: 10.1016/j.engfailanal.2008.06.018.
- [27] CEN/TC250. *Eurocode 1: Action on Structures. Part 2: Traffic Loads on Bridges. NS-EN 1991-2*. 2003.
- [28] CEN/TC250. *Eurocode 3: Design of Steel Structures. Part 1-9: Fatigue. NS-EN 1993-1-9*. 2005.
- [29] Central Bureau of Statistics of Norway. Norges Offisielle Statistikk, Norges Jernbaner 1867-1960 (in Norwegian). Technical report.
- [30] A. Cifuentes and M. Paz. A note on the determination of influence lines and surfaces using finite elements. *Finite Elements in Analysis and Design*, 7: 299–305, 1991.
- [31] P. Croce. Background to fatigue load models for Eurocode 1: Part 2 Traffic Loads. *Progress in Structural Engineering and Materials*, 3(4):335–345, 2001. doi: 10.1002/pse.93.
- [32] A. N. Daumueller and D. V. Jáuregui. Strain-Based Evaluation of a Steel Through-Girder Railroad Bridge. *Advances in Civil Engineering*, 2012:1–12, 2012.
- [33] J. D. DiBattista, D. E. J. Adamson, and G. L. Kulak. Evaluation of remaining fatigue life for riveted truss bridges. *Canadian Journal of Civil Engineering*, 25(4):678–691, 1998. doi: 10.1139/l98-011.
- [34] J. D. DiBattista, D. E. J. Adamson, and G. L. Kulak. Fatigue Strength of Riveted Connections. *Journal of Structural Engineering*, 124(7):792–797, 1998.
- [35] S. D. Downing and D. F. Socie. Simple Rainflow Counting Algorithms. *International Journal of Fatigue*, 4(1):31–40, 1982.

- [36] C. Esveld. *Modern Railway Track*. Koninklijke van de Garde, Zaltbommel, 2nd edition, 2001. ISBN 90-800324-3-3.
- [37] A. Fatemi and L. Yang. Cumulative fatigue damage and life prediction theories: A survey of the state of the art for homogeneous materials. *International Journal of Fatigue*, 20(1):9–34, 1998. doi: 10.1016/S0142-1123(97)00081-9.
- [38] J. W. Fisher, B. T. Yen, D. Wang, and J. E. Mann. Fatigue and fracture evaluation for rating riveted bridges final report. Technical Report 0309045738, 1987.
- [39] J. W. Fisher, G. L. Kulak, and I. F. C. Smith. *A Fatigue Primer for Structural Engineers*. National Steel Bridge Alliance, 1998.
- [40] G. T. Frøseth and A. Rönquist. System Reliability Analysis of Steel Railway Bridge Based on Historic Rolling Stock Records. In *13th Nordic Steel Construction Conference*, Tampere, Finland, 2015. Tampere University of Technology. ISBN 978-952-15-3579-6.
- [41] G. T. Frøseth and A. Rönquist. Finding the train composition causing greatest fatigue damage in railway bridges by Late Acceptance Hill Climbing. 2018. Submitted for journal publication.
- [42] G. T. Frøseth and A. Rönquist. Evolution of load conditions in the Norwegian railway network and imprecision of historic railway load data. *Structure and Infrastructure Engineering*, 15(2):152–169, 2019. doi: 10.1080/15732479.2018.1504087.
- [43] G. T. Frøseth and A. Rönquist. Load model of historic traffic for fatigue life estimation of Norwegian railway bridges. 2019. Submitted for journal publication.
- [44] G. T. Frøseth, P. Nåvik, and A. Rönquist. Close range photogrammetry for measuring the response of a railway catenary system. In *Proceedings of the Third International Conference on Railway Technology: Research, Development and Maintenance*, Stirlingshire, UK, 2016. Civil-Comp Press. doi: 10.4203/ccp.110.102.
- [45] G. T. Frøseth, P. Nåvik, and A. Rönquist. Operational displacement estimations of railway catenary systems by photogrammetry and the integration of acceleration time series. 2016. Accepted for publication in *International Journal of Railway Technology*.

- [46] G. T. Frøseth, A. Rönquist, and O. Øiseth. Operational Modal Analysis and Model Updating of Riveted Steel Bridge. In *Proceedings of the 34th IMAC, A Conference and Exposition on Structural Dynamics*, volume 2 of *Dynamics of Civil Structures*. Springer International Publishing, 2016. doi: 10.1007/978-3-319-29751-4\_23.
- [47] G. T. Frøseth, A. Rönquist, D. Cantero, and O. Øiseth. Influence line extraction by deconvolution in the frequency domain. *Computers & Structures*, 189:21–30, Sept. 2017. doi: 10.1016/j.compstruc.2017.04.014.
- [48] G. T. Frøseth, A. Rönquist, and O. Øiseth. Prediction Error in Strain Response in Finite Element Simulations with Moving Load Formulation of Train Passages of Open Deck Steel Bridges. In *First International Conference on Rail Transportation: Railway Development, Operations, and Maintenance*, Chengdu, China, 2017. ASCE. doi: 10.1061/9780784481257.077.
- [49] P. Grundy. Fatigue life of Australian railroad bridges. In *IABSE Symposium (Washington DC): Maintenance, Repair and Rehabilitation of Bridges*, pages 77–82, 1982.
- [50] T. Guo and Y.-W. Chen. Fatigue reliability analysis of steel bridge details based on field-monitored data and linear elastic fracture mechanics. *Structure and Infrastructure Engineering*, 9(5):496–505, 2013. ISSN 9780415621243. doi: 10.1080/15732479.2011.568508.
- [51] J. W. Hall. Uncertainty-based sensitivity indices for imprecise probability distributions. *Reliability Engineering and System Safety*, 91(10-11):1443–1451, 2006.
- [52] A. C. G. Hayward. Train loads on bridges, 1825 to 2010. *The International Journal for the History of Engineering & Technology*, 81(2):159–191, 2011. doi: 10.1179/175812111X13033852943273.
- [53] A. C. G. Hayward. The Construction of Railway Bridges Then and Now. *The International Journal for the History of Engineering & Technology*, 84(1): 59–87, 2014. doi: 10.1179/1758120613Z.00000000037.
- [54] K. Heie. *Veg- Og Jernbanebygging. (in Norwegian)*. H. Aschehoug & Co., Oslo, 2nd edition, 1941.
- [55] P. Hektoen, P. H. Sørli, and J. K. Andresen. Utviklingen av Brubyggingen ved NSB. (Development of bridge construction in the Norwegian State Railways). In *Norske sivilingeniørers forening: Jernbaneingeniørenes avdeling : 1891-1991 : jubileumsskrift*, pages 43–46. Norske sivilingeniørers forening, Jernbaneingeniørenes avdeling, Oslo, 1991. ISBN 82-992336-0-7.

- [56] J. C. Helton and W. L. Oberkampf. Alternative representations of epistemic uncertainty. *Reliability Engineering and System Safety*, 85(1-3):1–10, 2004. doi: 10.1016/j.res.2004.03.001.
- [57] M. A. Hirt. Remaining Fatigue Life of Bridges. In *IABSE Symposium (Washington DC): Maintenance, Repair and Rehabilitation of Bridges*, pages 113–129, 1982.
- [58] Hovestyret for Statsbanene. Norges Statsbaners moderniserings- og rasjonaliseringsplan (in Norwegian.). Technical report, Oslo, 1958.
- [59] B. Imam and P. A. Salter. Historical load effects on fatigue of metallic railway bridges. *Proceedings of the ICE - Bridge Engineering*, pages 1–14, 2017. doi: 10.1680/jbren.15.00046.
- [60] B. Imam, T. D. Righiniotis, M. K. Chryssanthopoulos, and B. Bell. Analytical fatigue assessment of riveted rail bridges. *Proceedings of the ICE - Bridge Engineering*, 159(3):105–116, Jan. 2006. doi: 10.1680/bren.2006.159.3.105.
- [61] B. M. Imam and T. D. Righiniotis. Fatigue evaluation of riveted railway bridges through global and local analysis. *Journal of Constructional Steel Research*, 66(11):1411–1421, 2010. doi: 10.1016/j.jcsr.2010.04.015.
- [62] B. M. Imam, T. D. Righiniotis, and M. K. Chryssanthopoulos. Numerical modelling of riveted railway bridge connections for fatigue evaluation. *Engineering Structures*, 29(11):3071–3081, Nov. 2007. doi: 10.1016/j.engstruct.2007.02.011.
- [63] B. M. Imam, T. D. Righiniotis, and M. K. Chryssanthopoulos. Probabilistic Fatigue Evaluation of Riveted Railway Bridges. *Journal of Bridge Engineering*, 13(3):237–244, 2008. doi: 10.1061/(ASCE)1084-0702(2008)13:3(237).
- [64] B. M. Imam, T. D. Righiniotis, and M. K. Chryssanthopoulos. Fatigue analysis of riveted railway bridge connections using the theory of critical distances. *Engineering Structures*, 30(10):2707–2715, Oct. 2008.
- [65] B. M. Imam, M. K. Chryssanthopoulos, and D. M. Frangopol. Fatigue System Reliability Analysis of Riveted Railway Bridge Connections. *Structure and Infrastructure Engineering*, 8(10):967–984, 2012.
- [66] S. D. Iwnicki, S. Stichel, A. Orlova, and M. Hecht. Dynamics of railway freight vehicles. *Vehicle System Dynamics*, 53(7):995–1033, 2015. doi: 10.1080/00423114.2015.1037773.

- [67] G. James. *Analysis of Traffic Load Effects on Railway Bridges*. PhD thesis, 2003.
- [68] M. S. Jepsen and L. Damkilde. A direct and fully general implementation of influence lines/surfaces in finite element software. *Advances in Engineering Software*, pages 1–7, 2016. doi: 10.1016/j.advengsoft.2016.04.006.
- [69] Jernbaneverket. Railway statistics 2015. Technical report, Oslo, 2015.
- [70] P.-A. Jönsson. Freight wagon running gear - a review. Technical report, Stockholm, 2002.
- [71] K. Kiss and L. Dunai. Stress history generation for truss bridges using multi-level models. *Computers and Structures*, 78(1):329–339, 2000. doi: 10.1016/S0045-7949(00)00079-1.
- [72] B. Kühn, M. Lukic, A. Nussbaumer, H.-P. Günther, R. Helmerich, S. Herion, M. H. Kolstein, S. Walbridge, B. Androic, O. Dijkstra, and O. Bucak. Assessment of Existing Steel Structures: Recommendations for Estimation of Remaining Fatigue Life. Technical report, 2008.
- [73] P. Kunz and M. A. Hirt. Reliability analysis of steel railway bridges under fatigue loading. In *IABSE Colloquium(Copenhagen): Remaining Structural Capacity*, 1993.
- [74] P. Kunz and G. Kulak. Fatigue Safety of Existing Steel Bridges. In *IABSE Symposium (San Francisco): Extending the Lifespan of Structures*, 1995.
- [75] J. Leander. *Refining the Fatigue Assessment Procedure of Existing Steel Bridges*. PhD thesis, 2013.
- [76] J. Leander and M. Al-Emrani. Reliability-based fatigue assessment of steel bridges using LEFM - A sensitivity analysis. *International Journal of Fatigue*, 93:82–91, 2016. doi: 10.1016/j.ijfatigue.2016.08.011.
- [77] J. Leander, A. Andersson, and R. Karoumi. Monitoring and Enhanced Fatigue Evaluation of a Steel Railway Bridge. *Engineering Structures*, 32(3):854–863, Mar. 2010.
- [78] J. Leander, B. Norlin, and R. Karoumi. Reliability-Based Calibration of Fatigue Safety Factors for Existing Steel Bridges. *Journal of Bridge Engineering*, (5):1–9, 2013. doi: 10.1061/(ASCE)BE.1943-5592.0000716.
- [79] K. Liu, H. Zhou, G. Shi, Y. Q. Wang, Y. J. Shi, and G. De Roeck. Fatigue assessment of a composite railway bridge for high speed trains. Part II: Conditions for which a dynamic analysis is needed. *Journal of Constructional Steel Research*, 82:246–254, 2013. doi: 10.1016/j.jcsr.2012.12.006.

- [80] S. C. Lovejoy. Determining Appropriate Fatigue Inspection Intervals for Steel Bridge Members. *Journal of Bridge Engineering*, 8(April):66–72, 2003. doi: 10.1061/(ASCE)1084-0702(2003)8:2(66).
- [81] F. Marques. *Fatigue Assessment of Old Riveted Railway Bridges*. PhD, University of Porto, Porto, 2016.
- [82] F. Marques, C. Moutinho, F. Magalhães, E. Caetano, and A. Cunha. Analysis of dynamic and fatigue effects in an old metallic riveted bridge. *Journal of Constructional Steel Research*, 99:85–101, 2014. doi: 10.1016/j.jcsr.2014.04.010.
- [83] F. Marques, C. Moutinho, W.-H. Hu, A. Cunha, and E. Caetano. Weigh-in-motion implementation in an old metallic railway bridge. *Engineering Structures*, 123:15–29, 2016.
- [84] R. E. Melchers. Assessment of Existing Structures – Approches and Research Needs. *Journal of Structural Engineering*, 127(4):406–411, 2001.
- [85] Norges Statsbaner. Illustrert fortegnelse over Personvogner, Trykk 751 [Illustrated record of passenger wagons, leaflet 751]. Technical report, NSB Hovedstyret, NSB Materiellavd., Oslo, 1900.
- [86] Norges Statsbaner. Illustrert fortegnelse over Lokomotiver, Trykk 750 [Illustrated record of Locomotives, leaflet 750]. Technical report, NSB Hovedstyret, NSB Materiellavd., Oslo, 1900.
- [87] Norges Statsbaner. Illustrert fortegnelse over Godsvogner, Trykk 752 [Illustrated record of freight wagons, leaflet 752]. Technical report, NSB Hovedstyret, NSB Materiellavd., Oslo, 1900.
- [88] Norges Statsbaner. Forskrifter om togs kjørehastighet, størrelse, utstyr med bremses, sammensetting og kobling samt om aksellast og lasteprofiler. Trykk 402 [Regulations on train speed, size, brakes, composition, coupling, axle loads and load profiles. Leaflet 402]. Technical report, Hovedstyret, Oslo, 1950.
- [89] Norges Statsbaner. Årsrapport for Norges Statsbaner [Annual report for Norwegian Railways]. Technical report, Hovedstyret, Oslo, 1953.
- [90] Norges Statsbaner. Illustrert fortegnelse over Motorvogner, Trykk 753 [Illustrated record of Multiple Units, leaflet 753]. Technical report, NSB Hovedstyret, NSB Materiellavd., Oslo, 1954.
- [91] Norges Statsbaner. NSB Historisk statistikk 1960-1987 (in Norwegian). Technical report, Oslo, 1988.

- [92] Norges Statsbaner. Jernbanestatistikk 1996-1998 [Railway statistics 1996-1998]. Technical report, Oslo, 1996.
- [93] M. Oberguggenberger, J. King, and B. Schmelzer. Classical and imprecise probability methods for sensitivity analysis in engineering: A case study. *International Journal of Approximate Reasoning*, 50(4):680–693, 2009. ISSN 0888-613X.
- [94] E. J. O'Brien, M. J. Quilligan, and R. Karoumi. Calculating an influence line from direct measurements. *Proceedings of the Institution of Civil Engineers, Bridge Engineering*, 159(BE1):31–34, 2006. doi: 10.1680/bren.2006.159.1.31.
- [95] E. Orakdöğen and K. Girgin. Direct determination of influence lines and surfaces by F.E.M. *Structural Engineering and Mechanics*, 20(3):279–292, 2005. doi: 10.12989/sem.2005.20.3.279.
- [96] J. Out, J. W. Fisher, and B. Yen. Fatigue strength of weathered and deteriorated riveted members. Technical report, 1984.
- [97] G. Parke and N. Hewson. ICE Manual of Bridge Engineering. Technical report, 2008.
- [98] R. Pasquier, J.-A. Goulet, C. Acevedo, and I. F. C. Smith. Improving Fatigue Evaluations of Structures Using In-Service Behavior Measurement Data. *Journal of Bridge Engineering*, 19(11), 2014. doi: 10.1061/(ASCE)BE.1943-5592.0000619.
- [99] B. Peeters, M. Finetto, G. De Roeck, V. Zabel, A. Braconi, C. Könke, H. Wenzel, W. Salvatore, F. Lippi, and A. Cunha. Fatigue damage control and assessment for railway bridges (FADLESS). 2014. ISSN 1831-9424. doi: 10.2777/59688.
- [100] U. Peil. Assessment of Bridges via Monitoring. *Structure and Infrastructure Engineering*, 1(2):101–117, 2005. ISSN 2331289387. doi: 10.1080/15732470412331289387.
- [101] A. Pipinato and C. Modena. Structural Analysis and Fatigue Reliability Assessment of the Paderno Bridge. *Practice Periodical on Structural Design and Construction*, 15(2):109–124, May 2010.
- [102] A. Pipinato, C. Pellegrino, O. S. Bursi, and C. Modena. High-cycle fatigue behavior of riveted connections for railway metal bridges. *Journal of Constructional Steel Research*, 65(12):2167–2175, 2009.



- [103] A. Pipinato, M. Molinari, C. Pellegrino, O. S. Bursi, and C. Modena. Fatigue tests on riveted steel elements taken from a railway bridge. *Structure and Infrastructure Engineering*, 7(12):907–920, 2011. doi: 10.1080/15732470903099776.
- [104] A. Pipinato, C. Pellegrino, and C. Modena. Fatigue Damage Estimation in Existing Railway Steel Bridges by Detailed Loading History Analysis. *ISRN Civil Engineering*, 2012:1–13, 2012.
- [105] A. Pipinato, C. Pellegrino, and C. Modena. Assessment procedure and rehabilitation criteria for the riveted railway Adige Bridge. *Structure and Infrastructure Engineering*, 8(8):747–764, 2012.
- [106] A. Pipinato, C. Pellegrino, and C. Modena. Residual life of historic riveted steel bridges: An analytical approach. *Proceedings of the Institution of Civil Engineers, Bridge Engineering*, 167(BE1):17–32, 2014. doi: 10.1680/bren.11.00014.
- [107] M. Prat. Traffic load models for bridge design: Recent developments and research. *Progress in Structural Engineering and Materials*, 3(4):326–334, 2001. doi: 10.1002/pse.91.
- [108] H. S. Reemsnyder. Fatigue Life Extension of Riveted Connections. *Journal of the Structural Division*, 101(12):2591–2608, 1976.
- [109] J. Schijve. Fatigue of structures and materials in the 20th century and the state of the art. *International Journal of Fatigue*, 25:679–702, 2003. doi: 10.1016/S0142-1123(03)00051-3.
- [110] J. Schijve. *Fatigue of Structures and Materials*. Springer Science, second edition, 2009. ISBN 978-1-4020-6807-2.
- [111] L. Schwarz. Measurements on railway bridges to determine axle loads and stress range spectra. In *Iabse Workshop (Lausanne): Evaluation of Existing Steel and Composite Bridges. Report*, pages 129–138, 1997.
- [112] S. Siriwardane, M. Ohga, R. Dissanayake, and K. Taniwaki. Application of new damage indicator-based sequential law for remaining fatigue life estimation of railway bridges. *Journal of Constructional Steel Research*, 64(2): 228–237, 2008. ISSN 0143-974X. doi: 10.1016/j.jcsr.2007.06.002.
- [113] S. S. Skiena. *The Algorithm Design Manual*. Springer-Verlag London, London, second edition, 2003. ISBN 978-1-84800-069-8.

- [114] G. N. Stamatopoulos. Fatigue assessment and strengthening measures to upgrade a steel railway bridge. *Journal of Constructional Steel Research*, 80: 346–354, 2013. doi: 10.1016/j.jcsr.2012.10.004.
- [115] Sustainable Bridges. Loads and Dynamic Effects - Background Document D4.3. Technical report, 2007.
- [116] Sustainable Bridges. Sustainable Bridges - Guideline for Load and Resistance Assessment of Existing European Railway Bridges - Advices on the use of advanced methods. Technical report, 2007.
- [117] Sustainable Bridges. Sustainable Bridges - Assessment for Future Traffic Demands and Longer Lives. Technical report, 2007.
- [118] R. A. P. Sweeney. Some remarks on the service behaviour of steel railway bridges. In *IABSE Symposium (Zürich): Bridges*, volume 32, pages 145–156, 1979.
- [119] A. Taras and R. Greiner. Development and Application of a Fatigue Class Catalogue for Riveted Bridge Components. *Structural Engineering International*, 20(1):91–103, Feb. 2010. doi: 10.2749/101686610790732535.
- [120] D. H. Tobias and D. A. Foutch. Reliability-Based Method for Fatigue Evaluation of Railway Bridges. *Journal of Bridge Engineering*, 2(2):53–60, 1997.
- [121] D. H. Tobias, D. A. Foutch, and J. Choros. Loading Spectra for Railway Bridges under Current Operating Conditions. *Journal of Bridge Engineering*, 1(4):127–134, 1996. ISSN 1084070219.
- [122] UIC. Leaflet 650 Standard designation of axle arrangements on locomotives and multiple-unit sets. 1983.
- [123] UIC. UIC Code 778-2 Recommendations for determining the carrying capacity of existing metal structures, 1986.



**DEPARTMENT OF STRUCTURAL ENGINEERING  
NORWEGIAN UNIVERSITY OF SCIENCE AND TECHNOLOGY**

N-7491 TRONDHEIM, NORWAY  
Telephone: +47 73 59 47 00    Telefax: +47 73 59 47 01

“Reliability Analysis of Structural Systems using Nonlinear Finite Element Methods”,

C. A. Holm, 1990:23, ISBN 82-7119-178-0.

“Uniform Stratified Flow Interaction with a Submerged Horizontal Cylinder”,

Ø. Arntsen, 1990:32, ISBN 82-7119-188-8.

“Large Displacement Analysis of Flexible and Rigid Systems Considering Displacement-Dependent Loads and Nonlinear Constraints”,

K. M. Mathisen, 1990:33, ISBN 82-7119-189-6.

“Solid Mechanics and Material Models including Large Deformations”,

E. Levold, 1990:56, ISBN 82-7119-214-0, ISSN 0802-3271.

“Inelastic Deformation Capacity of Flexurally-Loaded Aluminium Alloy Structures”,

T. Welo, 1990:62, ISBN 82-7119-220-5, ISSN 0802-3271.

“Visualization of Results from Mechanical Engineering Analysis”,

K. Aamnes, 1990:63, ISBN 82-7119-221-3, ISSN 0802-3271.

“Object-Oriented Product Modeling for Structural Design”,

S. I. Dale, 1991:6, ISBN 82-7119-258-2, ISSN 0802-3271.

“Parallel Techniques for Solving Finite Element Problems on Transputer Networks”,

T. H. Hansen, 1991:19, ISBN 82-7119-273-6, ISSN 0802-3271.

“Statistical Description and Estimation of Ocean Drift Ice Environments”,

R. Korsnes, 1991:24, ISBN 82-7119-278-7, ISSN 0802-3271.

“Properties of concrete related to fatigue damage: with emphasis on high strength concrete”,

G. Petkovic, 1991:35, ISBN 82-7119-290-6, ISSN 0802-3271.

“Turbidity Current Modelling”,

B. Brørs, 1991:38, ISBN 82-7119-293-0, ISSN 0802-3271.

- “Zero-Slump Concrete: Rheology, Degree of Compaction and Strength. Effects of Fillers as Part Cement-Replacement”,  
C. Sørensen, 1992:8, ISBN 82-7119-357-0, ISSN 0802-3271.
- “Nonlinear Analysis of Reinforced Concrete Structures Exposed to Transient Loading”,  
K. V. Høiseth, 1992:15, ISBN 82-7119-364-3, ISSN 0802-3271.
- “Finite Element Formulations and Solution Algorithms for Buckling and Collapse Analysis of Thin Shells”,  
R. O. Bjærum, 1992:30, ISBN 82-7119-380-5, ISSN 0802-3271.
- “Response Statistics of Nonlinear Dynamic Systems”,  
J. M. Johnsen, 1992:42, ISBN 82-7119-393-7, ISSN 0802-3271.
- “Digital Models in Engineering. A Study on why and how engineers build and operate digital models for decision support”,  
J. Høyte, 1992:75, ISBN 82-7119-429-1, ISSN 0802-3271.
- “Sparse Solution of Finite Element Equations”,  
A. C. Damhaug, 1992:76, ISBN 82-7119-430-5, ISSN 0802-3271.
- “Some Aspects of Floating Ice Related to Sea Surface Operations in the Barents Sea”,  
S. Løset, 1992:95, ISBN 82-7119-452-6, ISSN 0802-3271.
- “Modelling of Cyclic Plasticity with Application to Steel and Aluminium Structures”,  
O. S. Hopperstad, 1993:7, ISBN 82-7119-461-5, ISSN 0802-3271.
- “The Free Formulation: Linear Theory and Extensions with Applications to Tetrahedral Elements with Rotational Freedoms”,  
G. Skeie, 1993:17, ISBN 82-7119-472-0, ISSN 0802-3271.
- “Høyfast betongs motstand mot piggdekkslitasje. Analyse av resultater fra prøving i Veisliter'n”,  
T. Tveter, 1993:62, ISBN 82-7119-522-0, ISSN 0802-3271.
- “A Nonlinear Finite Element Based on Free Formulation Theory for Analysis of Sandwich Structures”,  
O. Aamlid, 1993:72, ISBN 82-7119-534-4, ISSN 0802-3271.
- “The Effect of Curing Temperature and Silica Fume on Chloride Migration and Pore Structure of High Strength Concrete”,  
C. J. Hauck, 1993:90, ISBN 82-7119-553-0, ISSN 0802-3271.

- “Failure of Concrete under Compressive Strain Gradients”,  
G. Markeset, 1993:110, ISBN 82-7119-575-1, ISSN 0802-3271.
- “An experimental study of internal tidal amphidromes in Vestfjorden”,  
J. H. Nilsen, 1994:39, ISBN 82-7119-640-5, ISSN 0802-3271.
- “Structural analysis of oil wells with emphasis on conductor design”,  
H. Larsen, 1994:46, ISBN 82-7119-648-0, ISSN 0802-3271.
- “Adaptive methods for non-linear finite element analysis of shell structures”,  
K. M. Okstad, 1994:66, ISBN 82-7119-670-7, ISSN 0802-3271.
- “On constitutive modelling in nonlinear analysis of concrete structures”,  
O. Fyrileiv, 1994:115, ISBN 82-7119-725-8, ISSN 0802-3271.
- “Fluctuating wind load and response of a line-like engineering structure with  
emphasis on motion-induced wind forces”,  
J. Bogunovic Jakobsen, 1995:62, ISBN 82-7119-809-2, ISSN 0802-3271.
- “An experimental study of beam-columns subjected to combined torsion,  
bending and axial actions”,  
A. Aalberg, 1995:66, ISBN 82-7119-813-0, ISSN 0802-3271.
- “Scaling and cracking in unsealed freeze/thaw testing of Portland cement and  
silica fume concretes”,  
S. Jacobsen, 1995:101, ISBN 82-7119-851-3, ISSN 0802-3271.
- “Damping of water waves by submerged vegetation. A case study of laminaria  
hyperborea”,  
A. M. Dubi, 1995:108, ISBN 82-7119-859-9, ISSN 0802-3271.
- “The dynamics of a slope current in the Barents Sea”,  
Sheng Li, 1995:109, ISBN 82-7119-860-2, ISSN 0802-3271.
- “Modellering av delmaterialenes betydning for betongens konsistens”,  
Ernst Mørtzell, 1996:12, ISBN 82-7119-894-7, ISSN 0802-3271.
- “Bending of thin-walled aluminium extrusions”,  
Birgit Søvik Opheim, 1996:60, ISBN 82-7119-947-1, ISSN 0802-3271.
- “Material modelling of aluminium for crashworthiness analysis”,  
Torodd Berstad, 1996:89, ISBN 82-7119-980-3, ISSN 0802-3271.

- “Estimation of structural parameters from response measurements on submerged floating tunnels”,  
Rolf Magne Larssen, 1996:119, ISBN 82-471-0014-2, ISSN 0802-3271.
- “Numerical modelling of plain and reinforced concrete by damage mechanics”,  
Mario A. Polanco-Loria, 1997:20, ISBN 82-471-0049-5, ISSN 0802-3271.
- “Nonlinear random vibrations - numerical analysis by path integration methods”,  
Vibeke Moe, 1997:26, ISBN 82-471-0056-8, ISSN 0802-3271.
- “Numerical prediction of vortex-induced vibration by the finite element method”,  
Joar Martin Dalheim, 1997:63, ISBN 82-471-0096-7, ISSN 0802-3271.
- “Time domain calculations of buffeting response for wind sensitive structures”,  
Ketil Aas-Jakobsen, 1997:148, ISBN 82-471-0189-0, ISSN 0802-3271.
- “A numerical study of flow about fixed and flexibly mounted circular cylinders”,  
Trond Stokka Meling, 1998:48, ISBN 82-471-0244-7, ISSN 0802-3271.
- “Estimation of chloride penetration into concrete bridges in coastal areas”,  
Per Egil Steen, 1998:89, ISBN 82-471-0290-0, ISSN 0802-3271.
- “Stress-resultant material models for reinforced concrete plates and shells”,  
Jan Arve Øverli, 1998:95, ISBN 82-471-0297-8, ISSN 0802-3271.
- “Chloride binding in concrete. Effect of surrounding environment and concrete composition”,  
Claus Kenneth Larsen, 1998:101, ISBN 82-471-0337-0, ISSN 0802-3271.
- “Rotational capacity of aluminium alloy beams”,  
Lars A. Moen, 1999:1, ISBN 82-471-0365-6, ISSN 0802-3271.
- “Stretch Bending of Aluminium Extrusions”,  
Arild H. Clausen, 1999:29, ISBN 82-471-0396-6, ISSN 0802-3271.
- “Aluminium and Steel Beams under Concentrated Loading”,  
Tore Tryland, 1999:30, ISBN 82-471-0397-4, ISSN 0802-3271.
- “Engineering Models of Elastoplasticity and Fracture for Aluminium Alloys”,  
Odd-Geir Lademo, 1999:39, ISBN 82-471-0406-7, ISSN 0802-3271.
- “Kapasitet og duktilitet av dybelforbindelser i trekonstruksjoner”,  
Jan Siem, 1999:46, ISBN 82-471-0414-8, ISSN 0802-3271.

- “Etablering av distribuert ingeniørarbeid; Teknologiske og organisatoriske erfaringer fra en norsk ingeniørbedrift”,  
Lars Line, 1999:52, ISBN 82-471-0420-2, ISSN 0802-3271.
- “Estimation of Earthquake-Induced Response”,  
Símon Ólafsson, 1999:73, ISBN 82-471-0443-1, ISSN 0802-3271.
- “Coastal Concrete Bridges: Moisture State, Chloride Permeability and Aging Effects”  
Ragnhild Holen Relling, 1999:74, ISBN 82-471-0445-8, ISSN 0802-3271.
- ”Capacity Assessment of Titanium Pipes Subjected to Bending and External Pressure”,  
Arve Bjørset, 1999:100, ISBN 82-471-0473-3, ISSN 0802-3271.
- “Validation of Numerical Collapse Behaviour of Thin-Walled Corrugated Panels”,  
Håvar Ilstad, 1999:101, ISBN 82-471-0474-1, ISSN 0802-3271.
- “Strength and Ductility of Welded Structures in Aluminium Alloys”,  
Miroslaw Matusiak, 1999:113, ISBN 82-471-0487-3, ISSN 0802-3271.
- “Thermal Dilation and Autogenous Deformation as Driving Forces to Self-Induced Stresses in High Performance Concrete”,  
Øyvind Bjøntegaard, 1999:121, ISBN 82-7984-002-8, ISSN 0802-3271.
- “Some Aspects of Ski Base Sliding Friction and Ski Base Structure”,  
Dag Anders Moldestad, 1999:137, ISBN 82-7984-019-2, ISSN 0802-3271.
- “Electrode reactions and corrosion resistance for steel in mortar and concrete”,  
Roy Antonsen, 2000:10, ISBN 82-7984-030-3, ISSN 0802-3271.
- “Hydro-Physical Conditions in Kelp Forests and the Effect on Wave Damping and Dune Erosion. A case study on Laminaria Hyperborea”,  
Stig Magnar Løvås, 2000:28, ISBN 82-7984-050-8, ISSN 0802-3271.
- “Random Vibration and the Path Integral Method”,  
Christian Skaug, 2000:39, ISBN 82-7984-061-3, ISSN 0802-3271.
- “Buckling and geometrical nonlinear beam-type analyses of timber structures”,  
Trond Even Eggen, 2000:56, ISBN 82-7984-081-8, ISSN 0802-3271.
- “Structural Crashworthiness of Aluminium Foam-Based Components”,  
Arve Grønsund Hanssen, 2000:76, ISBN 82-7984-102-4, ISSN 0809-103X.



“Measurements and simulations of the consolidation in first-year sea ice ridges, and some aspects of mechanical behaviour”,  
Knut V. Høyland, 2000:94, ISBN 82-7984-121-0, ISSN 0809-103X.

”Kinematics in Regular and Irregular Waves based on a Lagrangian Formulation”,  
Svein Helge Gjøsund, 2000-86, ISBN 82-7984-112-1, ISSN 0809-103X.

”Self-Induced Cracking Problems in Hardening Concrete Structures”,  
Daniela Bosnjak, 2000-121, ISBN 82-7984-151-2, ISSN 0809-103X.

“Ballistic Penetration and Perforation of Steel Plates”,  
Tore Børvik, 2000:124, ISBN 82-7984-154-7, ISSN 0809-103X.

“Freeze-Thaw resistance of Concrete. Effect of: Curing Conditions, Moisture Exchange and Materials”,  
Terje Finnerup Rønning, 2001:14, ISBN 82-7984-165-2, ISSN 0809-103X

“Structural behaviour of post tensioned concrete structures. Flat slab. Slabs on ground”,  
Steinar Trygstad, 2001:52, ISBN 82-471-5314-9, ISSN 0809-103X.

“Slipforming of Vertical Concrete Structures. Friction between concrete and slipform panel”,  
Kjell Tore Fosså, 2001:61, ISBN 82-471-5325-4, ISSN 0809-103X.

“Some numerical methods for the simulation of laminar and turbulent incompressible flows”,  
Jens Holmen, 2002:6, ISBN 82-471-5396-3, ISSN 0809-103X.

“Improved Fatigue Performance of Threaded Drillstring Connections by Cold Rolling”,  
Steinar Kristoffersen, 2002:11, ISBN: 82-421-5402-1, ISSN 0809-103X.

“Deformations in Concrete Cantilever Bridges: Observations and Theoretical Modelling”,  
Peter F. Takács, 2002:23, ISBN 82-471-5415-3, ISSN 0809-103X.

“Stiffened aluminium plates subjected to impact loading”,  
Hilde Giæver Hildrum, 2002:69, ISBN 82-471-5467-6, ISSN 0809-103X.

“Full- and model scale study of wind effects on a medium-rise building in a built up area”,  
Jónas Thór Snæbjörnsson, 2002:95, ISBN82-471-5495-1, ISSN 0809-103X.

- “Evaluation of Concepts for Loading of Hydrocarbons in Ice-infested water”, Arnor Jensen, 2002:114, ISBN 82-417-5506-0, ISSN 0809-103X.
- ”Numerical and Physical Modelling of Oil Spreading in Broken Ice”, Janne K. Økland Gjøsteen, 2002:130, ISBN 82-471-5523-0, ISSN 0809-103X.
- ”Diagnosis and protection of corroding steel in concrete”, Franz Pruckner, 20002:140, ISBN 82-471-5555-4, ISSN 0809-103X.
- “Tensile and Compressive Creep of Young Concrete: Testing and Modelling”, Dawood Atrushi, 2003:17, ISBN 82-471-5565-6, ISSN 0809-103X.
- “Rheology of Particle Suspensions. Fresh Concrete, Mortar and Cement Paste with Various Types of Lignosulfonates”, Jon Elvar Wallevik, 2003:18, ISBN 82-471-5566-4, ISSN 0809-103X.
- “Oblique Loading of Aluminium Crash Components”, Aase Reyes, 2003:15, ISBN 82-471-5562-1, ISSN 0809-103X.
- “Utilization of Ethiopian Natural Pozzolans”, Surafel Ketema Desta, 2003:26, ISSN 82-471-5574-5, ISSN:0809-103X.
- “Behaviour and strength prediction of reinforced concrete structures with discontinuity regions”, Helge Brå, 2004:11, ISBN 82-471-6222-9, ISSN 1503-8181.
- “High-strength steel plates subjected to projectile impact. An experimental and numerical study”, Sumita Dey, 2004:38, ISBN 82-471-6282-2 (printed version), ISBN 82-471-6281-4 (electronic version), ISSN 1503-8181.
- “Alkali-reactive and inert fillers in concrete. Rheology of fresh mixtures and expansive reactions.” Bård M. Pedersen, 2004:92, ISBN 82-471-6401-9 (printed version), ISBN 82-471-6400-0 (electronic version), ISSN 1503-8181.
- “On the Shear Capacity of Steel Girders with Large Web Openings”. Nils Christian Hagen, 2005:9 ISBN 82-471-6878-2 (printed version), ISBN 82-471-6877-4 (electronic version), ISSN 1503-8181.
- ”Behaviour of aluminium extrusions subjected to axial loading”. Østen Jensen, 2005:7, ISBN 82-471-6873-1 (printed version), ISBN 82-471-6872-3 (electronic version), ISSN 1503-8181.

- ”Thermal Aspects of corrosion of Steel in Concrete”.  
Jan-Magnus Østvik, 2005:5, ISBN 82-471-6869-3 (printed version), ISBN 82-471-6868 (electronic version), ISSN 1503-8181.
- ”Mechanical and adaptive behaviour of bone in relation to hip replacement. A study of bone remodelling and bone grafting.”  
Sébastien Muller, 2005:34, ISBN 82-471-6933-9 (printed version), ISBN 82-471-6932-0 (electronic version), ISSN 1503-8181.
- “Analysis of geometrical nonlinearities with applications to timber structures”.  
Lars Wollebæk, 2005:74, ISBN 82-471-7050-5 (printed version), ISBN 82-471-7019-1 (electronic version), ISSN 1503-8181.
- “Pedestrian induced lateral vibrations of slender footbridges”,  
Anders Rönquist, 2005:102, ISBN 82-471-7082-5 (printed version), ISBN 82-471-7081-7 (electronic version), ISSN 1503-8181.
- “Initial Strength Development of Fly Ash and Limestone Blended Cements at Various Temperatures Predicted by Ultrasonic Pulse Velocity”,  
Tom Ivar Fredvik, 2005:112, ISBN 82-471-7105-8 (printed version), ISBN 82-471-7103-1 (electronic version), ISSN 1503-8181.
- “Behaviour and modelling of thin-walled cast components”,  
Cato Dørum, 2005:128, ISBN 82-471-7140-6 (printed version), ISBN 82-471-7139-2 (electronic version), ISSN 1503-8181.
- “Behaviour and modelling of selfpiercing riveted connections”,  
Raffaele Porcaro, 2005:165, ISBN 82-471-7219-4 (printed version), ISBN 82-471-7218-6 (electronic version), ISSN 1503-8181.
- ”Behaviour and Modelling of Aluminium Plates subjected to Compressive Load”,  
Lars Rønning, 2005:154, ISBN 82-471-7169-1 (printed version), ISBN 82-471-7195-3 (electronic version), ISSN 1503-8181.
- ”Bumper beam-longitudinal system subjected to offset impact loading”,  
Satyanarayana Kokkula, 2005:193, ISBN 82-471-7280-1 (printed version), ISBN 82-471-7279-8 (electronic version), ISSN 1503-8181.
- “Control of Chloride Penetration into Concrete Structures at Early Age”,  
Guofei Liu, 2006:46, ISBN 82-471-7838-9 (printed version), ISBN 82-471-7837-0 (electronic version), ISSN 1503-8181.
- “Modelling of Welded Thin-Walled Aluminium Structures”,  
Ting Wang, 2006:78, ISBN 82-471-7907-5 (printed version), ISBN 82-471-7906-7 (electronic version), ISSN 1503-8181.

”Time-variant reliability of dynamic systems by importance sampling and probabilistic analysis of ice loads”,  
Anna Ivanova Olsen, 2006:139, ISBN 82-471-8041-3 (printed version), ISBN 82-471-8040-5 (electronic version), ISSN 1503-8181.

“Fatigue life prediction of an aluminium alloy automotive component using finite element analysis of surface topography”,  
Sigmund Kyrre Ås, 2006:25, ISBN 82-471-7791-9 (printed version), ISBN 82-471-7791-9 (electronic version), ISSN 1503-8181.

”Constitutive models of elastoplasticity and fracture for aluminium alloys under strain path change”,  
Dasharatha Achani, 2006:76, ISBN 82-471-7903-2 (printed version), ISBN 82-471-7902-4 (electronic version), ISSN 1503-8181.

“Simulations of 2D dynamic brittle fracture by the Element-free Galerkin method and linear fracture mechanics”,  
Tommy Karlsson, 2006:125, ISBN 82-471-8011-1 (printed version), ISBN 82-471-8010-3 (electronic version), ISSN 1503-8181.

“Penetration and Perforation of Granite Targets by Hard Projectiles”,  
Chong Chiang Seah, 2006:188, ISBN 82-471-8150-9 (printed version), ISBN 82-471-8149-5 (electronic version), ISSN 1503-8181.

“Deformations, strain capacity and cracking of concrete in plastic and early hardening phases”,  
Tor Arne Hammer, 2007:234, ISBN 978-82-471-5191-4 (printed version), ISBN 978-82-471-5207-2 (electronic version), ISSN 1503-8181.

“Crashworthiness of dual-phase high-strength steel: Material and Component behaviour”, Venkatapathi Tarigopula, 2007:230, ISBN 82-471-5076-4 (printed version), ISBN 82-471-5093-1 (electronic version), ISSN 1503-8181.

“Fibre reinforcement in load carrying concrete structures”,  
Åse Lyslo Døssland, 2008:50, ISBN 978-82-471-6910-0 (printed version), ISBN 978-82-471-6924-7 (electronic version), ISSN 1503-8181.

“Low-velocity penetration of aluminium plates”,  
Frode Grytten, 2008:46, ISBN 978-82-471-6826-4 (printed version), ISBN 978-82-471-6843-1 (electronic version), ISSN 1503-8181.

“Robustness studies of structures subjected to large deformations”,  
Ørjan Fyllingen, 2008:24, ISBN 978-82-471-6339-9 (printed version), ISBN 978-82-471-6342-9 (electronic version), ISSN 1503-8181.

- “Constitutive modelling of morsellised bone”,  
Knut Birger Lunde, 2008:92, ISBN 978-82-471-7829-4 (printed version), ISBN 978-82-471-7832-4 (electronic version), ISSN 1503-8181.
- “Experimental Investigations of Wind Loading on a Suspension Bridge Girder”,  
Bjørn Isaksen, 2008:131, ISBN 978-82-471-8656-5 (printed version), ISBN 978-82-471-8673-2 (electronic version), ISSN 1503-8181.
- “Cracking Risk of Concrete Structures in The Hardening Phase”,  
Guomin Ji, 2008:198, ISBN 978-82-471-1079-9 (printed version), ISBN 978-82-471-1080-5 (electronic version), ISSN 1503-8181.
- “Modelling and numerical analysis of the porcine and human mitral apparatus”,  
Victorien Emile Prot, 2008:249, ISBN 978-82-471-1192-5 (printed version), ISBN 978-82-471-1193-2 (electronic version), ISSN 1503-8181.
- “Strength analysis of net structures”,  
Heidi Moe, 2009:48, ISBN 978-82-471-1468-1 (printed version), ISBN 978-82-471-1469-8 (electronic version), ISSN 1503-8181.
- “Numerical analysis of ductile fracture in surface cracked shells”,  
Espen Berg, 2009:80, ISBN 978-82-471-1537-4 (printed version), ISBN 978-82-471-1538-1 (electronic version), ISSN 1503-8181.
- “Subject specific finite element analysis of bone – for evaluation of the healing of a leg lengthening and evaluation of femoral stem design”,  
Sune Hansborg Pettersen, 2009:99, ISBN 978-82-471-1579-4 (printed version), ISBN 978-82-471-1580-0 (electronic version), ISSN 1503-8181.
- “Evaluation of fracture parameters for notched multi-layered structures”,  
Lingyun Shang, 2009:137, ISBN 978-82-471-1662-3 (printed version), ISBN 978-82-471-1663-0 (electronic version), ISSN 1503-8181.
- “Modelling of Dynamic Material Behaviour and Fracture of Aluminium Alloys for Structural Applications”  
Yan Chen, 2009:69, ISBN 978-82-471-1515-2 (printed version), ISBN 978-82-471-1516-9 (electronic version), ISSN 1503-8181.
- “Nanomechanics of polymer and composite particles”  
Jianying He 2009:213, ISBN 978-82-471-1828-3 (printed version), ISBN 978-82-471-1829-0 (electronic version), ISSN 1503-8181.
- “Mechanical properties of clear wood from Norway spruce”  
Kristian Berbom Dahl 2009:250, ISBN 978-82-471-1911-2 (printed version), ISBN 978-82-471-1912-9 (electronic version), ISSN 1503-8181.

“Modeling of the degradation of TiB<sub>2</sub> mechanical properties by residual stresses and liquid Al penetration along grain boundaries”

Micol Pezzotta 2009:254, ISBN 978-82-471-1923-5 (printed version) ISBN 978-82-471-1924-2 (electronic version) ISSN 1503-8181.

“Effect of welding residual stress on fracture”

Xiabo Ren 2010:77, ISBN 978-82-471-2115-3 (printed version) ISBN 978-82-471-2116-0 (electronic version), ISSN 1503-8181.

“Pan-based carbon fiber as anode material in cathodic protection system for concrete structures”

Mahdi Chini 2010:122, ISBN 978-82-471-2210-5 (printed version) ISBN 978-82-471-2213-6 (electronic version), ISSN 1503-8181.

“Structural Behaviour of deteriorated and retrofitted concrete structures”

Irina Vasililjeva Sæther 2010:171, ISBN 978-82-471-2315-7 (printed version) ISBN 978-82-471-2316-4 (electronic version) ISSN 1503-8181.

“Prediction of local snow loads on roofs”

Vivian Meløysund 2010:247, ISBN 978-82-471-2490-1 (printed version) ISBN 978-82-471-2491-8 (electronic version) ISSN 1503-8181.

“Behaviour and modelling of polymers for crash applications”

Virgile Delhaye 2010:251, ISBN 978-82-471-2501-4 (printed version) ISBN 978-82-471-2502-1 (electronic version) ISSN 1503-8181.

“Blended cement with reduced CO<sub>2</sub> emission – Utilizing the Fly Ash-Limestone Synergy”,

Klaartje De Weerd 2011:32, ISBN 978-82-471-2584-7 (printed version) ISBN 978-82-471-2584-4 (electronic version) ISSN 1503-8181.

“Chloride induced reinforcement corrosion in concrete” Concept of critical chloride content – methods and mechanisms.

Ueli Angst 2011:113, ISBN 978-82-471-2769-9 (printed version) ISBN 978-82-471-2763-6 (electronic version) ISSN 1503-8181.

“A thermo-electric-Mechanical study of the carbon anode and contact interface for Energy savings in the production of aluminium”.

Dag Herman Andersen 2011:157, ISBN 978-82-471-2859-6 (printed version) ISBN 978-82-471-2860-2 (electronic version) ISSN 1503-8181.

“Structural Capacity of Anchorage Ties in Masonry Veneer Walls Subjected to Earthquake. The implications of Eurocode 8 and Eurocode 6 on a typical Norwegian veneer wall. ”

Ahmed Mohamed Yousry Hamed 2011:181, ISBN 978-82-471-2911-1 (printed version) ISBN 978-82-471-2912-8 (electronic ver.) ISSN 1503-8181.

“Work-hardening behaviour in age-hardenable Al-Zn-Mg(-Cu) alloys”.

Ida Westermann , 2011:247, ISBN 978-82-471-3056-8 (printed ver.) ISBN 978-82-471-3057-5 (electronic ver.) ISSN 1503-8181.

“Behaviour and modelling of selfpiercing riveted connections using aluminium rivets”. Nguyen-Hieu Hoang, 2011:266, ISBN 978-82-471-3097-1 (printed ver.) ISBN 978-82-471-3099-5 (electronic ver.) ISSN 1503-8181.

“Fibre reinforced concrete”.

Sindre Sandbakk, 2011:297, ISBN 978-82-471-3167-1 (printed ver.) ISBN 978-82-471-3168-8 (electronic ver.) ISSN 1503-8181.

“Dynamic behaviour of cablesupported bridges subjected to strong natural wind”.

Ole Andre Øiseth, 2011:315, ISBN 978-82-471-3209-8 (printed ver.) ISBN 978-82-471-3210-4 (electronic ver.) ISSN 1503-8181.

“Constitutive modeling of solargrade silicon materials”

Julien Cochard, 2011:307, ISBN 978-82-471-3189-3 (printed ver.) ISBN 978-82-471-3190-9 (electronic ver.) ISSN 1503-8181.

“Constitutive behavior and fracture of shape memory alloys”

Jim Stian Olsen, 2012:57, ISBN 978-82-471-3382-8 (printed ver.) ISBN 978-82-471-3383-5 (electronic ver.) ISSN 1503-8181.

“Field measurements in mechanical testing using close-range photogrammetry and digital image analysis”

Egil Fagerholt, 2012:95, ISBN 978-82-471-3466-5 (printed ver.) ISBN 978-82-471-3467-2 (electronic ver.) ISSN 1503-8181.

“Towards a better understanding of the ultimate behaviour of lightweight aggregate concrete in compression and bending”.

Håvard Nedrelid, 2012:123, ISBN 978-82-471-3527-3 (printed ver.) ISBN 978-82-471-3528-0 (electronic ver.) ISSN 1503-8181.

“Numerical simulations of blood flow in the left side of the heart”

Sigrid Kaarstad Dahl, 2012:135, ISBN 978-82-471-3553-2 (printed ver.) ISBN 978-82-471-3555-6 (electronic ver.) ISSN 1503-8181.

“Moisture induced stresses in glulam”

Vanessa Angst-Nicollier, 2012:139, ISBN 978-82-471-3562-4 (printed ver.) ISBN 978-82-471-3563-1 (electronic ver.) ISSN 1503-8181.

“Biomechanical aspects of distraction osteogenesis”

Valentina La Russa, 2012:250, ISBN 978-82-471-3807-6 (printed ver.) ISBN 978-82-471-3808-3 (electronic ver.) ISSN 1503-8181.

“Ductile fracture in dual-phase steel. Theoretical, experimental and numerical study”

Gaute Gruben, 2012:257, ISBN 978-82-471-3822-9 (printed ver.) ISBN 978-82-471-3823-6 (electronic ver.) ISSN 1503-8181.

“Damping in Timber Structures”

Nathalie Labonnote, 2012:263, ISBN 978-82-471-3836-6 (printed ver.) ISBN 978-82-471-3837-3 (electronic ver.) ISSN 1503-8181.

“Biomechanical modeling of fetal veins: The umbilical vein and ductus venosus bifurcation”

Paul Roger Leinan, 2012:299, ISBN 978-82-471-3915-8 (printed ver.) ISBN 978-82-471-3916-5 (electronic ver.) ISSN 1503-8181.

“Large-Deformation behaviour of thermoplastics at various stress states”

Anne Serine Ognedal, 2012:298, ISBN 978-82-471-3913-4 (printed ver.) ISBN 978-82-471-3914-1 (electronic ver.) ISSN 1503-8181.

“Hardening accelerator for fly ash blended cement”

Kien Dinh Hoang, 2012:366, ISBN 978-82-471-4063-5 (printed ver.) ISBN 978-82-471-4064-2 (electronic ver.) ISSN 1503-8181.

“From molecular structure to mechanical properties”

Jianyang Wu, 2013:186, ISBN 978-82-471-4485-5 (printed ver.) ISBN 978-82-471-4486-2 (electronic ver.) ISSN 1503-8181.

“Experimental and numerical study of hybrid concrete structures”

Linn Grepstad Nes, 2013:259, ISBN 978-82-471-4644-6 (printed ver.) ISBN 978-82-471-4645-3 (electronic ver.) ISSN 1503-8181.

“Mechanics of ultra-thin multi crystalline silicon wafers”

Saber Saffar, 2013:199, ISBN 978-82-471-4511-1 (printed ver.) ISBN 978-82-471-4513-5 (electronic ver.) ISSN 1503-8181.

“Through process modelling of welded aluminium structures”

Anizahyati Alisibramulisi, 2013:325, ISBN 978-82-471-4788-7 (printed ver.) ISBN 978-82-471-4789-4 (electronic ver.) ISSN 1503-8181.



- “Combined blast and fragment loading on steel plates”  
Knut Gaarder Rakvåg, 2013:361, ISBN 978-82-471-4872-3 (printed ver.) ISBN 978-82-4873-0 (electronic ver.) ISSN 1503-8181.
- “Characterization and modelling of the anisotropic behaviour of high-strength aluminium alloy”  
Marion Fourmeau, 2014:37, ISBN 978-82-326-0008-3 (printed ver.) ISBN 978-82-326-0009-0 (electronic ver.) ISSN 1503-8181.
- “Behaviour of threaded steel fasteners at elevated deformation rates”  
Henning Fransplass, 2014:65, ISBN 978-82-326-0054-0 (printed ver.) ISBN 978-82-326-0055-7 (electronic ver.) ISSN 1503-8181.
- “Sedimentation and Bleeding”  
Ya Peng, 2014:89, ISBN 978-82-326-0102-8 (printed ver.) ISBN 978-82-326-0103-5 (electric ver.) ISSN 1503-8181.
- “Impact against X65 offshore pipelines”  
Martin Kristoffersen, 2014:362, ISBN 978-82-326-0636-8 (printed ver.) ISBN 978-82-326-0637-5 (electronic ver.) ISSN 1503-8181.
- “Formability of aluminium alloy subjected to prestrain by rolling”  
Dmitry Vysochinskiy, 2014:363,, ISBN 978-82-326-0638-2 (printed ver.) ISBN 978-82-326-0639-9 (electronic ver.) ISSN 1503-8181.
- “Experimental and numerical study of Yielding, Work-Hardening and anisotropy in textured AA6xxx alloys using crystal plasticity models”  
Mikhail Khadyko, 2015:28, ISBN 978-82-326-0724-2 (printed ver.) ISBN 978-82-326-0725-9 (electronic ver.) ISSN 1503-8181.
- “Behaviour and Modelling of AA6xxx Aluminium Alloys Under a Wide Range of Temperatures and Strain Rates”  
Vincent Vilamosa, 2015:63, ISBN 978-82-326-0786-0 (printed ver.) ISBN 978-82-326-0787-7 (electronic ver.) ISSN 1503-8181.
- “A Probabilistic Approach in Failure Modelling of Aluminium High Pressure Die-Castings”  
Octavian Knoll, 2015:137, ISBN 978-82-326-0930-7 (printed ver.) ISBN 978-82-326-0931-4 (electronic ver.) ISSN 1503-8181.
- “Ice Abrasion on Marine Concrete Structures”  
Egil Møen, 2015:189, ISBN 978-82-326-1034-1 (printed ver.) ISBN 978-82-326-1035-8 (electronic ver.) ISSN 1503-8181.

“Fibre Orientation in Steel-Fibre-Reinforced Concrete”  
Giedrius Zirgulis, 2015:229, ISBN 978-82-326-1114-0 (printed ver.) ISBN 978-82-326-1115-7 (electronic ver.) ISSN 1503-8181.

“Effect of spatial variation and possible interference of localised corrosion on the residual capacity of a reinforced concrete beam”  
Mohammad Mahdi Kioumars, 2015:282, ISBN 978-82-326-1220-8 (printed ver.) ISBN 978-82-1221-5 (electronic ver.) ISSN 1503-8181.

“The role of concrete resistivity in chloride-induced macro-cell corrosion”  
Karla Horbostel, 2015:324, ISBN 978-82-326-1304-5 (printed ver.) ISBN 978-82-326-1305-2 (electronic ver.) ISSN 1503-8181.

“Flowable fibre-reinforced concrete for structural applications”  
Elena Vidal Sarmiento, 2015:335, ISBN 978-82-326-1324-3 (printed ver.) ISBN 978-82-326-1325-0 (electronic ver.) ISSN 1503-8181.

“Development of chushed sand for concrete production with microproportioning” Rolands Cepuritis, 2016:19, ISBN 978-82-326-1382-3 (printed ver.) ISBN 978-82-326-1383-0 (electronic ver.) ISSN 1503-8181.

“Withdrawal properties of threaded rods embedded in glued-laminated timber elements”  
Haris Stamatopoulos, 2016:48, ISBN 978-82-326-1436-3 (printed ver.) ISBN 978-82-326-1437-0 (electronic ver.) ISSN 1503-8181.

“An Experimental and numerical study of thermoplastics at large deformation”  
Marius Andersen, 2016:191, ISBN 978-82-326-1720-3 (printed ver.) ISBN 978-82-326-1721-0 (electronic ver.) ISSN 1503-8181.

“Modeling and Simulation of Ballistic Impact”  
Jens Kristian Holmen, 2016:240, ISBN 978-82-326-1818-7 (printed ver.) ISBN 978-82-326-1819-4 (electronic ver.) ISSN 1503-8181.

“Early age crack assessment of concrete structures”  
Anja B. Estensen Klausen, 2016:256, ISBN 978-82-326-1850-7 (printed ver.) ISBN 978-82-326-1851-4 (electronic ver.) ISSN 1503-8181.

“Uncertainty quantification and sensitivity analysis for cardiovascular models”  
Vinzenc Gregor Eck, 2016:234, ISBN 978-82-326-1806-4 (printed ver.) ISBN 978-82-326-1807-1 (electronic ver.) ISSN 1503-8181.

“Dynamic behaviour of existing and new railway catenary systems under Norwegian conditions”

Petter Røe Nåvik, 2016:298, ISBN 978-82-326-1935-1 (printed ver.) ISBN 978-82-326-1934-4 (electronic ver.) ISSN 1503-8181.

“Mechanical behaviour of particle-filled elastomers at various temperatures”

Arne Ilseng, 2016:295, ISBN 978-82-326-1928-3 (printed ver.) ISBN 978-82-326-1929-0 (electronic ver.) ISSN 1503-8181.

“Nanotechnology for Anti-Icing Application”

Zhiwei He, 2016:348, ISBN 978-82-326-2038-8 (printed ver.) ISBN 978-82-326-2019-5 (electronic ver.) ISSN 1503-8181.

“Conduction Mechanisms in Conductive Adhesives with Metal-Coated Polymer Spheres”

Sigurd Rolland Pettersen, 2016:349, ISBN 978-82-326-2040-1 (printed ver.) ISBN 978-82-326-2041-8 (electronic ver.) ISSN 1503-8181.

“The interaction between calcium lignosulfonate and cement”

Alessia Colombo, 2017:20, ISBN 978-82-326-2122-4 (printed ver.) ISBN 978-82-326-2123-1 (electronic ver.) ISSN 1503-8181.

“Behaviour and Modelling of Flexible Structures Subjected to Blast Loading”

Vegard Aune, 2017:101, ISBN 978-82-326-2274-0 (printed ver.) ISBN 978-82-326-2275-7 (electronic ver.) ISSN 1503-8181.

“Behaviour of steel connections under quasi-static and impact loading”

Erik Løhre Grimsø, 2017:159, ISBN 978-82-326-2390-7 (printed ver.) ISBN 978-82-326-2391-4 (electronic ver.) ISSN 1503-8181.

“An experimental and numerical study of cortical bone at the macro and Nano-scale”

Masoud Ramenzanzadehkoldeh, 2017:208, ISBN 978-82-326-2488-1 (printed ver.) ISBN 978-82-326-2489-8 (electronic ver.) ISSN 1503-8181.

“Optoelectrical Properties of a Novel Organic Semiconductor: 6,13-

Dichloropentacene” Mao Wang, 2017:130, ISBN 978-82-326-2332-7 (printed ver.) ISBN 978-82-326-2333-4 (electronic ver.) ISSN 1503-8181.

“Core-shell structured microgels and their behavior at oil and water interface”

Yi Gong, 2017:182, ISBN 978-82-326-2436-2 (printed ver.) ISBN 978-82-326-2437-9 (electronic ver.) ISSN 1503-8181.

“Aspects of design of reinforced concrete structures using nonlinear finite element analyses”

Morten Engen, 2017:149, ISBN 978-82-326-2370-9 (printed ver.) ISBN 978-82-326-2371-6 (electronic ver.) ISSN 1503-8181.

“Numerical studies on ductile failure of aluminium alloys”

Lars Edvard Dæhli, 2017:284, ISBN 978-82-326-2636-6 (printed ver.) ISBN 978-82-326-2637-3 (electronic ver.) ISSN 1503-8181.

“Modelling and Assessment of Hydrogen Embrittlement in Steels and Nickel Alloys”

Haiyang Yu, 2017:278, ISBN 978-82-326-2624-3 (printed. ver.) ISBN 978-82-326-2625-0 (electronic ver.) ISSN 1503-8181.

“Network arch timber bridges with light timber deck on transverse crossbeams”

Anna Weronika Ostrycharczyk, 2017:318, ISBN 978-82-326-2704-2 (printed ver.) ISBN 978-82-326-2705-9 (electronic ver.) ISSN 1503-8181.

“Splicing of Large Glued Laminated Timber Elements by Use of Long Threaded Rods”

Martin Cepelka, 2017:320, ISBN 978-82-326-2708-0 (printed ver.) ISBN 978-82-326-2709-7 (electronic ver.) ISSN 1503-8181.

“Thermomechanical behaviour of semi-crystalline polymers: experiments, modelling and simulation”

Joakim Johnsen, 2017:317, ISBN 978-82-326-2702-8 (printed ver.) ISBN 978-82-326-2703-5 (electronic ver.) ISSN 1503-8181.

“Small-Scale Plasticity under Hydrogen Environment”

Kai Zhao, 2017:356, ISBN 978-82-326-2782-0 (printed ver.) ISBN 978-82-326-2783-7 (electronic er.) ISSN 1503-8181.

“Risk and Reliability Based Calibration of Structural Design Codes”

Michele Baravalle, 2017:342, ISBN 978-82-326-2752-3 (printed ver.) ISBN 978-82-326-2753-0 (electronic ver.) ISSN 1503-8181.

“Dynamic behaviour of floating bridges exposed to wave excitation”

Knut Andreas Kvåle, 2017:365, ISBN 978-82-326-2800-1 (printed ver.) ISBN 978-82-326-2801-8 (electronic ver.) ISSN 1503-8181.

“Dolomite calcined clay composite cement – hydration and durability”

Alisa Lydia Machner, 2018:39, ISBN 978-82-326-2872-8 (printed ver.). ISBN 978-82-326-2873-5 (electronic ver.) ISSN 1503-8181.

“Modelling of the self-excited forces for bridge decks subjected to random motions: an experimental study”

Bartosz Siedziako, 2018:52, ISBN 978-82-326-2896-4 (printed ver.). ISBN 978-82-326-2897-1 (electronic ver.) ISSN 1503-8181.

“A probabilistic-based methodology for evaluation of timber facade constructions”

Klodian Gradeci, 2018:69, ISBN 978-82-326-2928-2 (printed ver.) ISBN 978-82-326-2929-9 (electronic ver.) ISSN 1503-8181.

“Behaviour and modelling of flow-drill screw connections”

Johan Kolstø Sønstabø, 2018:73, ISBN 978-82-326-2936-7 (printed ver.) ISBN 978-82-326-2937-4 (electronic ver.) ISSN 1503-8181.

“Full-scale investigation of the effects of wind turbulence characteristics on dynamic behavior of long-span cable-supported bridges in complex terrain”

Aksel Fenerci, 2018:100, ISBN 978-82-326-2990-9 (printed ver.) ISBN 978-82-326-2991-6 (electronic ver.) ISSN 1503-8181.

“Modeling and simulation of the soft palate for improved understanding of the obstructive sleep apnea syndrome”

Hongliang Liu, 2018:101, ISBN 978-82-326-2992-3 (printed ver.) ISBN 978-82-326-2993-0 (electronic ver.) ISSN 1503-8181.

“Long-term extreme response analysis of cable-supported bridges with floating pylons subjected to wind and wave loads”.

Yuwang Xu, 2018:229, ISBN 978-82-326-3248-0 (printed ver.) ISBN 978-82-326-3249-7 (electronic ver.) ISSN 1503-8181.

“Reinforcement corrosion in carbonated fly ash concrete”

Andres Belda Revert, 2018:230, ISBN 978-82-326-3250-3 (printed ver.) ISBN 978-82-326-3251-0 (electronic ver.) ISSN 1503-8181.

“Direct finite element method for nonlinear earthquake analysis of concrete dams including dam-water-foundation rock interaction”

Arnkjell Løkke, 2018:252, ISBN 978-82-326-3294-7 (printed ver.) ISBN 978-82-326-3295-4 (electronic ver.) ISSN 1503-8181.

“Electromechanical characterization of metal-coated polymer spheres for conductive adhesives”

Molly Strimbeck Bazilchuk, 2018:295, ISBN 978-82-326-3380-7 (printed. ver.) ISBN 978-82-326-3381-4 (electrical ver.) ISSN 1503-8181.

“Determining the tensile properties of Arctic materials and modelling their effects on fracture”

Shengwen Tu, 2018:269, ISBN 978-82-326-3328-9 (printed ver.) ISBN 978-82-326-3329-6 (electronic ver.) ISSN 1503-8181.

“Atomistic Insight into Transportation of Nanofluid in Ultra-confined Channel”

Xiao Wang, 2018:334, ISBN978-82-326-3456-9 (printed ver.) ISBN 978-82-326-3457-6 (electronic ver.) ISSN 1503-8181.

“An experimental and numerical study of the mechanical behaviour of short glass-fibre reinforced thermoplastics”.

Jens Petter Henrik Holmstrøm, 2019:79, ISBN 978-82-326-3760-7 (printed ver.) ISBN 978-82-326-3761-4 (electronic ver.) ISSN 1503-8181.